

**STUDIES ON DIFFUSION OF SOME
LABELLED TRANSITION METAL IONS
AND THEIR SALTS IN AGAR GEL MEDIUM**

S.K. UJLAMBKAR

AUGUST 1983

**STUDIES ON DIFFUSION OF SOME
LABELLED TRANSITION METAL IONS AND
THEIR SALTS IN AGAR GEL MEDIUM**

**A THESIS
SUBMITTED TO THE
UNIVERSITY OF POONA**

**FOR THE DEGREE OF
DOCTOR OF PHILOSOPHY
IN CHEMISTRY**

**BY
S. K. UJLAMBKAR**

**DEPARTMENT OF CHEMISTRY
UNIVERSITY OF POONA
PUNE - 411 007 (INDIA)**


AUGUST 1983



TO MY PARENTS

CERTIFICATE

This is to certify that the work incorporated in the thesis 'Studies on diffusion of some labelled transition metal ions and their salts in agar gel medium' being submitted by Shri S.K. Ujlambkar for the Ph.D. degree in Chemistry was carried out by the candidate under my supervision. Such material as has been obtained from other sources has been duly acknowledged in the thesis.



(Dr. S.F. Patil)
Research Guide

ACKNOWLEDGEMENTS

I wish to express a deep sense of gratitude towards Dr. S.F. Patil, Reader in Physical Chemistry, University of Poona, for suggesting the problem and for his invaluable guidance during the course of the thesis work.

My sincere thanks are due to Dr. H.J. Arnikar, Professor Emeritus, for his valuable discussions and timely help in this study. His views on academic and non-academic matters has influenced me greatly.

I would like to thank Professor V.K. Phansalkar, the Head of the Department of Chemistry, University of Poona, for providing the facilities during the progress of the present work.

My grateful thanks are also due to Professor S.Y. Gambhir, Principal, Modern College, Pune-411 005 and Professor Dr. L.H. Gadgil, Vice-Principal and the Head of the Chemistry Department, Modern College, for their constant and cheerful encouragement. The kind cooperation of all the staff members in Chemistry Department of Modern College is gratefully acknowledged.

I am deeply obliged to Dr.(Miss) H.G. Adhyapak for her kind and patient help at various phases of this work.

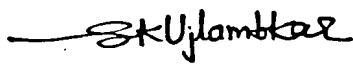
Thanks are due to my family members, my mother, father, Shashi, Sai, Nalini, Vidya, Mukund, Manasi and Dr. J.M. Athavale for their love, inspiration and kind cooperation.

I am indebted to all my friends : Shridhar P. Gejji, Dr. R.N. Bhave, P.R. Patil, Dr. D. Ravishanker, Dr.(Mrs.) Bhoite, Dr.(Miss) M.Y. Pandit, Micky Puri, Mrs. S.S. Joshi, Miss P. Bhatia, Miss Anita Agrawal and Miss Kavaljit Kaur for their good wishes.

I am very much thankful to Miss L.M. Pavangadkar for her excellent typing, Mr. B.B. Favar for tracing the figures, Mr. S.S. Sardesai for technical assistance and to all other technical staff for their timely help and cooperation.

Finally, financial assistance in the form of UOC Special Assistance Scholarship from Poona University is also deeply appreciated.

Department of Chemistry
University of Poona.


(S.K. Ujlambkar)

4th August, 1983.

C O N T E N T S

Page Nos.

CHAPTER 1 : INTRODUCTION

1.1	The Phenomenon of Diffusion	1
1.2	Fick's Laws of Diffusion	2
1.2.1	Fick's first law	2
1.2.2	Fick's second law	3
1.3	Types of Diffusion	5
1.3.1	Theory of electrolyte-diffusion	7
1.3.1.1	The electrophoretic effect	8
1.3.2	Theory of tracer-diffusion	15
1.3.2.1	The relaxation effect	15
1.4	Transition State Theory of Diffusion	17
1.5	Experimental Methods for Determining Diffusion Coefficient	20
1.5.1	Steady state methods	21
1.5.1.1	Clack's method	21
1.5.1.2	The porous diaphragm method	22
1.5.2	Non-steady state methods	24
1.5.2.1	Electrical conductivity method	25
1.5.2.2	Capillary tube method	23
1.6	Measurement of Changes in Concentration during Diffusion	31
1.7	Use of Gel Medium	32
1.8	Composition of Agar	34
1.9	Review of the Earlier Work	35
1.9.1	Electrolyte-diffusion	35
1.9.2	Tracer-diffusion	37
1.10	Scope of the Present Work	40

CHAPTER 2 : EXPERIMENTAL

2.1	Measurement of Diffusion Coefficient in Gel Medium	42
2.2	The Theory of Zone-diffusion	43
2.3	Experimental Details of the Zone-diffusion technique	47
2.3.1	Preparation of the diffusion column	47
2.3.2	Analysis of the diffusion column	49

CHAPTER 3 : DEPENDENCE OF DIFFUSION COEFFICIENT ON CONCENTRATION OF THE ELECTROLYTE

<u>Section A</u>	- Variation of the Tracer-diffusion Coefficient with Concentration of the Electrolyte	50
3.1A	Theoretical value of D^*	51
3.2A	Description of the Results	71
3.2.1A	Tracer-diffusion of $^{54}\text{Mn}^{2+}$ ions in manganese, magnesium, strontium and barium chlorides	71
3.2.2A	Tracer-diffusion of $^{54}\text{Mn}^{2+}$ ions in manganese, copper, nickel, cobalt and zinc sulphates	73
3.2.3A	Tracer-diffusion of $^{64}\text{Cu}^{2+}$ ions in copper, manganese, nickel and cobalt sulphates	73
3.2.4A	Tracer-diffusion of $^{65}\text{Zn}^{2+}$ ions in strontium, manganese and barium chlorides	74
3.3A	Discussion	74
3.3.1A	Relaxation effect	75
3.3.2A	Adsorption effect	76
3.3.3A	Obstruction effect	77
3.3.4A	water-gel interaction	77

3.3.5A	Ion-water and ion-ion interactions	78
3.3.5.1A	Structure of liquid water	79
3.3.5.2A	Structure of water near an ion	79
3.3.5.3A	Structure-breaking and structure-forming ions	82
3.3.5.4A	The model of Hertz <u>et al.</u>	83
3.4A	Interpretation of the Results	87
<u>Section B</u>	- Variation of Electrolyte-Diffusion Coefficient with Concentration of the Electrolyte	93
3.1B	Theoretical Value of D'	93
3.2B	Description of the Results	100
3.3B	Interpretation of the Results	100
<u>CHAPTER 4</u>	: EFFECT OF GEL CONCENTRATION AND TEMPERATURE ON THE DIFFUSION OF SOME LABELLED IONS AND ELECTROLYTES	
<u>Section A</u>	- Obstruction Effect	105
4.1A	Present work	106
4.2A	Results and Discussion	107
4.2.1A	Theoretical value of α	116
4.2.2A	Estimation of hydration of agar	118
<u>Section B</u>	- Temperature-dependence of Diffusion Coefficient	125
4.1B	Effect of Gel Concentration on the Activation Energy for the Process of Self- and Electrolyte-Diffusion	125
4.1.1B	Application of transition state theory of diffusion in gel medium	129
4.2B	Effect of Supporting Electrolytes on the Activation Energy in Tracer-Diffusion of Mn^{2+} and Zn^{2+} Ions	133
SUMMARY		138
REFERENCES		144



—● CHAPTER 1 ●—
• INTRODUCTION •

CHAPTER 1

INTRODUCTION

1.1 The Phenomenon of Diffusion

Diffusion is one of the irreversible phenomena whereby local differences in concentration in a system are reduced, till a system of homogeneous concentration results. This is due to activity of particles to disperse or intermingle by reason of their thermal energy. It is a spontaneous process which eliminates differences in concentration over different regions, if they existed initially.

Thomas Graham¹ was the first to study the process of diffusion in a systematic manner. He found that the mass of the substance that diffuses in the solution phase is largely dependent on the nature and concentration of the substance in solution. While Fick², assuming that the force responsible for diffusion flow in a binary mixture is the gradient of concentration, formulated the relationship now known as Fick's first and second laws of diffusion. These laws were adopted for different experimental conditions, and expressions relating the diffusion coefficient with various parameters involved

were proposed by different workers notably by Stokes, Eyring, Nernst, Hartley, Onsager and Fuoss.

1.2 Fick's Laws of Diffusion

1.2.1 Fick's first law

Diffusion in everyday practical applications is often a two or three dimensional process. However, most of the methods by which it is studied and measured involve a one-dimensional flow.

If the diffusion is restricted to a vertical column of uniform cross-section, then the flux of the matter J , defined as the amount of substance passing perpendicularly through a reference plane of unit area during unit time, is proportional to the concentration gradient $\partial C/\partial x$ at that level. Here C is the concentration of the diffusing substance and x is the distance, which is the co-ordinate chosen perpendicular to the reference plane. Hence,

$$J = -D \frac{\partial C}{\partial x} \quad \dots (1.1)$$

The proportionality factor D is the diffusion coefficient of the substance under consideration. The concentration gradient $\partial C/\partial x$ is the rate of increase of concentration with distance measured in the direction of flow. It is usual to take the direction of flow as the positive direction of the distance x .

The flux J is expressed in moles per cm^2 per second and the concentration in moles per cm^3 , then D has the dimensions cm^2/sec . The negative sign in equation (1.1) is introduced in order to make D a positive quantity, since $\partial C/\partial x$ is negative in virtue of our choice of sign for x , which increases as the concentration decreases. Fick's first law implies that D is a constant for a given medium, temperature and pressure, but this is not strictly true, as D is known to be concentration dependent. However, the equation (1.1) is of importance in the study of diffusion by steady state methods in which the concentration gradient $\partial C/\partial x$ does not change with time. It gives us a way to determine the flux through any cross-section, if we know the values of C throughout the system. It can serve as a basis for estimating how the system changes with time as a result of this flux.

1.2.2 Fick's second law

Most modern experimental techniques, however, are based on the observation of transient processes in which the concentration changes as a function of both time and distance. In such a situation, the phenomenon is better described by a second order partial differential equation, known as Fick's second law, wherein the dependent variable J is eliminated.

Let us consider a tube of uniform unit cross-section

intersected by two planes normal to the x-axis situated at x and $x + \delta x$ respectively (Fig. 1.1). Then the amount of the

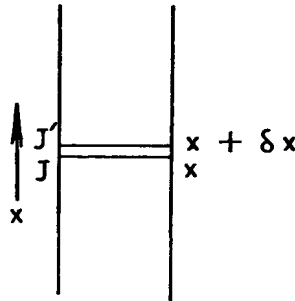


Fig.1.1- Diffusion through the column of uniform cross-section.

substance entering the volume-element between these planes through the plane at x and leaving through the plane at $x + \delta x$ in a time interval δt is given by

$$J \delta t = - \left(D \frac{\partial C}{\partial x} \right)_x \cdot \delta t$$

and

$$J' \delta t = - \left(D \frac{\partial C}{\partial x} \right)_{(x + \delta x)} \cdot \delta t \quad \text{respectively.}$$

The difference between $(D \cdot \partial C / \partial x)$ at the plane $x + \delta x$ and $(D \cdot \partial C / \partial x)$ at the plane x may be expressed as

$$(J - J') \delta t = D \left[\left(\frac{\partial C}{\partial x} \right)_{x + \delta x} - \left(\frac{\partial C}{\partial x} \right)_x \right] \cdot \delta t$$

Using the Taylor's theorem, this expression reduces to

$$(J - J') \delta t = \frac{\partial}{\partial x} \left(D \cdot \frac{\partial C}{\partial x} \right) \cdot \delta x \cdot \delta t$$

This accumulation, since it occurs in an element of volume δx , gives rise to a concentration increase δC which is given by

$$\delta C = \frac{\partial}{\partial x} D \frac{\partial C}{\partial x} \cdot \delta t$$

and in the limit $\delta x \rightarrow 0$, one obtains the relation

$$\frac{\partial C}{\partial t} = D \frac{\partial^2 C}{\partial x^2} \quad \dots (1.2)$$

Equation (1.2) is called Fick's second law of diffusion derived on the assumption that D is constant.

If diffusion occurs in an arbitrary direction, we have to add at the right hand side of the equation (1.2), two corresponding expressions for the y and z co-ordinates giving

$$\frac{\partial C}{\partial t} = D(\partial^2 C / \partial x^2 + \partial^2 C / \partial y^2 + \partial^2 C / \partial z^2) = D \nabla^2 C$$

where ∇^2 is Laplace's operator.

Berthollet's³, Fourier's⁴ and Ohm's analogy between heat conduction and diffusion, was rediscovered by Fick, and can be immediately adapted to diffusion problems.

1.3 Types of Diffusion

The diffusion of an electrolyte in any medium may be studied in two different ways. First is electrolyte-diffusion, in which a single salt diffuses in the solvent medium and both the positive and negative ions move with the same velocity in

order to maintain electrical neutrality at the macroscopic level. Under this condition, the ionic atmosphere suffers no deformation and the relaxation effect vanishes. Further, the electrolyte moves in one direction and the solvent by replacing it moves in the opposite direction. Thus, the electrophoretic effect becomes an important factor in single electrolyte diffusion and its computation becomes necessary. Finally, since the activity coefficient of the electrolyte is not constant throughout the diffusing system, it appears as a thermodynamic term $(1 + C \frac{\partial \ln \gamma_{\pm}}{\partial C})$ in the theoretical equation.

Alternatively, the diffusion may also be studied in a solution containing three or more different ions. Since more than two ions are present in the solution, all the ions need not move with the same velocity. While a general treatment of this case is very complicated, a simple limiting law has been derived by Onsager⁵ for the diffusion coefficient of an ion at very low concentration compared to that of the other ions present. The concentration of the latter remains essentially constant throughout the solution. The activity coefficient of the ion in question is then constant, as the ionic strength of the solution containing it is kept constant and the thermodynamic term which affects the electrolyte-diffusion, is simply unity. Since, however, the migrating ion has a velocity relative to the other ions, its atmosphere is asymmetric and the time of

relaxation is not zero and its computation provides the necessary and sufficient basis for the calculation of the limiting law for the variation of the diffusion coefficient of the trace-ion with the total ionic concentration. The concentration dependent electrophoretic effect is negligible here. This type of diffusion is termed as tracer-diffusion and when the trace-ion is isotopic with one of the solution components, the term self-diffusion is often used.

1.3.1 Theory of electrolyte-diffusion

The history of the theory of electrolyte-diffusion begins with the work of Long⁶ in 1830 when he formulated a relation between the diffusion coefficient of an electrolyte and the mobilities of its constituent ions.

Eight years after Long's work, the same relationship was developed quantitatively by Nernst⁷, who considered the driving force of diffusion to be the osmotic pressure gradient. This view was supported by Shreiner⁸ while developing the theory. But it was Gibbs⁹, who first suggested that it is the gradient of chemical potential in a solution which is the virtual force causing diffusion. This idea was later elaborated by others : notably Guggenheim¹⁰, Hartley¹¹, Onsager and Fuoss¹² to describe the manner in which the diffusivity of an electrolyte varies with concentration. The result of this approach is the so-called

Hernst-Hartley relation in which they have considered that each ion is moving under the influence of two forces; (1) The gradient of chemical potential for that ionic species and (2) The gradient of electrical potential produced by the motion of the oppositely charged ions. The corresponding expression is as follows :

$$D' = \frac{RT}{F^2} \cdot \frac{(\nu_1 + \nu_2) \lambda_1^\circ \cdot \lambda_2^\circ}{\nu_1 |Z_1| (\lambda_1^\circ + \lambda_2^\circ)} \left(1 + C \frac{\partial \ln \gamma_{\pm}}{\partial C} \right) \quad \dots (1.3)$$

where ν_1 and ν_2 are the number of cations and anions with algebraic valency Z_1 , Z_2 and limiting ionic conductances λ_1° and λ_2° respectively.

Onsager and Fuoss¹² in 1932 had shown that Nernst and Hartley failed to take into account the electrophoretic effect which is prominent in the electrolyte diffusion. The following discussion deals with the computation of this effect.

1.3.1.1 The electrophoretic effect

The electrophoretic effect arises due to the tendency of a moving ion to drag a part of the solvent along with it due to the viscosity of the medium. The distribution function i.e. the probability of finding a particular ion in a given position relative to another given ion, is the chief controlling parameter in this effect.

All the ions are surrounded by solvent molecules which are, in turn, in contact with others which are under the influence of the external fields of neighbouring ions. As any ion moves, it tends to drag other ions along with it, the force being transmitted through the solvent molecules. Neighbouring ions, therefore, have to move not in a stationary medium, but with or against the stream, as the case may be. The effect will be clearly concentration dependent falling to zero at infinite dilution and its computation will require the use of the distribution function, since it involves the distance between the ions. The following treatment of the electrophoretic effect was given by Onsager and Fuoss,¹² based on Debye-Huckel¹³ theory.

Around the selected ion, the atmosphere may be considered to be arranged as shown in Fig. 1.2, in spherical shells of radius r and thickness dr , in each of which the force per unit volume F is constant.

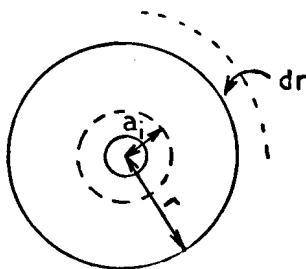


Fig.1.2 - The electrophoretic effect.

Let us consider the simplest case viz. that of two ions in a neutral solvent. If diffusion velocity alone is considered, the net force on cations, anions and the solvent for the whole volume of solution must be zero. If the bulk concentrations in moles per unit volume for cation, anion and neutral solvent are respectively C_+ , C_- , C_1 and the forces per mole being X_+ , X_- , X_1 , then it follows that

$$C_+X_+ + C_-X_- + C_1X_1 = 0 \dots \quad \dots (1.4)$$

Within the ion atmosphere surrounding any ion, the net force per unit volume is not zero, because the local ion concentrations C'_+ , C'_- , differ from the bulk concentrations. This force per unit volume is the same at all points on any sphere surrounding the central ion, and the net force on a spherical shell of radius r and thickness dr is therefore,

$$F = (C'_+X_+ + C'_-X_- + C_1X_1)4\pi r^2dr \quad \dots (1.5)$$

Neglecting any variation in C_1 from its bulk value (which is true in dilute solutions) we can eliminate C_1X_1 by using equation (1.4). Hence,

$$F = [(C'_+ - C_+)X_+ + (C'_- - C_-)X_-]4\pi r^2dr \quad \dots (1.6)$$

and this force is assumed to cause the shell and all points within it to move with a velocity V_1 which is given by Stokes' law

$$F = 6\pi\eta r v_1$$

Therefore,

$$V_1 = \frac{2}{3\eta} [(C_+^i - C_+)X_+ + (C_-^i - C_-)X_-] r \cdot dr \quad \dots (1.7)$$

The motion of this shell provides a velocity increment for the central ion, and the total increment ΔV_1 can be obtained by integrating the velocity of each shell from the distance $r = a$ (distance of closest approach to the central ion) to infinity. This gives

$$\Delta V_1 = \frac{2}{3} \int_{r=a}^{r=\infty} [(C_+^i - C_+)X_+ + (C_-^i - C_-)X_-] r \cdot dr \quad \dots (1.8)$$

Using the values C_+^i and C_-^i as given by Boltzmann distribution law and expressing the concentrations C_+ and C_- in terms of quantity ka ($k =$ reciprocal of ion atmosphere radius), we get the expression for ΔV_+ , by solving the exponentials involved in it, as follows :

$$\Delta V_+ = \sum_{j=1}^{\infty} A_j \left(\frac{Z_+}{a}\right)^j \frac{Z_+^{(j-1)} X_+ - Z_-^{(j-1)} X_-}{Z_+^j - Z_-^j} \quad \dots (1.9)$$

where

$$A_j = \frac{(1)^j}{6\pi\eta j!} \left(\frac{e^{-2}}{kT}\right)^{j-1} \phi_j(ka)$$

where ϕ_j is the exponential integral function.

In diffusion, the forces X_+ and X_- are the combination

of a virtual force produced by the gradient of chemical potential and electrical force due to the diffusion potential which results from the electrical attraction of the faster moving ions for the slower moving ionic species, these forces can be conveniently evaluated in terms of the velocity of the ions and their absolute mobilities and the expressions for ΔV for cation and anion come out respectively to be

$$\frac{\Delta V_+}{V} = \frac{F^2}{N} \sum_j \lambda_j \frac{\frac{z_+^{2j}}{\lambda_+} + \frac{z_+^j \cdot z_-^j}{\lambda_-}}{a^j(z_+ - z_-)} = \delta_+$$

and

$$\frac{\Delta V_-}{V} = \frac{F^2}{N} \sum_j \lambda_j \frac{\frac{z_+^j \cdot z_-^j}{\lambda_+} + \frac{z_-^{2j}}{\lambda_-}}{a^j(z_+ - z_-)} = \delta_- \quad \dots (1.10)$$

These velocities are additional to the velocity produced by the diffusion force. Thus the electrophoretic effect enhances the mobility of the cation by the factor $(1 + \delta_+)$ and that for the anion by $(1 + \delta_-)$. By substituting the values for the increment, the Nernst-Hartley equation takes the form

$$D' = \left(1 + C \cdot \frac{\partial \ln \gamma_{\pm}}{\partial C}\right) (D^0 + \sum_j \Delta_j) \quad \dots (1.11)$$

Where D^0 is the Nernst limiting value of D' and the Δ_j term represents the electrophoretic corrections

$$\Delta j = kT \cdot A_j \frac{(z_+^j t_+^0 + z_-^j t_-^0)^2}{a^j |z_+ \cdot z_-|} \quad \dots (1.12)$$

Taking into consideration this electrophoretic effect Onsager and Fuoss arrived at a more refined theory of electrolyte-diffusion. The improvement introduced by them is expressed as

$$D' = 1000 RT (\gamma_+ + \gamma_-) \left(\frac{\bar{M}}{C} \right) \left(1 + C \cdot \frac{\partial \ln \gamma_{\pm}}{\partial C} \right) \quad \dots (1.13)$$

where $\frac{\bar{M}}{C}$ is the electrophoretic term and $(1 + C \cdot \frac{\partial \ln \gamma_{\pm}}{\partial C})$ is the thermodynamic term. They are given by the following expressions :

$$\frac{\bar{M}}{C} = 1.074 \times 10^{-20} \cdot \frac{\lambda_+^0 \cdot \lambda_-^0}{|z_+| |z_-| \Lambda^0} + \frac{\Delta n^I}{C} + \frac{\Delta n^{II}}{C} \quad \dots (1.14)$$

where

$$\frac{\Delta n^I}{C} = \frac{-(|z_-| \lambda_+^0 - |z_+| \lambda_-^0)^2}{\Lambda^2 |z_+| \cdot |z_-| (\gamma_+ + \gamma_-)} \cdot \frac{3.11 \times 10^{-19}}{\eta_0 \sqrt{\epsilon T}} \cdot \frac{\sqrt{T}}{1 + \Lambda' \sqrt{C}} \quad \dots (1.15)$$

$$\frac{\Delta n^{II}}{C} = \frac{(z_-^2 \lambda_+^0 + z_+^2 \lambda_-^0)^2}{\Lambda^2} \cdot \frac{9.18 \times 10^{-13}}{\eta_0 (\epsilon T)^2} \cdot C \cdot \phi \Lambda' \sqrt{C} \quad \dots (1.16)$$

and

$$\left(1 + C \cdot \frac{\partial \ln \gamma_{\pm}}{\partial C} \right) = 1 - \frac{1.1514 \cdot S_f \sqrt{C}}{(1 + \Lambda' \sqrt{C})^2} + 4.606 \cdot B \cdot C \quad \dots (1.17)$$

where R is the gas constant expressed in J mole⁻¹ K⁻¹, ϵ and η_0 are the dielectric constant and viscosity of the medium respectively, γ_+ and γ_- are the number of cations and anions

for the given electrolyte with charges Z_+ and Z_- and their limiting equivalent conductances λ_+^0 and λ_-^0 respectively. $\phi A'\sqrt{C}$ is the exponential integral function, S_f is the limiting slope of the Debye-Huckel theory, B is the salting constant and A' is another constant depending upon the nature of the electrolyte.

$\frac{\Delta \eta^+}{C}$ and $\frac{\Delta \eta^-}{C}$ terms are first and second order electrophoretic terms and as it can be seen from equations (1.15) and (1.16) they are functions of the temperature, ionic strength of the solution, viscosity and dielectric constant of solvent, the radii and valencies of the ions and their limiting electrolyte conductances. The first order effect results because the anions in the neighbourhood of a given anion are partly replaced by cation and vice-versa. When one species of ions is more mobile than the other, then the sluggish ions will move counter-currently, while the mobile ions will be aided by the motion of environment. The second order term of electrophoretic effect depends simply on an overall reduction of the mean distances between the ions in the sense that the distances between ions of opposite sign are reduced more than the distances between ions of the same sign are increased. This effect always decreases the resistance to diffusion.

1.3.2 Theory of tracer-diffusion

The important factor in the discussion of tracer-diffusion theory is the computation of relaxation effect which gives a quantitative theoretical relationship between diffusion coefficient and concentration of the ion.

1.3.2.1 The relaxation effect

In the case of an electrolyte solution in equilibrium, the ionic atmosphere is on a time average distributed with a spherical symmetry. It, therefore, exerts no resultant force on the central ion when the latter moves, whether under an external force as in conduction, or purely as Brownian motion as in self-diffusion. The central ion moves to an off-centre position and the ion-atmospheric symmetry is destroyed as shown in Fig. 1.3. In this act, the ion experiences a restoring force which, however, rapidly dies out as the fragments of the old atmosphere disintegrate and a new atmosphere builds around the ion at its new site. The time lag for this arrangement is referred to as the relaxation time, and the mean retarding force on the forward motion of the ion due to the momentary asymmetry of the ion-atmosphere is the relaxation effect. In other words, the relaxation field opposes the force causing conduction or tracer diffusion.

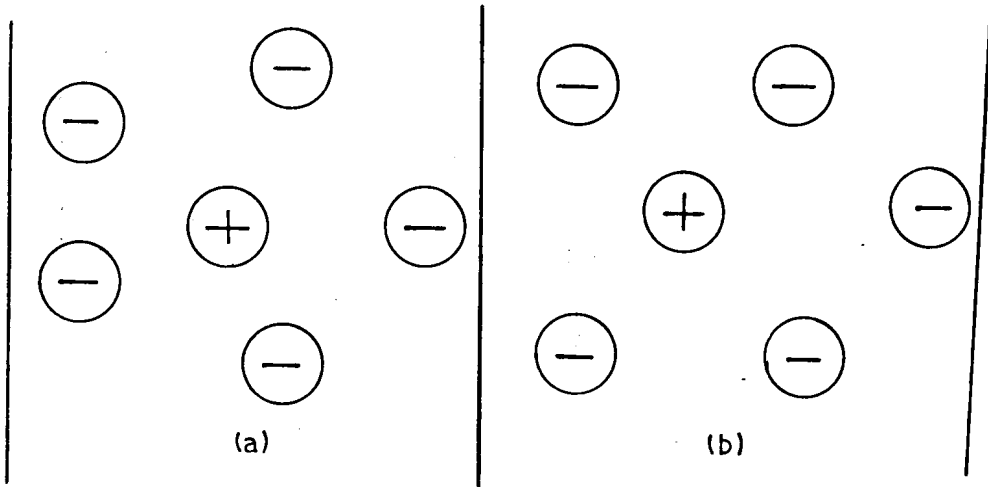


Fig.1.3-(a) Symmetric ionic atmosphere surrounding ion at rest

(b) Asymmetric ionic atmosphere surrounding moving ion

Taking into consideration the relaxation effect, Onsager⁵ had derived the following expression for the tracer-diffusion coefficient

$$D_j^* = D_j^{*0} \left[1 - \frac{k Z_j e^2}{3 \epsilon k T} (1 - \sqrt{d(w_j)}) \right] \quad \dots (1.18)$$

The term in the square brackets corresponds to the relaxation effect which lowers the mobility of the ion. D_j^{*0} represents the Nernst limiting value, Z_j is the valency of the ions and the other terms have their usual significance.

For the practical application of equation (1.18)

Costing and Earned¹⁴ obtained the following expression for the

variation of tracer diffusion coefficient of an ion with the concentration of the electrolyte :

$$D_j^* = \frac{RT \lambda_j^0}{|Z_j| F^2} - \frac{\lambda_j^0 |Z_j| F}{3\pi \epsilon} \cdot 2.694 \times 10^{16} \times \sqrt{\frac{4\pi}{\epsilon RT}} \cdot [(1 - \sqrt{d(\omega)})] \\ \times \sqrt{\sum_i c_i Z_i^2} \quad \dots (1.19)$$

1.4 Transition State Theory of Diffusion

A far more general kinetic theory of diffusion has been developed by Eyring and his collaborators¹⁵⁻¹⁷ by applying the theory of rate processes to the problem. This was published in a series of papers which have been summarized in a major review¹⁵ and in the well-known book 'The Theory of Rate Processes' by Glasstone, Laidler and Eyring¹⁶. Most, if not all, processes which occur at a measurable rate, can be regarded as proceeding through an intermediate transition state.

Eyring applied the theory of absolute reaction rate to diffusion in condensed phase by considering each jump to be an activated process of a definite frequency and length related to the size of the solvent and solute particles. Suppose the distance between two successive equilibrium positions is λ , so that this is the distance through which a solute particle is transported in each jump, the change in the standard free energy with distance can then be represented by the curve in Fig. 1.4.

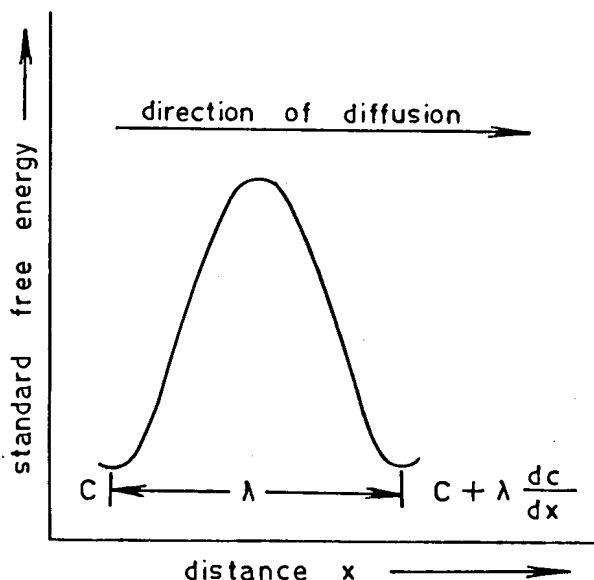


Fig.1.4 - Free energy barrier for diffusion in an ideal solution.

If we assume that the standard free energy of the solute particle in any of the equilibrium positions is same, it follows that there exists a symmetrical potential barrier between the two states or between the two equilibrium positions. Hence, the energy of activation needed for forward and backward directions is same and therefore the specific rate constant K' is same for flow in either direction.

Let C and $C + \lambda \frac{dC}{dx}$ be the molar concentrations in the initial and final states of diffusion, where $C > C + \lambda \frac{dC}{dx}$ i.e. $\frac{dC}{dx}$ is negative. Then the number of molecules moving in

the forward direction through 1 cm^2 is given by

$$K_f = N C \lambda K' \text{ molecules cm}^{-2} \text{ s}^{-1} \quad \dots (1.20)$$

where N is the Avogadro number and K' is the specific reaction rate for diffusion (i.e. number of times a molecule moves from one position to the next per second). Similarly, for the rate of movement in the backward direction, we have

$$K_b = N(C + \lambda \frac{dC}{dx}) \lambda K' \text{ molecules cm}^{-2} \text{ s}^{-1} \quad \dots (1.21)$$

The net flow in the forward direction is therefore represented by

$$K = -N \lambda^2 K' \frac{dC}{dx} \text{ molecules cm}^{-2} \text{ s}^{-1} \quad \dots (1.22)$$

Taking into consideration Fick's first law, the resultant flow per cm^2 per sec can be expressed in terms of the diffusion coefficient as

$$K = -D \cdot N \cdot \frac{dC}{dx} \text{ molecules cm}^{-2} \text{ s}^{-1} \quad \dots (1.23)$$

comparing equations (1.22) and (1.23)

$$D \cdot N \cdot \frac{dC}{dx} = N \cdot \lambda^2 \cdot K' \cdot \frac{dC}{dx}$$

$$\therefore D = \lambda^2 K' \quad \dots (1.24)$$

This is valid only for dilute solutions where the free energy may be considered to be independent of the concentration changes.

1.5 Experimental Methods for Determining Diffusion Coefficient

Essentially the determination of diffusion coefficient consists in measuring sets of simultaneous values of time, distance and concentration (or concentration gradient). These measured values are then fitted to a solution of Fick's law, describing the phenomenology of the experiment, in order to derive optimum estimates of the constants appearing in the theoretical equation. These constants are known functions of D and of various geometric and physical parameters characteristic of the experiment, therefore, the diffusivity follows directly.

The accurate measurement of diffusion coefficient is one of the more difficult tasks facing the experimentalist. Small rise in temperature or slight mechanical vibrations transmitted to the diffusion cell, can cause much more rapid mixing of the diffusing substances than the pure diffusion process itself. It is not surprising that a large number of methods for studying the diffusion phenomenon have been suggested, most of which soon got dropped out of use.

Methods of measuring D can be classified in several ways, one of the most convenient being that based on the nature of diffusion process occurring.

1.5.1 Steady state methods

In these, the diffusion is allowed to occur within a column of solution in such a way that a steady (time-invariant) state is set up within the column. Material is supplied to the bottom and removed from the top and the concentration at each point within the column remains constant and independent of time. The important methods under this category are :

(1) Clack's method and (2) The porous diaphragm method.

1.5.1.1 Clack's method

In this method¹⁸, the concentration of the lower end of a column was maintained at saturation by means of a reservoir of solid salt, while at the other end, the concentration was maintained effectively zero by means of a slow flow of water. The flux was determined analytically and the concentration gradient was measured at any desired level by an optical determination of the refractive index gradient. The value of diffusion coefficient for different concentrations was calculated by integrating the concentration gradient. Thus, a single successful run provided values of D at all concentrations upto saturation. In this respect, the method is advantageous. However, the experimental difficulties of establishing and maintaining the steady state were very great, chief among these were the thermally and mechanically induced convection currents.

1.5.1.2 The porous diaphragm method

This method was originally introduced by Northrop and Anson¹⁹ and further developed by a number of workers²⁰⁻²⁴, particularly by Gordon²⁵ and Stokes²⁶.

The diaphragm cell consists of two compartments separated by a thin porous disk, usually made of sintered glass (Fig. 1.5). When the cell is positioned vertically and the

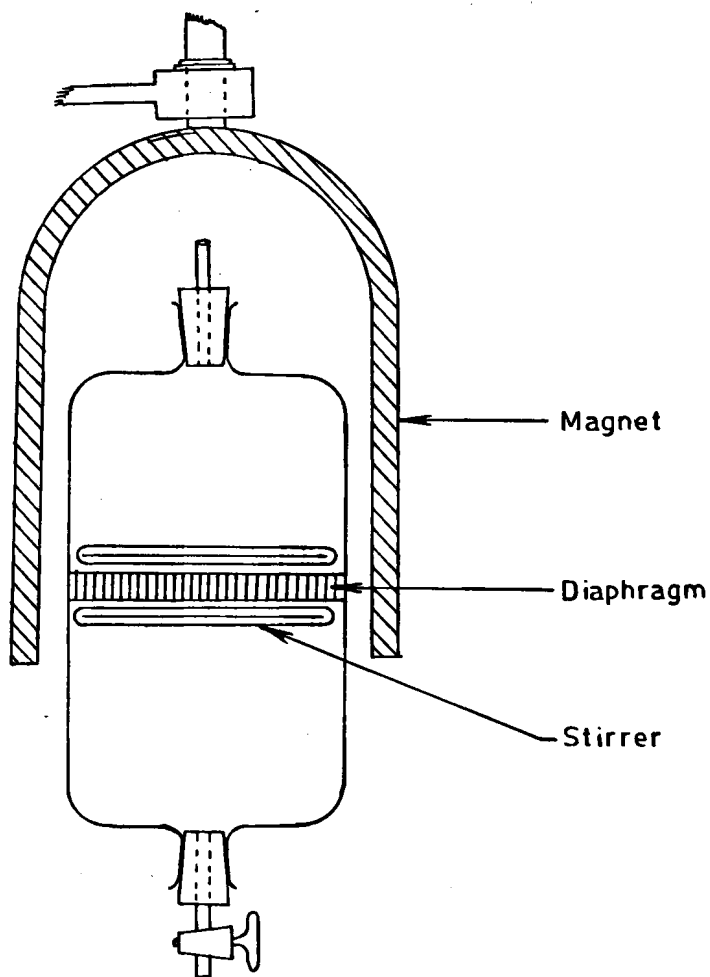


Fig. 1.5 - Magnetically stirred diaphragm cell.

compartments are filled with solutions of differing concentration (the denser liquid on the bottom), diffusion will be confined to the interior of the porous diaphragm provided that adequate stirring eliminates the formation of stationary layers on its surfaces. If the volumes of the upper and lower compartments are large so that the concentrations in the compartments do not change appreciably during the experiment, the flux within the diaphragm is independent of time and position. Therefore, it is fairly accurate assumption that the flux is in a steady state. The solution in the compartments are analysed at a known time, and diffusion coefficient is calculated by the equation

$$\bar{D} = \frac{1}{C_m' - C_m''} \int_{C_m'}^{C_m''} D \cdot dC \quad \dots (1.25)$$

where C_m' and C_m'' are mean of the concentrations after and before diffusion in the two compartments and

$$\bar{D} = \frac{1}{\beta t} \cdot \ln \frac{C_1 - C_2}{C_3 - C_4}$$

C_1 and C_3 are the concentrations in the lower cell at time $t = 0$ and $t = t$ respectively and C_2 and C_4 are the concentrations in the upper cell at time $t = 0$ and $t = t$, respectively. β is the cell constant given by

$$\beta = \frac{A}{l} \left(\frac{1}{V_1} + \frac{1}{V_2} \right)$$

where A is the total effective cross-section of the diaphragm

pores, l is their effective average length along the diffusion path and V_1 and V_2 are the volumes of the lower and upper compartments respectively.

The advantage of the diaphragm method is in the experimental simplicity. The precision of the method is about 0.2 - 0.3%. The disadvantage is that the accuracy (as distinguished from the precision) hinges entirely on the cell calibration and that extraneous phenomena may occur during the diffusion process which cannot be calibrated. For example, electrical double layers or adsorption effects may develop within the diaphragm which has a tremendous surface area in its pores. Such effects become particularly serious for dilute solutions. Though the method appears to be reliable in the higher concentration ranges, it cannot be recommended for use at concentrations less than 0.05 M.

1.5.2 Non-steady state methods

In non-steady state methods, all parameters of the diffusion process change both with the position and time. It is necessary, therefore, to use equations obtained by integration of Fick's second law with the boundary conditions appropriate to the arrangement of the experiment. A suitable form of the function $D(x, t)$ should be assumed. Usually, however, the diffusion coefficient is assumed constant and the resulting

integrated equations are used only for small concentration differences for which the change of the diffusion coefficient may reasonably be neglected. We describe below some of these methods in common use.

1.5.2.1 Electrical conductivity method

This technique is based on the fact that the electrical conductivity of dilute electrolytes varies linearly with change in concentration, provided this change is small. Harned and French²⁷ have used this principle to measure diffusivity in very dilute solutions where the sensitivity of optical methods become poor.

The method is applicable under condition of restricted diffusion taking place in a sheared boundary cell, shown in Fig. 1.6. The diffusion channels T and B are rectangular and have the same length a and same cross-section. At a given distance measured from the top and bottom of both channels, two pairs of electrodes are installed on the opposing walls at distances $a/6$ and $5a/6$, the electrodes are made of copper faced with platinum foil.

The top channel T is filled with the pure solvent, and the bottom channel B with the more concentrated solution, the two channels are initially positioned so that the two liquid

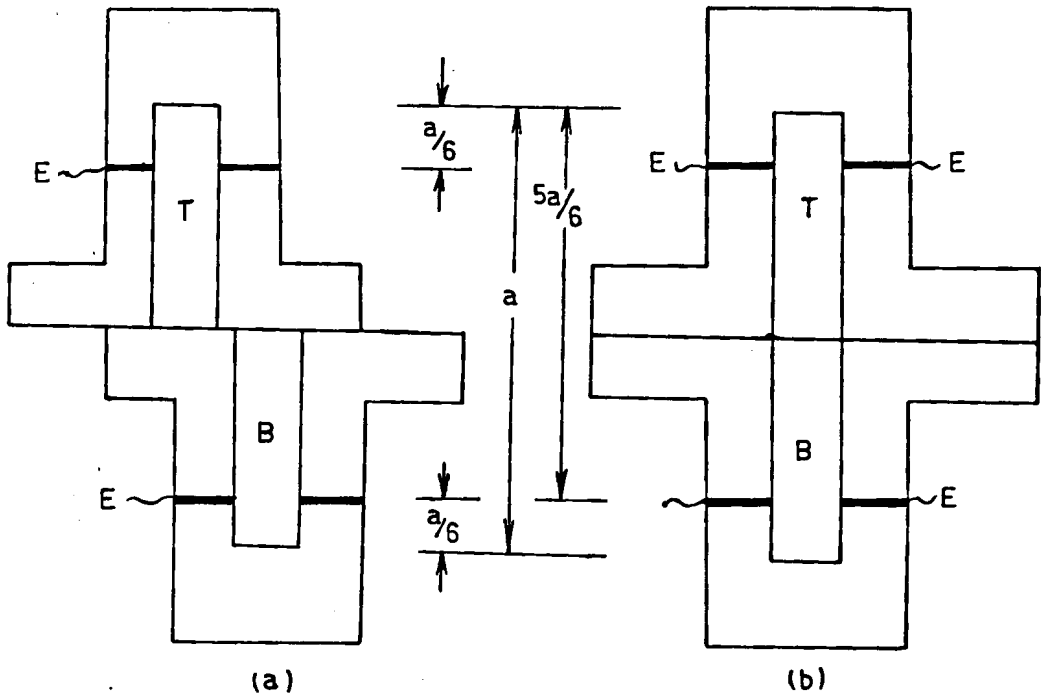


Fig.1.6- The Harned - French conductance cell.

columns are not in contact (Fig. 1.6a). Then by sliding the upper part of the cell in position with the lower part (Fig. 1.6b), a sharp boundary is formed and the diffusion process begins. The concentration changes are measured by following the conductivity at the two electrode pairs.

Since both ends are closed, $\frac{\partial C}{\partial x} = 0$ at $x = 0$ and $x = a$.

Under these boundary conditions, the appropriate Fourier-series solution of Fick's second law for the concentration C at a height x is

$$C = C_0 + \sum_{n=1}^{n=C_0} B_n \exp(-n^2 \pi^2 Dt/a^2) \cdot \cos n\pi x/a \quad \dots (1.27)$$

where C_0 and B_n are constants. Hence this difference in concentration between the planes $x = a/6$ and $x = 5a/6$ is given by the following expression

$$C_{a/6} - C_{5a/6} = \sum_{n=1}^{n=C_0} B_n \exp(-n^2 \pi^2 Dt/a^2) \times \left[\cos \frac{n\pi}{6} - \cos \frac{5n\pi}{6} \right] \quad \dots (1.28)$$

for even values of n , $\cos \frac{5n\pi}{6} = \cos \frac{n\pi}{6}$ and for odd n , $\cos \frac{5n\pi}{6} = -\cos \frac{n\pi}{6}$ so that all the terms for even n vanish (since the term in square brackets is zero) and for odd n values the square brackets becomes $2 \cdot \cos \cdot n \cdot \pi/6$ which is equal to $\sqrt{3}$ for $n = 1$, 0 for $n = 3$, $-\sqrt{3}$ for $n = 5$ and 7 etc.

Equation (1.28) takes the following form :

$$C_{a/6} - C_{5a/6} = B_1' \exp(-\pi^2 Dt/a^2) + B_5' \exp(-25 \cdot \pi^2 \cdot Dt/a^2) + \dots$$

where $B_1' = B_1 \sqrt{3}$... etc. This expression exceeds the second term by the factor $\exp(24 \pi^2 \cdot Dt/a^2)$; and the series converges very rapidly even for small values of Dt/a^2 and after a few days of diffusion only the first term need be considered at all. This rapid convergence is a result of the ingenious choice of the

heights $a/6$ and $5a/6$ for the electrode pairs, which makes the term for $n = 3$ vanish at all times. The coefficient B_1' need not be determined, for by logarithmic differentiation, one obtains

$$\frac{d}{dt} \cdot \ln[C_{a/6} - C_{5a/6}] = - \frac{\pi^2 D}{a^2}$$

Thus, if we plot $\ln [C_{a/6} - C_{5a/6}]$ against time t , a straight line results the slope of which is $-\frac{\pi^2 D}{a^2}$. The value of diffusion coefficient is thus readily obtained.

The method is applicable to even very dilute solutions and the value of differential diffusion coefficient is directly obtained at the average concentrations of the solution in the cell. This method is best adaptable for use at low concentrations. On the other hand, it demands great care and elaborate precautions to avoid trouble from vibration and thermal convection due to the long duration of the runs.

Modification in the above method, was proposed by Arnika²⁸, based on measuring the activity of a labelled solution at $a/6$ and $5a/6$ levels.

1.5.2.2 Capillary tube method

A more widely used method in the study of tracer-diffusion is the capillary tube method developed by Anderson and

Saddington²⁹ in 1949. In this method, the labelled ions are placed in a narrow thick-walled capillary of uniform cross-section and known length. The capillary is then lowered vertically into a large volume of the inactive solution and the solution is gently stirred (see Fig. 1.7) so that concentration

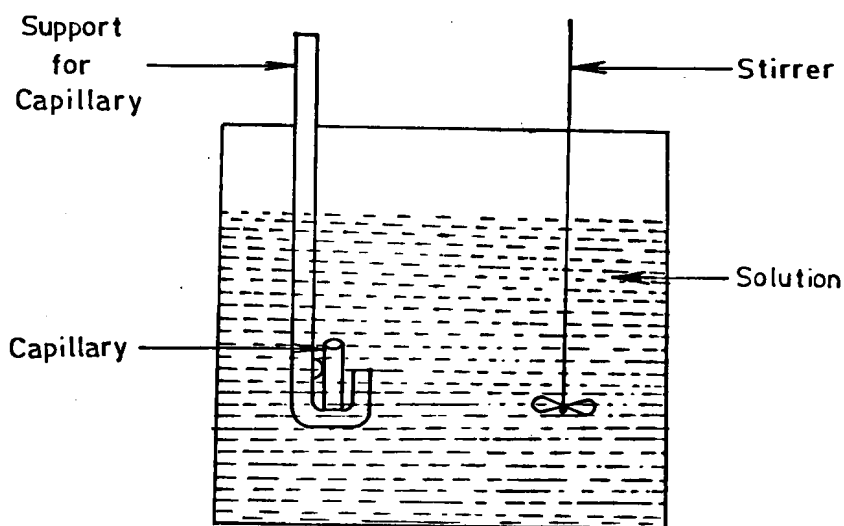


Fig.1.7 - Capillary tube method

of the labelled form remains effectively zero at the mouth of capillary throughout the experiment. Diffusion of the labelled species from the capillary into the bulk of the solution takes place and at the end of the experiment, the amount remaining in the capillary is measured. The initial concentration of the

labelled species in the external solution³⁰ is assumed to be zero.

The boundary conditions for a tube closed at $x = 0$ and open at $x = a$ are :

$$\text{At } t = 0 \quad C = C_0 \text{ for } 0 < x < a$$

$$C = 0 \text{ for } x > a$$

$$\text{At } t > 0 \quad C = 0 \text{ at } x = a$$

$$\text{and } \frac{\partial C}{\partial x} = 0 \text{ at } x = 0$$

Under these conditions, the solution of the diffusion equation for this one-dimensional case takes the following form :

$$\frac{C_{av}}{C_0} = \frac{8}{\pi^2} \sum_{n=0}^{\infty} \frac{(-1)^n}{(2n+1)^2} \exp \left[-(2n+1)^2 \frac{\pi^2 D^* t}{4a^2} \right] \quad \dots (1.29)$$

where C_0 is the initial concentration in the capillary tube, C_{av} is the average concentration after the diffusion, D^* is the diffusion coefficient, t is the time of diffusion and a is the length of the capillary.

When $\frac{D^* t}{a^2}$ is sufficiently great (> 0.2 , cf. Wang³¹) this series converges so rapidly that only the first term needs to be considered, and the equation (1.29) simplifies to

$$\frac{D^* t}{a^2} = \frac{4}{\pi^2} \ln \left(\frac{8}{\pi^2} \times \frac{C_0}{C_{av}} \right) \quad \dots (1.30)$$

If the logarithm of the ratio C_{av}/C_0 is plotted against the

time t , at which the observations are made, the tracer-diffusion coefficient D^* can be calculated from the slope of the line³².

There has been much discussion of the best experimental conditions, partly because of the discrepancies which have been observed between the results of different workers on the tracer-diffusion of ions in aqueous solution. The process of immersing the capillaries in the large bulk of solution might be expected to produce mechanical convection, but the loss of labelled material from the capillaries immediately on immersion has been shown to be small^{33,34} and can be neglected. The problem of stirring the bulk solution outside the capillary is more important. If the solution is stirred at a gradually increasing speed, at a certain stage turbulent flow across the end of the capillary will draw some labelled material out of it, the effective length being $(a - \delta a)$. On the other hand, if the solution is unstirred, the effective length of the capillary will be slightly greater than a , namely $(a + \delta a)$. Some workers have preferred not to stir the solution outside the capillaries at all^{29,34-37}; others have done so³³⁻⁴².

1.6 Measurement of Changes in Concentration during Diffusion

Depending upon any set of the initial and boundary conditions of the experiment, the final concentration distribution after a time t , can be determined by any

convenient method. These include analytical, electrical, optical and tracer methods.

All these methods have their own limitations, for example, electrical methods are restricted to systems whose components carry electrical charges, optical and chemical methods are susceptible to slight disturbances in the system. When self-diffusion is to be studied, none of the above methods, except tracer technique in which the diffusing ion is labelled, can be used as there is no concentration change and the diffusant is chemically identical with the medium. The technique of using labelled systems, specially with radioactive isotopes is simpler than any other technique and even under ordinary conditions, it provides the possibility of analyzing concentrations as low as 10^{-10} to 10^{-14} M.

1.7 Use of Gel Medium

The experimental methods for the determination of D described in Section 1.5 reveal that there are several difficulties in obtaining accurate data on diffusion. The numerical difficulties inherent in the computation of the diffusion coefficients from rate measurements, the elimination of turbulent flow, the very accurate control of temperature and the analytical accuracy required are all contributing obstacles to the attainment of high accuracy. The above mentioned errors

in the study of diffusion are reduced to a minimum by immobilizing the system in gel medium⁴³, as has been pointed out by several workers⁴⁴⁻⁵⁰. The gel structure is capable of holding almost all water in a practically immobilized and semi-rigid state, eliminating the direct streaming and convectional flow of the solution. Thus, it provides an ideal medium for the study of diffusion. As the ion-atmosphere does not change in gel medium, Onsager-Fuoss and Onsager's theory of diffusion can also be applied in gel medium. Further, with the diffusion taking place in gel medium, it is possible to get a sharper boundary surface, the danger of mixing is negligible and other outside disturbances are also minimized. The layers may be separated by slicing the gel at the desired length at the conclusion of the experiment. However, the use of gel medium for the study of diffusion has some demerits. Adsorption of the diffusing species by the gel structure and impurities in the gel introduce complications in its use. The rate of diffusion also gets affected by the presence of macromolecules of the gel which causes a mechanical obstruction in the diffusion path, besides involving effects due to high viscosity.

Of the different gel media, that of agar is found to be the best suited for its ready availability, ease of preparation and above all because of its property of easy extrusion from the diffusion tube.

1.8 Composition of Agar

Agar, the dried mucilaginous water extract of certain seaweeds, is known to be a heteropolysaccharide. According to Araki⁵¹, agar is composed of the two polysaccharides, agarose and agarpectin, with a constitution similar to that produced in starch by amylose and amylopectin. Molecules of agarose, the chief component of agar, are composed of a neutral chain of β -D-galactopyranose residues linked through 1,3-positions and 3,6-anhydro- α -L-galactopyranose residues connected through 1,4-positions and repeated alternately. The empirical composition of agarose can be represented as $[C_{12}H_{14}O_5(OH)]_n$. Agarpectin is a more complex polysaccharide having the same backbone but comprising of ester sulphates, glucuronic and pyruvic acids, it resembles agarose structurally in having disaccharide agaro-biose as the structural unit. The molecular weights of agarose and agarpectin have been found to be 120,000 and 2,600 respectively. The gels formed by agar melt when warmed and reset on cooling. This process is readily reversible and reproducible. Agar gel by virtue of its structure holds nearly 98% water in a practically immobilized semi-rigid state reducing direct streaming and convection to a minimum.

1.9 Review of the Earlier Work

The diffusion of electrolytes through liquids is a common phenomenon and has been extensively studied in a quantitative way. But the theory of diffusion in electrolytes is not nearly so well developed, partly due to reliable experimental data being scanty and partly due to the more complicated nature of the process. The theoretical interpretation of the experimental results is important as it leads to a better understanding of the properties of electrolyte solutions. We give here a brief outline of the present status of the subject in relation to the Onsager-Fuoss phenomenological theory of diffusion. First we shall discuss more important results reported in the electrolyte-diffusion followed by tracer-diffusion.

1.9.1 Electrolyte-diffusion

Subsequent to Onsager-Fuoss theory of diffusion, numerous studies have been made on different electrolytes in order to verify its validity for both dilute and concentrated solutions.

Among the various electrolytes studied, extensive work is reported on the diffusion of the alkali⁵²⁻⁶⁹, alkaline earth^{62,70-80} ^{metal salts} both in pure aqueous solution and in agar gel

medium. While comparatively less work has been done in transition metal salts⁸¹⁻⁹¹. In most of the cases, the measured diffusion coefficient deviates from the theory specially in the case of unsymmetrical and higher valence type of electrolytes.

A careful analysis by Stokes⁹² of the validity of Onsager's treatment of the electrophoretic effect showed that the equation (1.13) incorporating the first and second order electrophoretic terms should be adequate for uni-univalent electrolytes, and as has been shown, the experimental data are not inconsistent with this view in the cases where the activity coefficient term can be calculated with sufficient accuracy. For unsymmetrical valence type salts the two term Onsager equation is not self-consistent, and Stokes⁹² examined the possibility that the exclusion of the second term might provide a better agreement between theory and experiment.

To explain the deviations of experimental values from the theoretical, Stokes⁹² put forward an equation to correlate both these values with the solvation number. However, this equation was not very satisfactory as the hydration values obtained from this equation vary with those determined by other techniques. Good⁹³ has proposed a theoretical equation by eliminating the hydration number in the Stokes' equation and incorporating a new correlation between D and concentration of the electrolyte.

The lower values of D obtained for CaCl_2 ⁷⁰ and for ammonium salts and LiNO_3 ⁹⁴, were interpreted in terms of the hydration of ions while the higher values obtained in the case of ZnSO_4 were explained by Harned and Hudson⁹⁵ by considering the formation of ion pairs. Using the same concept Tanaka *et al.*⁹⁶ explained their results of diffusion in K_2SO_4 and NiSO_4 systems. Sood and Kaur⁶⁹ also suggested that the ion association is responsible for the deviations from the theory observed in the case of 1-1 electrolytes.

Gupta^{62,89} in his diffusion studies of some alkali and alkaline earth chlorides in gel medium observed a divergence between the theoretical and experimental values. He explained this observation in the light of gel interaction and partial desolvation effect. Patil and Adhyapak⁹⁷ also explained their results of different salts in gel medium by considering the different types of interactions occurring in the gel-water-electrolyte system. Further, they attributed the observed minimum in the diffusion curve of all the salts studied to the increase in the activity coefficient of an electrolyte caused by desolvation of the ions.

1.9.2 Tracer-diffusion

A great deal of attention has been paid to the tracer-diffusion of ions in alkali halide solutions. Almost always,

the diffusion of the tracer ion has been followed by radioactive assay, the exception being the work of Stokes on the diffusion of iodide ions in alkali chlorides^{98,99}. The experimental techniques for the determination of tracer-diffusion coefficient are not easy and there are many pitfalls³³; so it is not surprising that the results of the different workers on the same system sometimes differ considerably.

Wang and Miller³⁸ determined the tracer-diffusion coefficient of sodium ions in aqueous sodium and potassium chlorides. The hump observed in the plot of D^* versus square-root of ionic strength was attributed to the effect of the ions upon the structure of the solvent. This has been found only in measurements made with open-end capillaries and not in diaphragm cell measurements. In the case of sodium ion in sodium chloride solutions, a careful comparative study of the two methods, using a stirring system designed to give streamline flow in the case of open-end capillary work^{42,100} did not confirm the existence of the hump. Wang and Miller's result at higher concentrations were well reproduced, and those of Nielsen, Adamson and Cobble¹⁰¹ using a stirred diaphragm cell shown to be incorrect, a conclusion later confirmed independently by Vitagliano and Lyons¹⁰². This was attributed to the use of very high stirring speeds by these authors which may have led to bulk flow through the diaphragm. Similarly,

the even more pronounced maximum reported for the tracer-diffusion coefficient of sodium ions in potassium chloride⁴⁰ was not confirmed by Mills. Friedmann and Kennedy¹⁰³ obtained a maximum in the curves for K^+ , Ca^{2+} and I^- , Cl^- ions and these were explained on the basis of ion-dipole interaction as well as hydration of the ion. Hertz et al.⁶⁶ also obtained a similar type of diffusion curve as that of Wang for the diffusion of Li^+ , K^+ and I^- ions. They discussed this in terms of structure breaking and structure making properties of the diffusing ion.

Gupta⁶² and Shukla⁶⁴ had explained the higher values of D^* for different ions in gel medium by considering the gel interaction and partial desolvation effect. They suggested that gel interaction depends on the size as well as the charge of the hydrated ion. Recently Fatil et al. in their studies on diffusion in gel medium observed a minimum in the D^* versus \sqrt{C} curve for Cd^{2+} 104, Mn^{2+} 105, CrO_4^{2-} 106 and Cl^- 107 ions while in addition to the minimum, a maximum also was observed in the case of Zn^{2+} 108 ion. These facts were explained on the basis of different types of interactions taking place in the ion-gel-water system.

Mills et al.¹⁰⁹ in the study of diffusion of Ni^{2+} and Cl^- ions in $NiCl_2$ solutions observed a markedly lower mobility of Ni^{2+} ions due to the hydration cloud around Ni^{2+} ions, while

the mobility of Cl^- ion was found to be higher. From these observations they established that Ni^{2+} and Cl^- ions are not closely correlated. Yagodarov and Fhranov¹¹⁰ in their studies in some 2-1 electrolytes at low concentrations observed D values higher than expected from theory. This they explained as due to effects of hydrolysis.

1.10 Scope of the Present Work

The above brief review of earlier work on tracer- and electrolyte-diffusion shows that the theoretical implications of the phenomenon of diffusion are only incompletely understood except at very low concentrations. This is partly due to the lack of experimental values of diffusion coefficients over an extended range of conditions and is mainly due to the difficulties encountered in studying the process. The survey of literature shows that the bulk of work on diffusion has been carried out in 1-1 type of electrolytes, while only limited data on self- and electrolyte-diffusion coefficients are available in 1-2 and 2-1 electrolytes, specially involving transition metals.

The present work was undertaken to see the applicability of the Onsager and Fuoss theory to tracer-diffusion of manganese, copper and zinc ions and electrolyte-diffusion of manganese and copper salts by labelling with the respective

isotopes over a wide range of concentration in gel medium by using zone-diffusion technique. Further, in order to investigate the obstruction effect caused by agar macromolecules in the diffusion path, and to examine the applicability of transition state theory, the diffusion coefficients were measured at different gel concentrations and temperatures.



— • CHAPTER 2 • —
• EXPERIMENTAL •

CHAPTER 2

EXPERIMENTAL

2.1 Measurement of Diffusion Coefficient in Gel Medium

The basic problem of measuring diffusion is to determine the transport of matter under conditions where it can be ensured that the transport is due to diffusion alone, free from transport by flow or convection. It is, therefore, essential to reduce to a minimum direct streaming, turbulence, and convection currents due to temperature variations. Though the most commonly employed techniques to achieve this are the diaphragm or the capillary tube methods, Arnika¹¹⁰ was amongst the early workers to study the possibility of employing a gel medium (of agar-agar) for these studies.

Gels have been looked upon historically as colloidal solutions consisting of two phases, one a solid disperse phase and the other a continuous liquid phase. If an agar-agar sol is cooled to below 40°C, the viscosity is found to have suffered an increase. In the course of gelation the particles in the sol unite to form a number of chains or fibrils which become interlocked and eventually a semi-solid form is acquired. Part of the dispersion medium may be involved in

solvation but the major portion is believed to be held by capillary forces between the fibrils and it is possible to immobilize as much as 98% water in these interstices whereby streaming and convection currents are practically eliminated.

In the present studies, we have chosen ^{54}Mn , ^{64}Cu and ^{65}Zn radioactive isotopes in the form of their different salts, to study the different aspects of diffusion in the agar gel medium using the zone-diffusion technique. These isotopes ^{54}Mn (half-life : 312 days), ^{64}Cu (half-life : 12.7 hours) and ^{65}Zn (half-life : 244 days) were obtained from the Khabha Atomic Research Centre, Trombay, Bombay, in the form of MnCl_2 , CuSO_4 and ZnCl_2 respectively.

As the isotope ^{54}Mn in the form of MnCl_2 was carrier-free, the experiments for the diffusion of MnSO_4 were carried out by simply adding appropriate quantity of MnSO_4 to it.

2.2 The Theory of Zone-Diffusion

The zone-diffusion technique was modified by Arnikar¹¹¹ and used in the study of electromigration in agar columns. This technique has since then been used by several workers^{60,62,112,113} in the study of diffusion of different ions and electrolytes in agar gel medium.

The basic principle involved in the zone-diffusion

technique is shown in Fig. 2.1

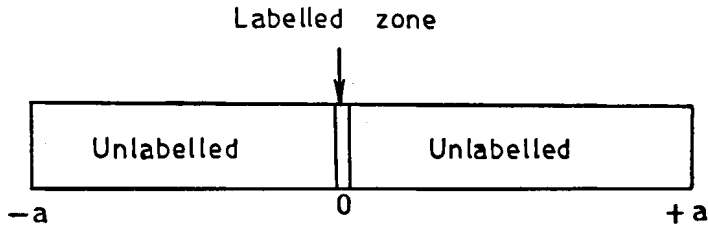


Fig.2.1 - Boundary conditions of zone - diffusion.

A uniform and infinitely thin layer of tracer is allowed to diffuse into semi-infinitely long diffusion column of length, a , of the medium corresponding to the boundary conditions for the activity $\Lambda(x,t)$ at distance x from the origin and at time t :

$$\begin{aligned}\Lambda(0,0) &= \Lambda_0 \\ \Lambda(x,0) &= 0 \text{ for } x \geq 0 \text{ at } t = 0 \\ \Lambda(x,t) &= 0 \text{ for } x = \pm a\end{aligned}$$

The solution of the Fick's II law for the given boundary conditions is the probability or error integral. The following derivation is based on the requirement, first noted by Boltzmann, that although the concentration varies with both distance x and time t , these two variables must always occur in the ratio x^2/t for D to have the proper dimensions.

Consequently, if diffusion proceeds from an initially sharp boundary at $x = t = 0$ a new variable, y , may be defined by the relation $y = x/\sqrt{t}$. Then

$$\frac{\partial}{\partial t} = \frac{\partial y}{\partial t} \cdot \frac{d}{dy} = -\frac{1}{2} \cdot \frac{x}{t^{3/2}} \cdot \frac{d}{dy} \quad \dots (2.1)$$

and

$$\frac{\partial}{\partial x} = \frac{\partial y}{\partial x} \cdot \frac{\partial}{\partial y} = \frac{1}{\sqrt{t}} \cdot \frac{d}{dy} \quad \dots (2.2)$$

Hence, Fick's II law takes the following form

$$\frac{y}{2} \cdot \frac{dc}{dy} = -D \cdot \frac{d^2 c}{dy^2} \quad \dots (2.3)$$

Substituting $p = \frac{dc}{dy}$ and integrating equation (2.3) we get $-y^2/4 = D \cdot \ln I$ where I is constant of integration. Rewriting the equation in terms of x and t , one obtains,

$$\frac{\partial c}{\partial x} = \frac{1}{I \sqrt{t}} e^{-x^2/4Dt} \quad (2.4)$$

The integration constant I may be evaluated from the condition that the total area of the gradient curve $\int_{-\infty}^{+\infty} (\partial c / \partial x) dx$ must equal at all times the initial concentration C_0 . Since each end of the column is at a physical infinity and since the

function (2.4) is symmetrical about the concentration axis,
we can write as

$$C_0 = \frac{1}{I \sqrt{t}} \int_{-\infty}^{+\infty} e^{-x^2/4Dt} \cdot dx = \frac{2}{I \sqrt{t}} \int_{-\infty}^{+\infty} e^{-x^2/4Dt} dx \quad \dots (2.5)$$

This integral has the value $\sqrt{\pi Dt}$ and $I = 2 \sqrt{D \cdot \pi / C_0}$

Then equation (2.4) becomes

$$\frac{\partial c}{\partial x} = \frac{C_0}{2 \sqrt{\pi Dt}} \cdot e^{-x^2/4Dt} \quad \dots (2.6)$$

and

$$C = \frac{C_0}{2 \sqrt{\pi Dt}} \int_x^{\infty} e^{-x^2/4Dt} dx$$

$$\therefore C = \frac{C_0}{2 \sqrt{\pi Dt}} e^{-x^2/4Dt} \quad \dots (2.7)$$

Replacing the concentration in terms of activity A, equation
(2.7) can be written as

$$A_{(x,t)} = \frac{A_0}{\sqrt{4 \pi Dt}} e^{-x^2/4Dt} \quad (2.8)$$

where A_0 is the constant representing the total activity in the

initial zone at $t = 0$ and $A(x,t)$ is the radioactivity at distance x from the origin at time t .

2.3 Experimental Details of the Zone-Diffusion Technique

The experimental details are given below under two heads
(i) The preparation of the diffusion column and (ii) Analysis of the diffusion column.

2.3.1 Preparation of the diffusion column

A required amount of agar (Dacto-Agar, Difco Laboratories, Detroit Michigan, USA) was weighed and dissolved in water in case of electrolyte-diffusion and in solution containing appropriate salt in case of tracer-diffusion. Then this solution is heated slowly and gently to above 80°C on a hot-plate. Sudden and excessive heating was avoided as it leads to charring of the gel. The solution on cooling sets into a semi-rigid solid state containing the aqueous phase electrolyte solution immobilized in the interstitial space of the agar-agar network. This gel which appears homogeneous and really translucent, was used for the preparation of the column.

A clean dry pyrex tube with plane edges and uniform diameter of 1.2 cm and length 30 cm was taken. With one end closed, this tube was filled with the viscous gel solution to half the length with desired concentration containing

unlabelled electrolyte in the case of tracer-diffusion and without electrolyte in the case of electrolyte-diffusion. This was cooled to a solid. Then after removing the cork, one end of the gel is brought out and from it a small piece was cut off with a clean, sharp blade along the edge of the tube so that plane boundary is obtained. The gel column was then allowed to slip back a little and 1 cm^3 of gel containing the labelled electrolyte was added above it and immediately cooled to a solid gel. Leaving a 0.5 cm band of this gel in the column, the remaining part was chopped off to a plane surface as before. The whole gel column was then moved to one side of the tube so that 0.5 cm band remained at the middle of the tube. The remaining part of the tube was then filled with the same gel which was used for the first column before the labelled zone and then immediately cooled. Once the column was ready, both ends of the tube were tightly corked and suspended horizontally in an automatically temperature regulated thermostat maintained to within $\pm 0.1^\circ\text{C}$ at the desired temperature.

In setting the diffusion column, three things were taken care off :

- (i) No enclosure of air bubbles in the gel,
- (ii) Good contact between the central zone and the column on the either side of it,

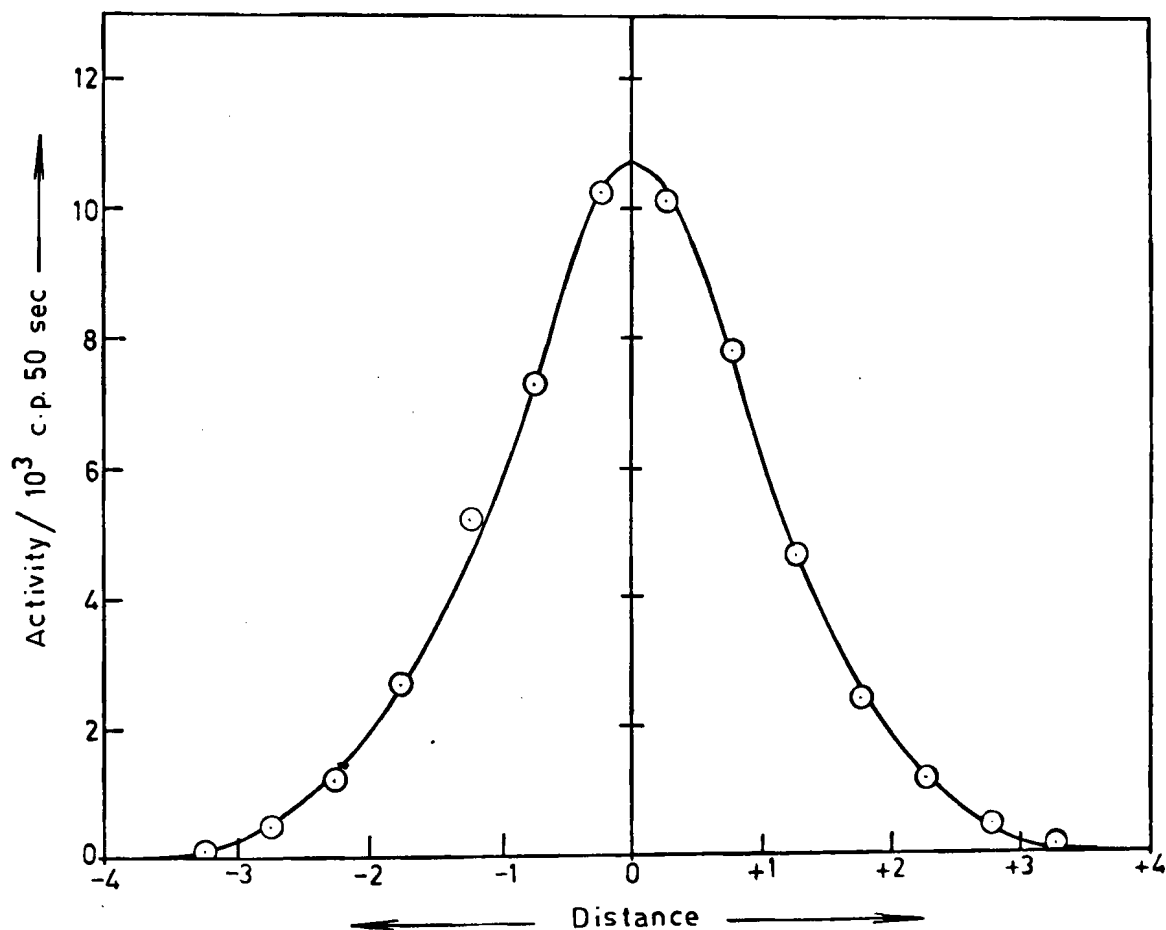


Fig.2.2- Gaussian distribution curve for the electrolyte- diffusion of MnSO_4 ($1 \times 10^{-5} \text{ M}$) at 25°C in 1% agar gel.

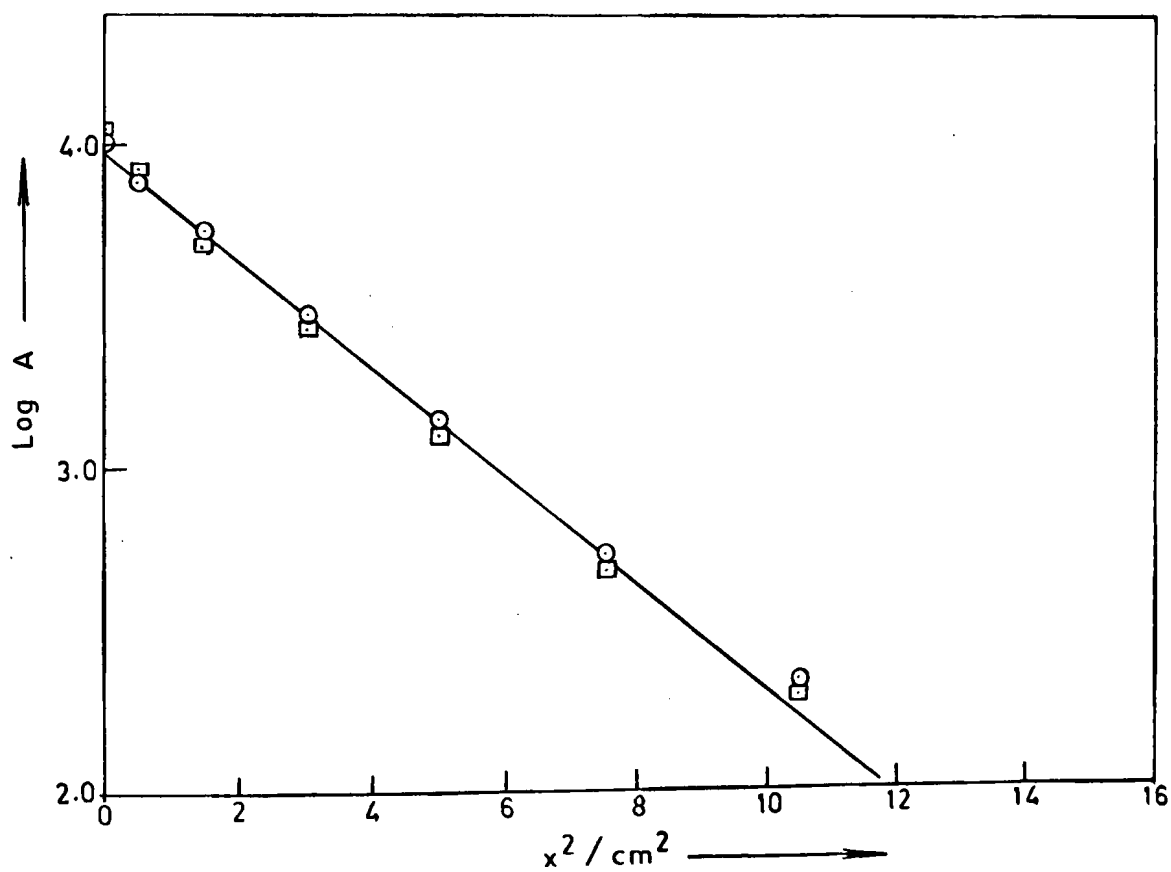


Fig. 2.3 - Electrolyte-diffusion of MnSO_4 ($1 \times 10^{-5} \text{M}$) at 25°C . in 1% agar gel.

(iii) No part of the gel sticks to the sides of the glass while being moved to and fro in the tube.

2.3.2 Analysis of the diffusion column

Diffusion is allowed to proceed for a definite time of the order of 24 hours, the gel column was then extruded carefully and the region of 5 cm on either side of the central zone was sliced into 0.5 cm long samples. These were transferred to aluminium planchettes and dehydrated under an infrared lamp. The radioactivity in each sample was measured using a well-type single channel gamma ray scintillation counter.

When the activity A is plotted versus distance, a Gaussian distribution curve is obtained which is shown in Fig. 2.2

The plot of $\log A$ versus x^2 gives a straight line as expected, with

$$\text{Slope} = - \frac{1}{2.303 \times 4 \times D \times t}$$

Knowing the time of diffusion t for a specific run, the diffusion coefficient is calculated. A typical plot of $\log A$ versus x^2 is shown in Fig. 2.3. Each value of D presented in the tables is an average of at least four independent measurements.



—● CHAPTER 3 ●—

• DEPENDENCE OF DIFFUSION COEFFICIENT
ON CONCENTRATION OF THE ELECTROLYTE •

CHAPTER 3

DEPENDENCE OF DIFFUSION COEFFICIENT ON CONCENTRATION OF THE ELECTROLYTE

In the present work, tracer-diffusion coefficients and electrolyte-diffusion coefficients of some labelled transition metal ions in a number of electrolytes are reported over a wide range of concentration in gel medium. The applicability of the Onsager⁵ and Onsager-Fuoss¹² theory to the experimental data of tracer- and electrolyte-diffusion coefficients respectively is examined in various systems in this chapter. As the mechanism and hence the theoretical treatment for the two diffusion processes are different, the results obtained in these studies are discussed separately under two heads.

Section A : Variation of the Tracer-Diffusion Coefficient with Concentration of the Electrolyte

This section deals with the measurement of diffusion in coefficientsⁱⁿ tracer-diffusion of

- (1) $^{54}\text{Mn}^{2+}$ in (a) MnCl_2 , MgCl_2 , SrCl_2 and BaCl_2 electrolytes
and

(b) MnSO_4 , CuSO_4 , NiSO_4 , CoSO_4 and ZnSO_4 electrolytes.

(2) $^{64}\text{Cu}^{2+}$ in (a) CuSO_4 , NiSO_4 , CoSO_4 and MnSO_4 electrolytes.
and

(3) $^{65}\text{Zn}^{2+}$ in (a) BaCl_2 , SrCl_2 and MnCl_2 electrolytes.

The diffusion coefficients in all the systems were measured in 1% agar gel medium.

Before discussing the experimental results obtained in these systems let us first see how the theoretical value of tracer-diffusion coefficient (D^*) is computed.

3.1A Theoretical Value of D^*

As we have seen in Chapter 1, the theoretical value of tracer-diffusion coefficient is calculated by using the Onsager-Gosting-Harned^{5,14} equation. They have shown that the diffusion coefficient D_j^* of a tracer amount of ions of jth kind in a salt solution of uniform composition is given by the following limiting law expression applicable for dilute solutions :

$$D_j^* = \frac{RT \lambda_j^\circ}{|Z_j| F^2} - \left[\frac{\lambda_j^\circ |Z_j| F}{3N\epsilon} \times 2.694 \times 10^{16} \sqrt{\frac{4\pi}{\epsilon RT}} \times [1 - \sqrt{d(u_j)}] \sqrt{\sum C_i Z_i^2} \right] \quad \dots (1.20)$$

The mobility function $d(u_j)$ in the above equation (1.20) is given by :

$$d(w_j) = \frac{1}{\sum_i C_i Z_i} \sum \frac{C_i |Z_i| \lambda_i^\circ}{\frac{\lambda_i^\circ}{|Z_i|} + \frac{\lambda_j^\circ}{|Z_j|}} \quad \dots (3.1)$$

In the case of tracer-diffusion only three kinds of ions are present and let diffusing ion be denoted as $j=1$ with its valence Z_1 and concentration C_1 which is negligibly small. Further, we have $C_2 |Z_2| = C_3 |Z_3|$ where C_2 and C_3 are the concentrations of the cations and anions of the supporting electrolyte with their valences Z_2 and Z_3 respectively. Under these conditions equation (3.1) takes the following form :

$$d(w_j) = \frac{|Z_1|}{|Z_2| + |Z_3|} \left[\frac{|Z_2| \lambda_2^\circ}{|Z_1| \lambda_2^\circ + |Z_2| \lambda_1^\circ} + \frac{|Z_3| \lambda_3^\circ}{|Z_1| \lambda_3^\circ + |Z_3| \lambda_1^\circ} \right] \quad \dots (3.2)$$

In the case of self-diffusion, a special case of tracer-diffusion, we have $|Z_1| = |Z_2|$ and also $\lambda_1^\circ = \lambda_2^\circ$ because the ionic conductances of the normal ion and the radioactive ion are practically identical. Hence the value of $d(w_j)$ for 2-1 electrolytes, in which the cation is diffusing, becomes

$$d(w_j) = \frac{2}{3} \left[\frac{1}{2} + \frac{\lambda_3^\circ}{\lambda_2^\circ + 2\lambda_3^\circ} \right] \quad \dots (3.3)$$

while for 2-2 electrolytes; the value of $d(w_j)$ simplifies to

$$d(w_j) = \frac{1}{2} \left[\frac{1}{2} + \frac{\lambda_3^\circ}{\lambda_3^\circ + \lambda_2^\circ} \right] \quad \dots (3.4)$$

In deriving the equation (1.20), the ions were treated as point charges, justifiable at very low concentrations only. However, at higher concentrations, one has to take into consideration the sizes of the ions. Taking this into account, Stokes et al.⁹⁸ made empirical correction to the equation given by Costing and Harned, by replacing,

$$\sqrt{C} \quad \text{by} \quad \sqrt{C} / (1 + ka) (1 + ka/\sqrt{2})$$

where a is the closest distance of approach of opposite ions and k the reciprocal radius of the ionic atmosphere.

The values of different parameters involved in equation (1.20) for the calculation of D_{theo}^+ for different ions are presented in Table 3.1; while the different constants involved in it have the values :

$$\begin{aligned} R &= 8.314 \text{ JK}^{-1} \text{ mol}^{-1}, \\ F &= 96500 \text{ C mol}^{-1}, \\ N &= 6.023 \times 10^{23} \text{ mole}^{-1}, \\ e &= 78.5 \text{ and } T = 298 \text{ K.} \end{aligned}$$

Table 3.1 : Values of different parameters for the calculation of theoretical diffusion coefficient

(A) Tracer-diffusion of Mn^{2+} in					
	$MnCl_2$	$MgCl_2$	$SrCl_2$	$BaCl_2$	
$ Z_1 $	2	2	2	2	
$ Z_2 $	2	2	2	2	
$ Z_3 $	1	1	1	1	
λ_1° /siemens	53.5	53.5	53.5	53.5	
λ_2° /siemens	53.5	53.0	59.4	63.6	
λ_3° /siemens	76.35	76.35	76.35	76.35	
$d(w_j)$	0.580	0.579	0.598	0.609	
a/λ°	6.713	3.187	6.663	6.955	
(B) Tracer-diffusion of Mn^{2+} in					
	$MnSO_4$	$CuSO_4$	$NiSO_4$	$CoSO_4$	$ZnSO_4$
$ Z_1 $	2	2	2	2	2
$ Z_2 $	2	2	2	2	2
$ Z_3 $	2	2	2	2	2
λ_1° /siemens	53.5	53.5	53.5	53.5	53.5
λ_2° /siemens	53.5	53.6	54.0	55.0	52.8
λ_3° /siemens	80.0	80.0	80.0	80.0	80.0
$d(w_j)$	0.550	0.550	0.550	0.553	0.543
a/λ°	2.917	3.026	2.917	7.088	3.026

Table 3.1 (contd.)

(C) Tracer-diffusion of Cu^{2+} in				
	CuSO_4	NiSO_4	CoSO_4	MnSO_4
$ Z_1 $	2	2	2	2
$ Z_2 $	2	2	2	2
$ Z_3 $	2	2	2	2
λ_1° /siemens	53.6	53.6	53.6	53.6
λ_2° /siemens	53.6	54.0	55.0	53.5
λ_3° /siemens	80.0	80.0	80.0	80.0
$d(\omega_j)$	0.549	0.550	0.553	0.549
a/λ°	3.023	2.917	7.033	2.917

(D) Tracer-diffusion of Zn^{2+} in			
	BaCl_2	SrCl_2	MnCl_2
$ Z_1 $	2	2	2
$ Z_2 $	2	2	2
$ Z_3 $	1	1	1
λ_1° /siemens	52.8	52.8	52.8
λ_2° /siemens	63.6	59.4	53.5
λ_3° /siemens	76.35	76.35	76.35
$d(\omega_j)$	0.612	0.601	0.583
a/λ°	6.023	5.775	5.814

By substituting these values into equation (1.20) the limiting law and the extended limiting law expressions of D^* for different ions at 25°C take the following forms :

(I) Tracer-diffusion of Mn^{2+} ions in different transition metal chlorides

(i) Mn^{2+} in $MnCl_2$

Limiting law expression

$$D_{Mn}^{*2+}/10^{-6} \text{ cm}^2 \text{ s}^{-1} = 7.117 - 9.201 \sqrt{C} \quad \dots (3.5a)$$

Extended limiting law expression

$$D_{Mn}^{*2+}/10^{-6} \text{ cm}^2 \text{ s}^{-1} = 7.117 - 9.201 \frac{\sqrt{C}}{(1+2.7016\sqrt{C})(1+2.7016\sqrt{C}/\sqrt{2})} \quad \dots (3.5b)$$

(ii) Mn^{2+} in $MgCl_2$

Limiting law expression

$$D_{Mn}^{*2+}/10^{-6} \text{ cm}^2 \text{ s}^{-1} = 7.117 - 9.242 \sqrt{C} \quad \dots (3.6a)$$

Extended limiting law expression

$$D_{Mn}^{*2+}/10^{-6} \text{ cm}^2 \text{ s}^{-1} = 7.117 - 9.242 \frac{\sqrt{C}}{(1+1.2327\sqrt{C})(1+1.2327\sqrt{C}/\sqrt{2})} \quad \dots (3.6b)$$

(iii) Mn^{2+} in $SrCl_2$

Limiting law expression

$$D_{Mn}^{*2+}/10^{-6} \text{ cm}^2 \text{ s}^{-1} = 7.117 - 8.763 \sqrt{C} \quad \dots (3.7a)$$

Extended limiting law expression

$$D_{Mn}^{*2+}/10^{-6} \text{ cm}^2 \text{ s}^{-1} = 7.117 - 8.763 \frac{\sqrt{C}}{(1+2.6936\sqrt{C})(1+2.6936\sqrt{C}/\sqrt{2})} \quad \dots (3.7b)$$

(iv) Mn^{2+} in BaCl_2

Limiting law expression

$$D_{\text{Mn}}^* \times 10^{-6} \text{ cm}^2 \text{ s}^{-1} = 7.117 - 8.493 \sqrt{C} \quad \dots (3.8a)$$

Extended limiting law expression

$$D_{\text{Mn}}^* \times 10^{-6} \text{ cm}^2 \text{ s}^{-1} = 7.117 - 8.493 \frac{\sqrt{C}}{(1+2.7989\sqrt{C})(1+2.7989\sqrt{C}/\sqrt{2})} \quad \dots (3.8b)$$

(II) Tracer-diffusion of Mn^{2+} in different transition metal sulphates

(i) Mn^{2+} in MnSO_4

Limiting law expression

$$D_{\text{Mn}}^* \times 10^{-6} \text{ cm}^2 \text{ s}^{-1} = 7.117 - 11.529 \sqrt{C} \quad \dots (3.9a)$$

Extended limiting law expression

$$D_{\text{Mn}}^* \times 10^{-6} \text{ cm}^2 \text{ s}^{-1} = 7.117 - 11.529 \frac{\sqrt{C}}{(1+1.3557\sqrt{C})(1+1.3557\sqrt{C}/\sqrt{2})} \quad \dots (3.9b)$$

(ii) Mn^{2+} in ZnSO_4

Limiting law expression

$$D_{\text{Mn}}^* \times 10^{-6} \text{ cm}^2 \text{ s}^{-1} = 7.117 - 11.578 \sqrt{C} \quad \dots (3.10a)$$

Extended limiting law expression

$$D_{\text{Mn}}^* \times 10^{-6} \text{ cm}^2 \text{ s}^{-1} = 7.117 - 11.578 \frac{\sqrt{C}}{(1+1.4071\sqrt{C})(1+1.4071\sqrt{C}/\sqrt{2})} \quad \dots (3.10b)$$

(iii) Mn^{2+} in NiSO_4

Limiting law expression

$$D_{\text{Mn}}^* \times 10^{-6} \text{ cm}^2 \text{ s}^{-1} = 7.117 - 11.493 \sqrt{C} \quad \dots (3.11a)$$

Extended limiting law expression

$$D_{Mn}^{*2+}/10^{-6} \text{ cm}^2 \text{ s}^{-1} = 7.117 - 11.493 \frac{\sqrt{C}}{(1+1.3557\sqrt{C})(1+1.3557\sqrt{C}/\sqrt{2})} \quad \dots (3.11b)$$

(iv) Mn^{2+} in $CoSO_4$

Limiting law expression

$$D_{Mn}^{*2+}/10^{-6} \text{ cm}^2 \text{ s}^{-1} = 7.117 - 11.427 \sqrt{C} \quad \dots (3.12a)$$

Extended limiting law expression

$$D_{Mn}^{*2+}/10^{-6} \text{ cm}^2 \text{ s}^{-1} = 7.117 - 11.427 \frac{\sqrt{C}}{(1+3.2938\sqrt{C})(1+3.2938\sqrt{C}/\sqrt{2})} \quad \dots (3.12b)$$

(v) Mn^{2+} in $CuSO_4$

Limiting law expression

$$D_{Mn}^{*2+}/10^{-6} \text{ cm}^2 \text{ s}^{-1} = 7.117 - 11.525 \sqrt{C} \quad \dots (3.13a)$$

Extended limiting law expression

$$D_{Mn}^{*2+}/10^{-6} \text{ cm}^2 \text{ s}^{-1} = 7.117 - 11.525 \frac{\sqrt{C}}{(1+1.4071\sqrt{C})(1+1.4071\sqrt{C}/\sqrt{2})} \quad \dots (3.13b)$$

(III) Tracer-diffusion of Cu^{2+} in different transition

metal sulphates

(1) Cu^{2+} in $CuSO_4$

Limiting law expression

$$D_{Cu}^{*2+}/10^{-6} \text{ cm}^2 \text{ s}^{-1} = 7.130 - 11.560 \sqrt{C} \quad \dots (3.14a)$$

Extended limiting law expression

$$D_{Cu}^{*2+}/10^{-6} \text{ cm}^2 \text{ s}^{-1} = 7.130 - 11.560 \frac{\sqrt{C}}{(1+1.4071\sqrt{C})(1+1.4071\sqrt{C}/\sqrt{2})} \quad \dots (3.14b)$$

(11) Cu^{2+} in MnSO_4

Limiting law expression

$$D_{\text{Cu}^{2+}}^*/10^{-6} \text{ cm}^2 \text{ s}^{-1} = 7.130 - 11.567\sqrt{C} \quad \dots (3.15a)$$

Extended limiting law expression

$$D_{\text{Cu}^{2+}}^*/10^{-6} \text{ cm}^2 \text{ s}^{-1} = 7.130 - 11.567 \frac{\sqrt{C}}{(1+1.4071\sqrt{C})(1+1.4071\sqrt{C}/\sqrt{2})} \quad \dots (3.15b)$$

(111) Cu^{2+} in NiSO_4

Limiting law expression

$$D_{\text{Cu}^{2+}}^*/10^{-6} \text{ cm}^2 \text{ s}^{-1} = 7.130 - 11.530 \sqrt{C} \quad \dots (3.16a)$$

Extended limiting law expression

$$D_{\text{Cu}^{2+}}^*/10^{-6} \text{ cm}^2 \text{ s}^{-1} = 7.130 - 11.530 \frac{\sqrt{C}}{(1+1.3557\sqrt{C})(1+1.3557\sqrt{C}/\sqrt{2})} \quad \dots (3.16b)$$

(iv) Cu^{2+} in CoSO_4

Limiting law expression

$$D_{\text{Cu}^{2+}}^*/10^{-6} \text{ cm}^2 \text{ s}^{-1} = 7.130 - 11.462 \sqrt{C} \quad \dots (3.17a)$$

Extended limiting law expression

$$D_{\text{Cu}^{2+}}^*/10^{-6} \text{ cm}^2 \text{ s}^{-1} = 7.130 - 11.462 \frac{\sqrt{C}}{(1+3.2938\sqrt{C})(1+3.2938\sqrt{C}/\sqrt{2})} \quad \dots (3.17b)$$

(IV) Tracer-diffusion of Zn^{2+} in different transition metal chlorides

(1) Zn^{2+} in BaCl_2

Limiting law expression

$$D_{\text{Zn}^{2+}}^*/10^{-6} \text{ cm}^2 \text{ s}^{-1} = 7.023 - 8.297 \sqrt{C} \quad \dots (3.18a)$$

Extended limiting law expression

$$D_{Zn^{2+}}^*/10^{-6} \text{ cm}^2 \text{ s}^{-1} = 7.023 - 8.297 \frac{\sqrt{C}}{(1+2.7939\sqrt{C})(1+2.7939\sqrt{C}/\sqrt{2})} \quad \dots (3.13b)$$

(ii) Zn^{2+} in $SrCl_2$

Limiting law expression

$$D_{Zn^{2+}}^*/10^{-6} \text{ cm}^2 \text{ s}^{-1} = 7.023 - 8.574 \sqrt{C} \quad \dots (3.19a)$$

Extended limiting law expression

$$D_{Zn^{2+}}^*/10^{-6} \text{ cm}^2 \text{ s}^{-1} = 7.023 - 8.574 \frac{\sqrt{C}}{(1+2.6936\sqrt{C})(1+2.6936\sqrt{C}/\sqrt{2})} \quad \dots (3.19b)$$

(iii) Zn^{2+} in $MnCl_2$

Limiting law expression

$$D_{Zn^{2+}}^*/10^{-6} \text{ cm}^2 \text{ s}^{-1} = 7.023 - 8.835 \sqrt{C} \quad \dots (3.20a)$$

Extended limiting law expression

$$D_{Zn^{2+}}^*/10^{-6} \text{ cm}^2 \text{ s}^{-1} = 7.023 - 8.885 \frac{\sqrt{C}}{(1+2.7016\sqrt{C})(1+2.7016\sqrt{C}/\sqrt{2})} \quad \dots (3.20b)$$

The theoretical values of tracer-diffusion coefficients calculated using equations (3.5-3.20) for manganese, copper and zinc ions in different electrolytes are tabulated along with their experimental values in Tables 3.2-3.10 and are shown in Figs. 3.1-3.7 as a function of square root of concentration. The curve a in these figures shows the diffusion coefficient values expected from the Onsager's limiting law, curve b shown

by dotted lines represents the theoretical D^* values according to the extended limiting law while the curve with open circles (curve C) shows experimental values of D^* obtained in the present work.

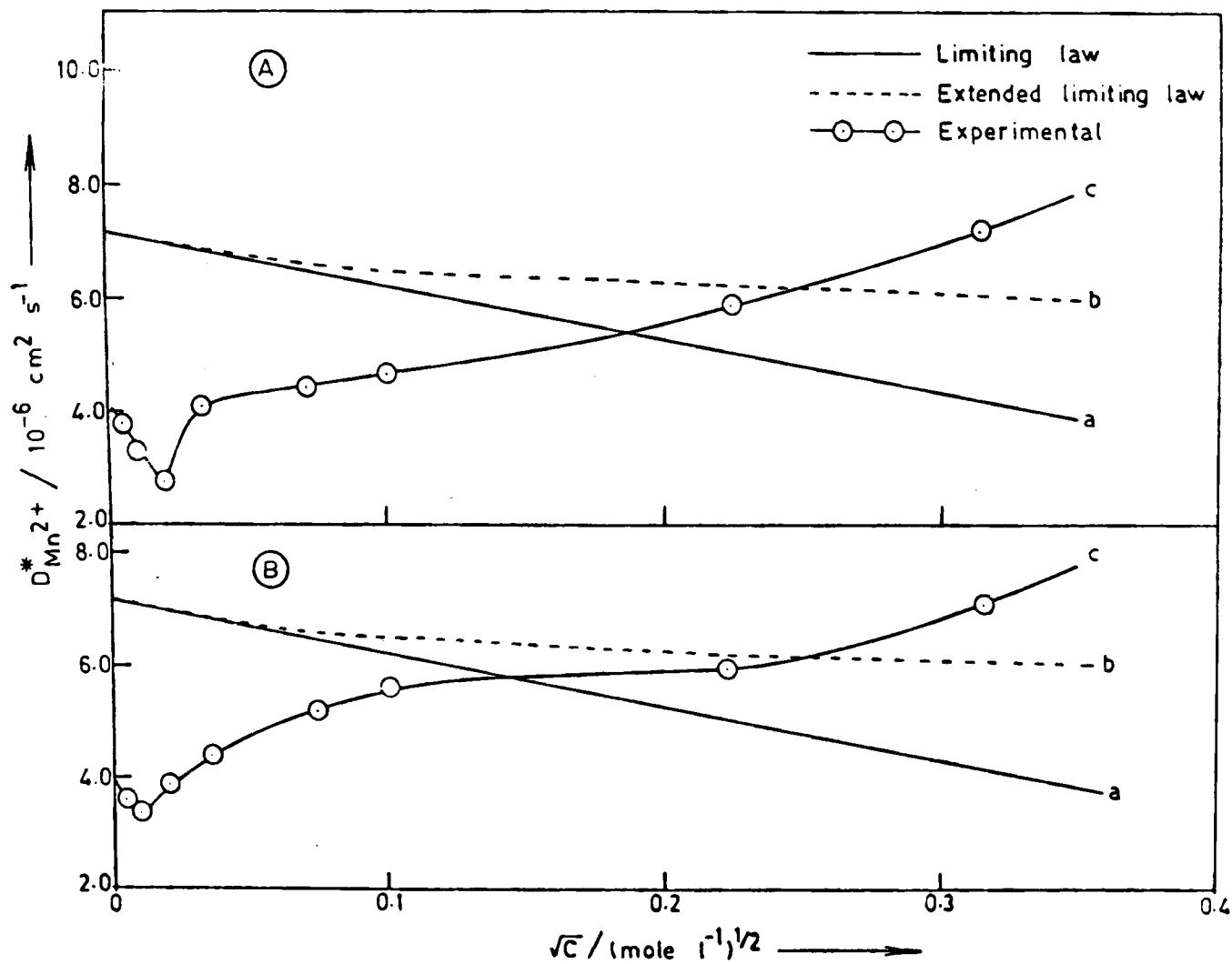


Fig. 3.1: Variation of tracer-diffusion coefficient of Mn^{2+} ions with square root of concentration of (A) MnCl_2 and (B) MgCl_2 in 1 % agar gel at 25°C .

Table 3.2 : Variation of tracer-diffusion coefficient of $^{54}\text{Mn}^{2+}$ with concentration of (A) MnCl_2 and (B) MgCl_2 in 1% agar gel at 25°C

(A) MnCl_2

Conc./mole l^{-1}	$D_{\text{Mn}^{2+}}^*/10^{-6} \text{ cm}^2 \text{ s}^{-1}$		
	Limiting law	Theoretical Extended limiting law	Experimental
0	7.117	-	-
5×10^{-5}	7.051	7.054	3.753
1×10^{-4}	7.024	7.029	3.466
5×10^{-4}	6.911	6.930	2.706
1×10^{-3}	6.825	6.864	4.036
5×10^{-3}	6.466	6.635	4.497
1×10^{-2}	6.198	6.508	4.612
5×10^{-2}	5.059	6.218	5.901
0.1	4.207	6.138	7.143

(B) MgCl_2

0	7.117	-	-
5×10^{-5}	7.051	7.053	3.606
1×10^{-4}	7.024	7.028	2.881
5×10^{-4}	6.910	6.930	3.794
1×10^{-3}	6.824	6.863	4.850
5×10^{-3}	6.463	6.635	5.281
1×10^{-2}	6.192	6.509	5.641
5×10^{-2}	5.050	6.224	5.982
0.1	4.194	6.143	7.120

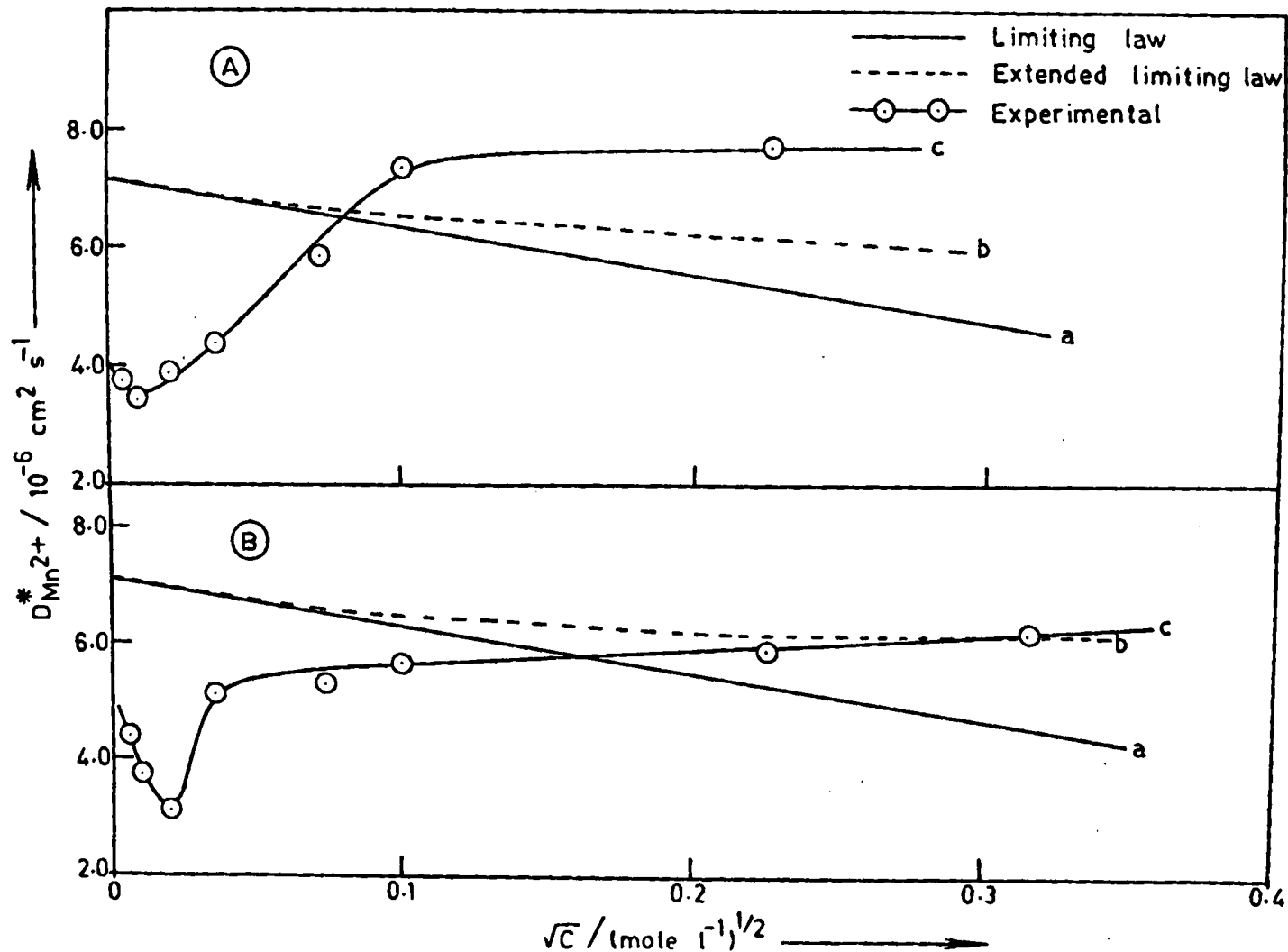


Fig.3.2: Variation of tracer - diffusion coefficient of Mn^{2+} ions with square root of concentration of (A) SrCl_2 and (B) BaCl_2 in 1 % agar gel at 25°C .

Table 3.3 : Variation of tracer-diffusion coefficient of $^{54}\text{Mn}^{2+}$ with concentration of (A) SrCl_2 and (B) BaCl_2 in 1% agar gel at 25°C

(A) SrCl_2

Conc./mole l^{-1}	$D_{\text{Mn}^{2+}}^*/10^{-6} \text{ cm}^2 \text{ s}^{-1}$		
	Limiting law	Theoretical Extended limiting law	Experimental
0	7.117	-	-
5×10^{-5}	7.054	7.056	3.634
1×10^{-4}	7.029	7.033	3.492
5×10^{-4}	6.920	6.939	3.938
1×10^{-3}	6.839	6.876	4.345
5×10^{-3}	6.497	6.657	5.962
1×10^{-2}	6.240	6.536	7.447
5×10^{-2}	5.157	6.257	7.637

(B) BaCl_2

0	7.117	-	-
5×10^{-5}	7.056	7.053	4.439
1×10^{-4}	7.032	7.036	3.652
5×10^{-4}	6.927	6.946	3.012
1×10^{-3}	6.848	6.885	5.064
5×10^{-3}	6.517	6.677	5.339
1×10^{-2}	6.268	6.563	5.671
5×10^{-2}	5.220	6.303	5.893
0.1	4.434	6.241	6.234

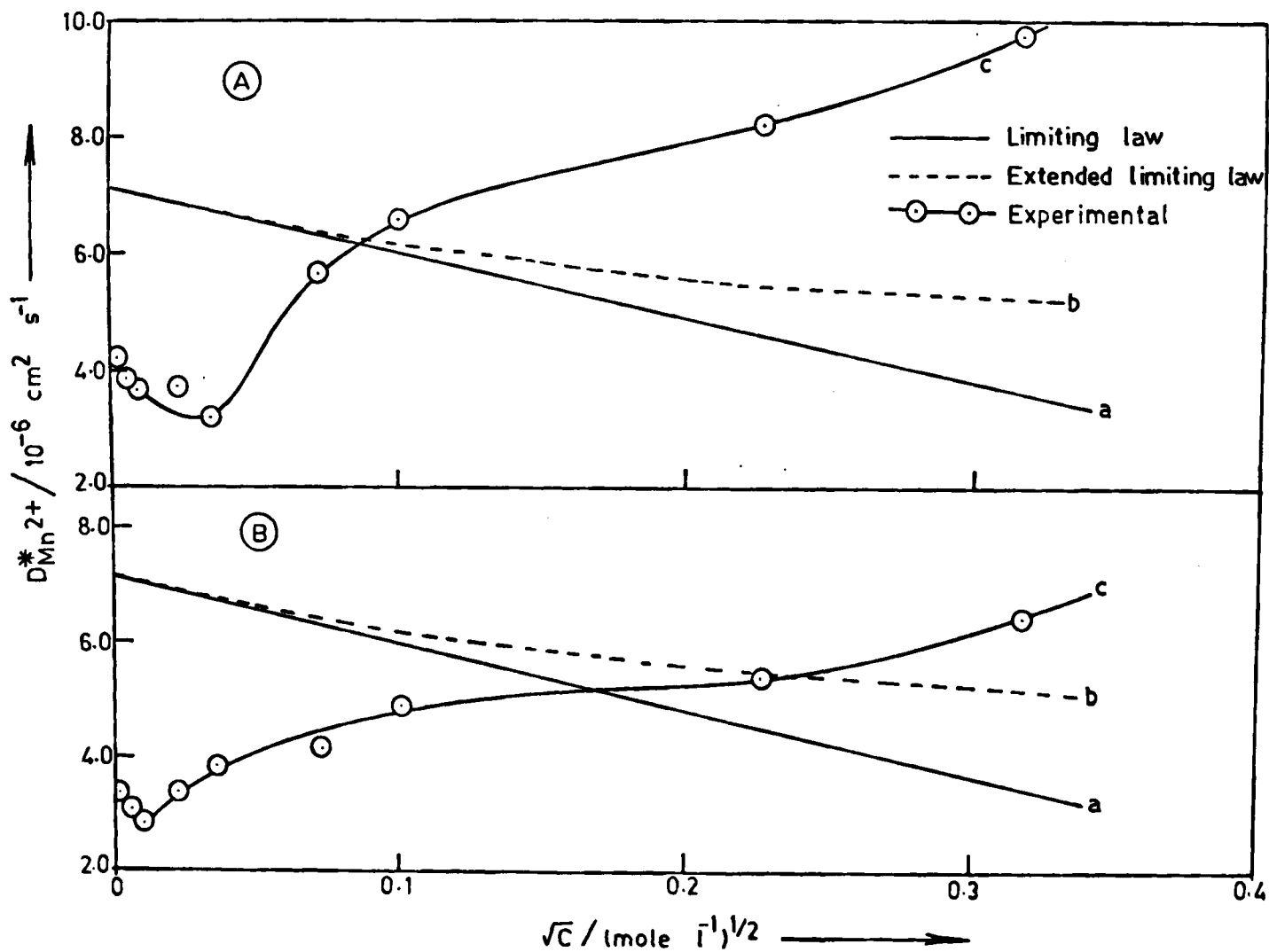


Fig.3.3: Variation of tracer-diffusion coefficient of Mn^{2+} ions with square root of concentration of (A) MnSO_4 and (B) CuSO_4 in 1% agar gel at 25°C .

Table 3.4 : Variation of tracer-diffusion coefficient of $^{54}\text{Mn}^{2+}$ with concentration of (A) MnSO_4 and (B) CuSO_4 in 1% agar gel at 25°C

(A) MnSO_4

Conc/mole l^{-1}	$D_{\text{Mn}}^* \times 10^{-6} \text{ cm}^2 \text{ s}^{-1}$		
	Theoretical Limiting law	Extended limiting law	Experimental
0	7.117	-	-
1×10^{-5}	7.080	7.080	4.225
5×10^{-5}	7.035	7.036	3.801
1×10^{-4}	7.001	7.004	3.637
5×10^{-4}	6.859	6.871	3.562
1×10^{-3}	6.752	6.777	3.196
5×10^{-3}	6.301	6.420	5.779
1×10^{-2}	5.963	6.190	6.533
5×10^{-2}	4.533	5.437	8.105
0.1	3.470	5.158	9.875

(B) CuSO_4

0	7.117	-	-
1×10^{-5}	7.080	7.080	3.416
5×10^{-5}	7.035	7.036	3.071
1×10^{-4}	7.001	7.004	2.831
5×10^{-4}	6.850	6.877	3.425
1×10^{-3}	6.752	6.773	3.865
5×10^{-3}	6.302	6.424	4.062
1×10^{-2}	5.964	6.197	4.896
5×10^{-2}	4.540	5.513	5.462
0.1	3.472	5.193	6.387

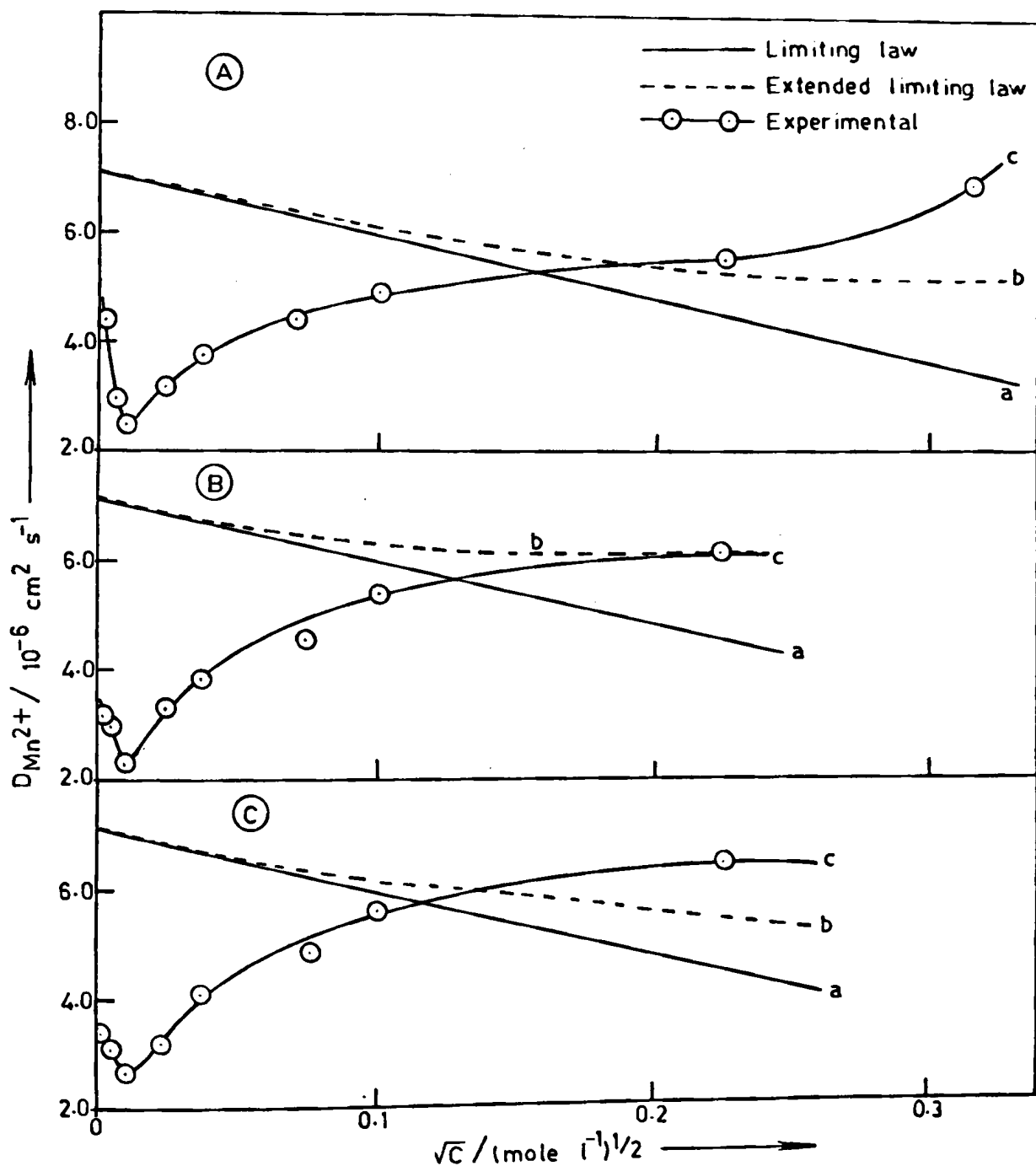


Fig.3.4: Variation of tracer-diffusion coefficient of Mn^{2+} ions with square root of concentration of
 (A) $NiSO_4$, (B) $CoSO_4$ and (C) $ZnSO_4$ in 1% agar gel at 25°C .

Table 3.5 : Variation of tracer-diffusion coefficient of $^{54}\text{Mn}^{2+}$ with concentration of (A) HISO_4 and (B) CoSO_4 in 1% agar gel at 25°C

(A) HISO_4

Conc./mole l^{-1}	$D_{\text{Mn}^{2+}}^*/10^{-6} \text{ cm}^2 \text{ s}^{-1}$		
	Limiting law	Theoretical Extended limiting law	Experimental
0	7.117	-	-
1×10^{-5}	7.030	7.031	4.393
5×10^{-5}	7.036	7.037	2.890
1×10^{-4}	7.002	7.004	2.504
5×10^{-4}	6.860	6.872	3.153
1×10^{-3}	6.753	6.779	3.774
5×10^{-3}	6.304	6.422	4.395
1×10^{-2}	5.967	5.192	4.912
5×10^{-2}	4.546	5.492	5.682
0.1	3.481	5.164	6.914

(B) CoSO_4

0	7.117	-	-
1×10^{-5}	7.030	7.031	3.256
5×10^{-5}	7.036	7.039	3.001
1×10^{-4}	7.002	7.009	2.464
5×10^{-4}	6.861	6.891	3.433
1×10^{-3}	6.755	6.812	3.819
5×10^{-3}	6.308	6.554	4.649
1×10^{-2}	5.970	6.420	5.432
5×10^{-2}	4.561	6.149	6.146

Table 3.6 : Variation of tracer-diffusion coefficient of $^{54}\text{Mn}^{2+}$ with concentration of ZnSO_4 in 1% agar gel at 25°C

Conc./mole l^{-1}	$D_{\text{Mn}^{2+}}^*/10^{-6} \text{ cm}^2 \text{ s}^{-1}$		
	Limiting law	Theoretical Extended limiting law	Experimental
0	7.117	-	-
1×10^{-5}	7.080	7.030	3.367
5×10^{-5}	7.035	7.036	3.119
1×10^{-4}	7.001	7.003	2.625
5×10^{-4}	6.853	6.871	3.065
1×10^{-3}	6.751	6.770	4.177
5×10^{-3}	6.299	6.421	4.926
1×10^{-2}	5.960	6.193	5.634
5×10^{-2}	4.530	5.505	6.467

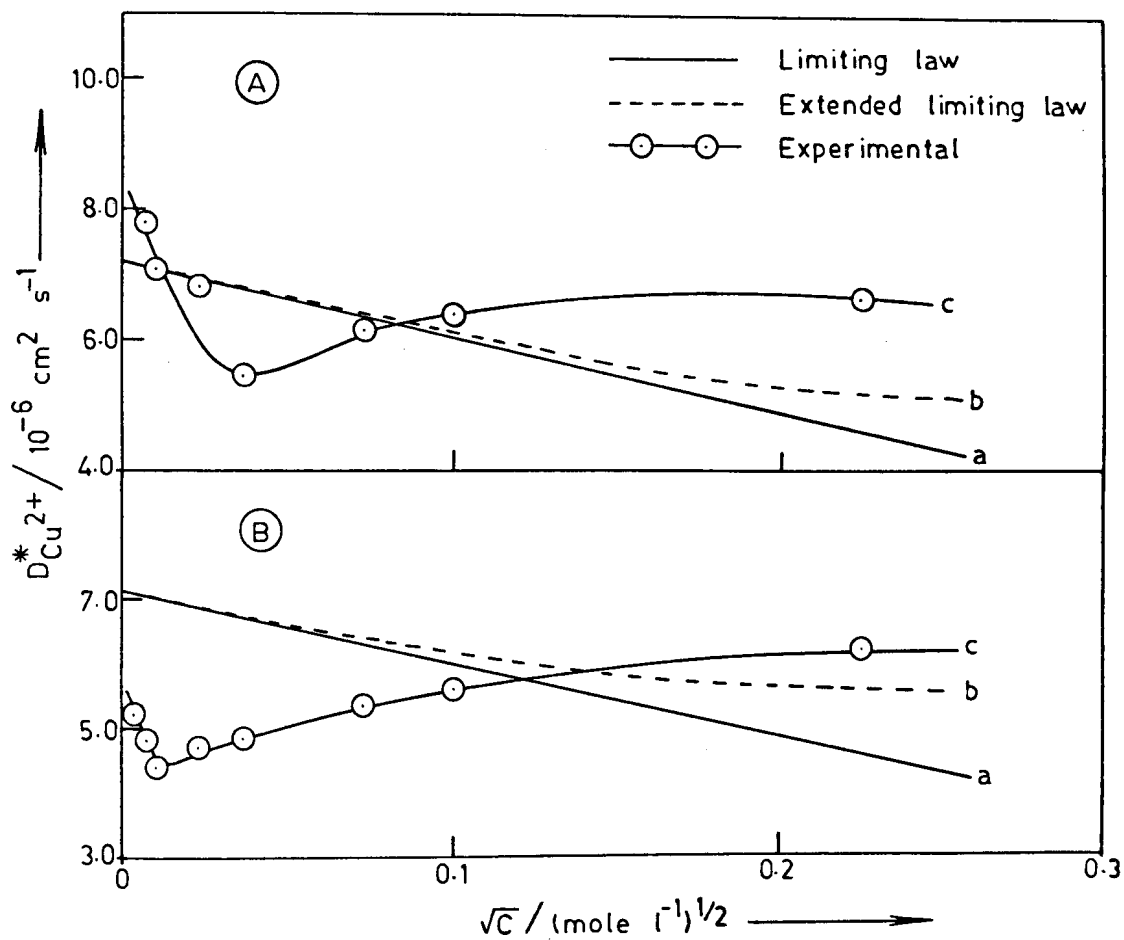


Fig. 3.5: Variation of tracer - diffusion coefficient of Cu^{2+} ions with square root of concentration of (A) CuSO_4 and (B) NiSO_4 in 1% agar gel at 25°C .

Table 3.2 : Variation of tracer-diffusion coefficient of $^{64}\text{Cu}^{2+}$ with concentration of (A) CuSO_4 and (B) NiSO_4 in 1% agar gel at 25°C

(A) CuSO_4

Conc./mole l^{-1}	$D_{\text{Cu}^{2+}}^* / 10^{-6} \text{ cm}^2 \text{ s}^{-1}$		
	Limiting law	Theoretical Extended limiting law	Experimental
0	7.130	-	-
5×10^{-5}	7.043	7.050	7.711
1×10^{-4}	7.014	7.017	7.034
5×10^{-4}	6.871	6.836	6.833
1×10^{-3}	6.764	6.791	5.435
5×10^{-3}	6.312	6.436	6.223
1×10^{-2}	5.974	6.209	6.414
5×10^{-2}	4.545	5.521	6.542

(B) NiSO_4

0	7.130	-	-
1×10^{-5}	7.094	7.094	5.195
5×10^{-5}	7.043	7.050	4.793
1×10^{-4}	7.014	7.013	4.374
5×10^{-4}	6.872	6.836	4.709
1×10^{-3}	6.765	6.790	4.832
5×10^{-3}	6.314	6.434	5.452
1×10^{-2}	5.977	6.204	5.696
5×10^{-2}	4.551	5.501	6.305

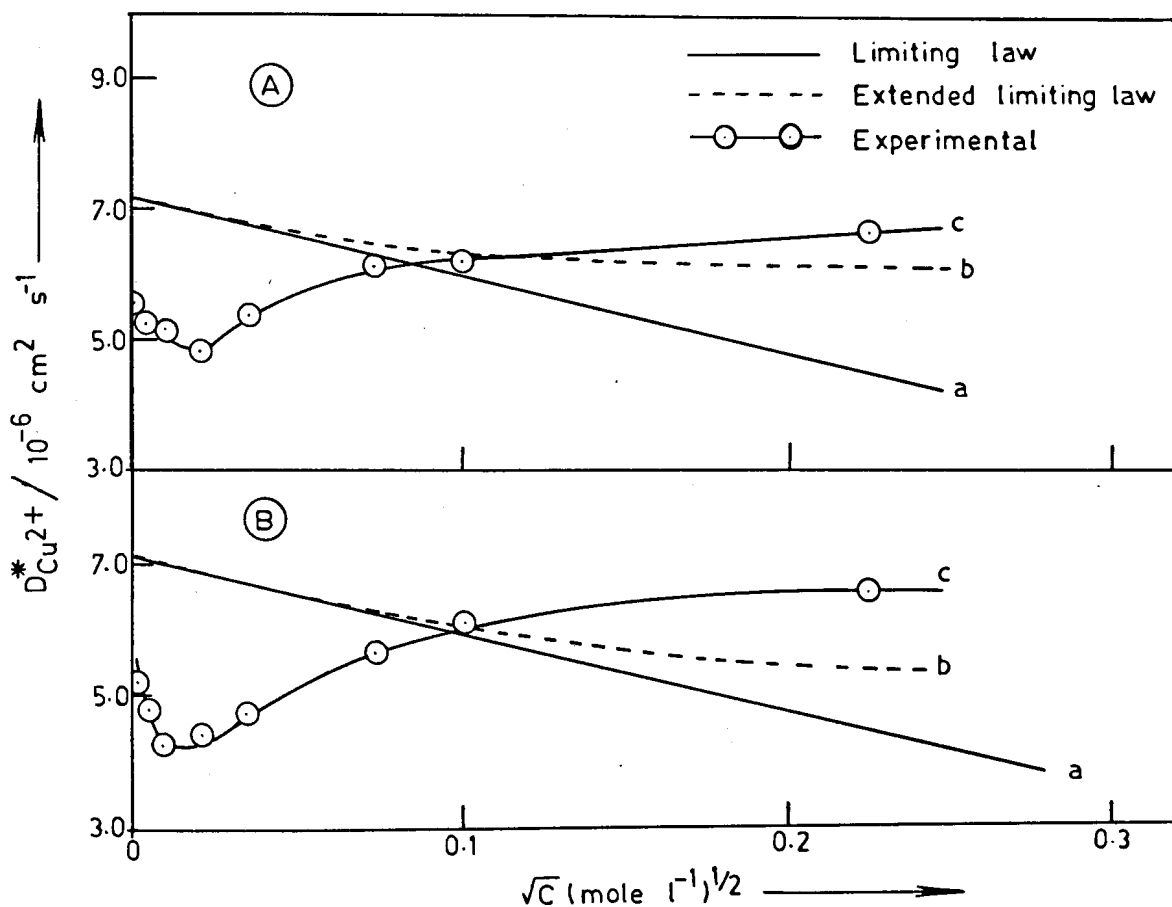


Fig.3.6: Variation of tracer - diffusion coefficient of Cu^{2+} ions with square root of concentration of
 (A) CoSO_4 and (B) MnSO_4 in 1% agar gel at 25°C .

Table 3.8 : Variation of tracer-diffusion coefficient of $^{64}\text{Cu}^{2+}$ with concentration of (A) CoSO_4 and (B) MnSO_4 in 1% agar gel at 25°C

(A) CoSO_4

Conc./mole l^{-1}	$D_{\text{Cu}^{2+}}^*/10^{-6} \text{ cm}^2 \text{ s}^{-1}$		
	Limiting law	Theoretical Extended limiting law	Experimental
0	7.130	-	-
1×10^{-5}	7.094	7.095	5.591
5×10^{-5}	7.049	7.052	5.330
1×10^{-4}	7.016	7.021	5.133
5×10^{-4}	6.874	6.903	5.769
1×10^{-3}	6.786	6.824	5.551
5×10^{-3}	6.320	6.566	6.091
1×10^{-2}	5.984	6.430	6.192
5×10^{-2}	4.567	6.160	6.641

(B) MnSO_4

0	7.130	-	-
1×10^{-5}	7.093	7.094	5.079
5×10^{-5}	7.048	7.050	4.727
1×10^{-4}	7.014	7.017	4.276
5×10^{-4}	6.871	6.894	4.476
1×10^{-3}	6.764	6.790	4.741
5×10^{-3}	6.312	6.431	5.521
1×10^{-2}	5.973	6.200	6.033
5×10^{-2}	4.544	5.496	6.541

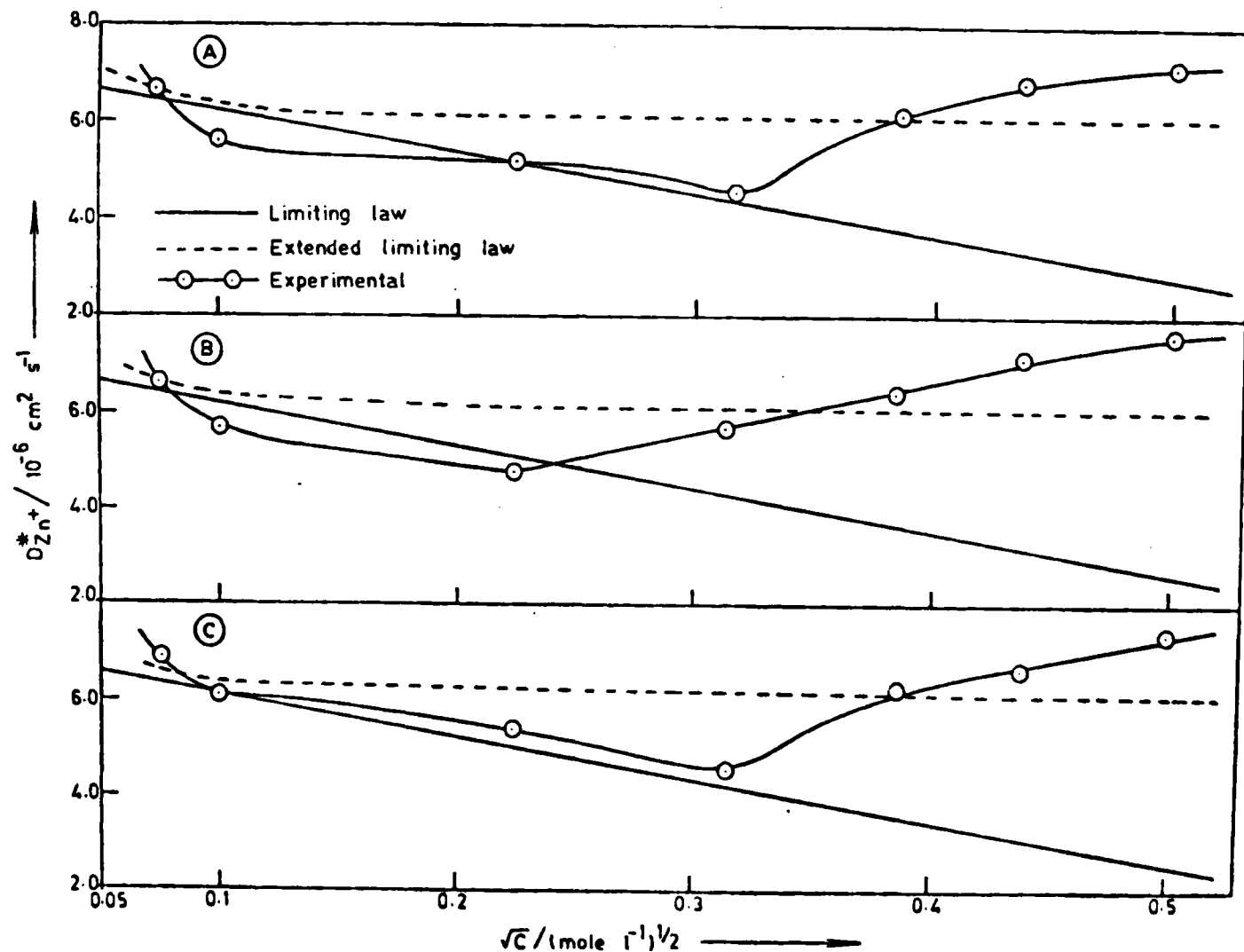


Fig.3.7: Variation of tracer-diffusion coefficient of Zn^{2+} ions with square root of concentration of (A) BaCl_2 (B) SrCl_2 and (C) MnCl_2 in 1% agar gel at 25°C .

Table 3.9 : Variation of tracer-diffusion coefficient of $^{65}\text{Zn}^{2+}$ with concentration of (A) BaCl_2 and (B) SrCl_2 in 1% agar gel at 25°C

(A) BaCl_2

Conc./mole l^{-1}	$D_{\text{Zn}^{2+}}^*/10^{-6} \text{ cm}^2 \text{ s}^{-1}$		
	Limiting law	Theoretical Extended limiting law	Experimental
0	7.024	-	-
1×10^{-2}	6.194	6.350	5.630
5×10^{-2}	5.168	6.232	5.233
0.1	4.399	6.168	4.517
0.15	3.810	6.150	6.233
0.2	3.313	6.150	6.823
0.25	2.876	6.155	7.239

(B) SrCl_2

0	7.024	-	-
1×10^{-2}	6.167	6.456	5.571
5×10^{-2}	5.107	6.182	4.847
0.1	4.312	6.107	5.754
0.15	3.702	6.035	6.430
0.2	3.189	6.030	7.135
0.25	2.737	6.034	7.619

Table 3.10 : Variation of tracer-diffusion coefficient of $^{65}\text{Zn}^{2+}$ with concentration of MnCl_2 in 1% agar gel at 25°C

Conc./mole L^{-1}	$D_{\text{Zn}^{2+}}^*/10^{-6} \text{ cm}^2 \text{ s}^{-1}$		
	Limiting law	Theoretical Extended limiting law	Experimental
0	7.024	-	-
1×10^{-2}	6.135	6.436	6.105
5×10^{-2}	5.037	6.156	5.427
0.1	4.214	6.079	4.707
0.15	3.532	6.057	6.306
0.20	3.050	6.053	6.640
0.25	2.530	6.057	7.469

3.2A Description of the Results

An examination of Figs. 3.1-3.7 (Tables 3.2-3.10) shows the presence of a minimum in the D_{expt}^* VERSUS \sqrt{C} plot for all the systems studied, in contradiction to the Onsager's theory. Usually this minimum is observed in the lower concentration range mostly between 10^{-3} - 10^{-4} M concentration except in the case of tracer-diffusion of Zn^{2+} ions. Further, another point of interest to note here is that at lower concentrations of the electrolytes D_{expt}^* is always less than the theoretical value while at the higher concentrations the case is exactly the reverse. It should be mentioned here that the theoretical values obtained by extended limiting law are only considered for comparison of experimental and theoretical diffusion coefficients in the subsequent text.

3.2.1A Tracer-diffusion of Mn^{2+} ions in manganese, magnesium, strontium and barium chlorides

It can be seen from Tables 3.2 and 3.3 (Figs. 3.1 and 3.2) that the theoretical value of $D_{\text{Mn}^{2+}}^*$ (equations 3.5b-3.8b) is always greater than the experimental one at all the concentrations studied and at concentrations $\geq 10^{-2}$ M the reverse case is observed i.e. $D_{\text{expt}}^* > D_{\text{theo}}^*$; with the exception of the $D_{\text{Mn}^{2+}}^*$ values obtained at 0.1 M concentration

in MnCl_2 and MgCl_2 systems and beyond 10^{-2} M concentration in BaCl_2 system. It is also seen from the $D_{\text{Mn}^{2+}}^*$ versus \sqrt{C} plots (Figs. 3.1 and 3.2) that the minimum occurs at 10^{-4} M concentration in MgCl_2 and SrCl_2 systems and at 5×10^{-4} M concentration in MnCl_2 and BaCl_2 systems as against its absence in the theoretical curves.

Careful examination of the Tables 3.2 and 3.3 reveals that the theoretical diffusion coefficient of Mn^{2+} in the four systems increases in the following order :



but the same trend is not observed in the case of experimental diffusion coefficients. Further, the trend in the experimental $D_{\text{Mn}^{2+}}^*$ values is also found to change with the concentration of the electrolyte; for example, the trend in experimental $D_{\text{Mn}^{2+}}^*$ at 10^{-3} M concentration of the different electrolytes is found to be



while at 0.05 M concentration this order becomes



3.2.2A Tracer-diffusion of $^{54}\text{Mn}^{2+}$ ions in manganese, copper, nickel, cobalt and zinc sulphates

It can be seen from the Tables 3.4-3.6 (Figs. 3.3 and 3.4) that the measured rate of diffusion of manganese ions decreases with concentration upto 10^{-4} M in all the transition metal sulphates studied. However, the decreasing trend in the D_{expt}^* value extends upto 10^{-3} M concentration in MnSO_4 system. Beyond these concentrations, the rate of diffusion increases with increasing concentration of the electrolytes in contrast to the Onsager's theory. Further, the experimental value is always less than the theoretical one in the lower concentration range in all the systems studied. At concentrations $\geq 10^{-2}$ M, D_{expt}^* values are found to be higher than the D_{theo}^* values with the exception at 0.05 M in CuSO_4 . However, these values are less than the Nernst limiting value, the only exception being the MnSO_4 system.

3.2.3A Tracer-diffusion of $^{64}\text{Cu}^{2+}$ ions in copper, manganese, nickel and cobalt sulphates

A glance at Tables 3.7 and 3.8 (Figs. 3.5 and 3.6) shows that at all concentrations in manganese, nickel and cobalt sulphates, the theoretical value of $D_{\text{Cu}^{2+}}^*$ is greater than the experimental one with the exception of 0.05 M concentration,

while no trend is observed between experimental and theoretical values in CuSO_4 system. Further, it may be noted from Figs. 3.5 and 3.6 that the minimum occurs at 10^{-4} M concentration in all the systems studied with the exception of CuSO_4 system wherein it occurs at 10^{-3} M.

3.2.4A Tracer-diffusion of $^{65}\text{Zn}^{2+}$ ions in strontium, manganese and barium chlorides

Similar to the earlier systems, a minimum in the plot of D_{expt}^* versus \sqrt{C} for the tracer-diffusion of Zn^{2+} ions in different systems is observed (Fig. 3.7). It occurs at 0.1 M in BaCl_2 and MnCl_2 systems and at 5×10^{-2} M in SrCl_2 system. Further, it is also seen from Fig. 3.7 (Tables 3.9 and 3.10) that the experimental value of $D_{\text{Zn}^{2+}}^*$ is less than the theoretical one, upto 0.1 M electrolyte concentration while as the concentration increases beyond this the reverse trend is observed.

3.3A Discussion

The Onsager-Fuoss¹² theory of transport processes in electrolyte solutions was based on the Debye-Huckel¹³ treatment of ion-atmosphere in dilute solutions and was never meant to be applied to solutions of concentrations higher than 0.01 M even for uni-univalent electrolytes. Hence the deviations of

the observed diffusion coefficients from the theoretically expected ones are not surprising in the present work which involves multivalent systems. Many workers have reported such deviations at higher concentrations of the electrolytes both in aqueous^{66,31,114} and in gel^{106,115} medium.

In order to bridge the gap between the experimental results and the theoretical values, the Onsager-Fuoss theory needs to be modified. But attempts to extend the Onsager-Fuoss theory to higher concentrations would encounter the same difficulties as the extension of the Debye-Huckel theory itself. Hence it is very difficult to account for the deviations quantitatively. However, the discrepancies in the observed results over the entire range of concentration studied in gel medium can be explained only qualitatively in terms of different types of interactions occurring between ions, water and the gel macromolecules.

These interactions which affect the rate of diffusion in gel medium are discussed one by one in the following section.

3.3.1A Relaxation effect

Among the different effects to be discussed in the following sections, the relaxation effect is the only one whose contribution towards the diffusion coefficient is estimated

quantitatively. The relaxation effect which gives a negative contribution towards the diffusion coefficient increases with increasing concentration of the electrolyte giving a decreasing trend in the diffusion coefficient with concentration. The theoretical treatment of the relaxation effect and its influence on tracer-diffusion coefficient of an ion is discussed in detail in Chapter 1 (Section 1.3.2.1).

3.3.2A Adsorption effect

As mentioned earlier (Section 1.8), agar is composed of agarose and agarpectin containing a sulphonyl group which confers on the gel a small cation exchange capacity. The presence of these cation exchange sites causes the adsorption of cations on the agar gel. According to Langdon and Thomas¹¹⁶, these adsorbed cations presumably migrate with a mobility lower than that of the free cations, causing the diffusion coefficient in gels to decrease when electrolyte concentrations are such that a significant fraction of the ion present in the gel is adsorbed. However, the contribution of the adsorption effect towards the overall diffusion coefficient is insignificant at higher concentrations of the electrolyte, as the ratio of the ions which get adsorbed and exchanged to the unadsorbed ions becomes very small.

The effect of adsorption on the diffusion of the cations studied in the present work is examined by giving the following treatment to agar. The solution of the respective metal salt was kept in contact with the agar for about eight days, with daily change of the solution. After eight days, this solution was filtered and agar was washed thoroughly with distilled water and dried to powder. The agar thus obtained was used for the diffusion experiments and the results were compared with that obtained using agar without the above treatment. The comparison shows that the latter D^* value is less than the former one at low concentration of the electrolyte. This observation confirms the role of adsorption in the diffusion of cation.

3.3.3A Obstruction effect

The presence of gel in the diffusion medium makes the diffusion path tortuous. This is mainly due to the irregular network of macromolecules present in it and therefore, the ions in the agar gel have to diffuse along longer paths. As the effective length of diffusion increases, the diffusion coefficient in gel medium decreases. The detailed description of this obstruction effect is given in Chapter 4.

3.3.4A Water-gel interaction

The water molecule has a permanent dipole moment. The

positive and negative charges are supposed to be situated at the four corners of a regular tetrahedron and thus each dipole is associated to four neighbouring molecules of water. This association of dipoles in water gets affected in the presence of agar molecules. These macromolecules bind the water molecules by hydrogen bonding¹¹⁷, adsorption¹¹⁸, and dipole-dipole interactions¹¹⁹ between the polar sulphonic groups and water molecules. Due to these interactions, the short range crystalline structure of water gets distorted and a loose gel-water structure is formed throughout the gel network. The distortion thus caused in the water structure increases the mobility of the ion in gel medium compared to that in aqueous solution. Hence, water-gel interactions tend to increase the diffusion coefficient of the ion in gel medium.

3.3.5A Ion-water and ion-ion interactions

When we confine ourselves to only lower concentrations of the electrolyte, the contribution of ion-ion interactions towards the diffusion of ions can be neglected¹²⁰ as the distance between the ions is sufficiently large. However, the interpretation of the results at higher concentrations demands a consideration of the contribution of ion-ion interactions towards the diffusion coefficient. These ion-ion interactions

are intimately associated with the ion-water interactions, hence we shall discuss both these interactions together.

3.3.5.1A Structure of liquid water

It has been found by many workers¹²¹ using different techniques that liquid water, under most conditions, shows a semicrystalline structure with a considerable degree of short range order, characteristic of tetrahedral bonding. This tetrahedral bonding results in a network structure somewhat similar to the structure of ice.

Frank and Wen^{122,123} in their flickering-cluster model postulated that the formation of hydrogen bonds in liquid water is predominantly a cooperative phenomena. The net result of this cooperative hydrogen bonding is that when one bond forms, there is a tendency for several to form, whereas when one breaks, an entire group tends to break. Accordingly, short lived (10^{-10} to 10^{-11} s) ice-like flickering clusters of varying sizes, consisting of highly hydrogen-bonded molecules are produced.

3.3.5.2A Structure of water near an ion

When we add an electrolyte to water, this structure of the liquid water gets affected due to ion-water interactions. The ions not only alter the dielectric polarization, binding and compression of near-neighbour molecules, but also alter the

structure of water due to its structure-breaking action. Moreover, the effects of ionic structure disturbing centres are not limited to the hydration shell immediately adjacent to the ion. Through the torque, which their electric fields exert on water dipoles, ions both interfere with the initiation of clusters (i.e. hydrogen-bonding) and hasten cluster disruption.

Frank and Wen¹²² introduced a simple model to describe the structure of water near an ion. The central consideration of their model is that the ions orient water dipoles. The spherically symmetrical electric field of the ion may tear water dipoles out of the water lattice and make them point with the appropriate charged end towards the central ion giving rise to ion-dipole forces. Due to the operation of those ion-dipole forces, a certain number of water molecules in the immediate vicinity of the ion may be trapped and oriented in the ionic field (Fig. 3.8). Such water molecules cease to associate with other water molecules to form the networks, characteristic of water. They are immobilized except in so far as the ion moves, in which case the sheath of immobilized water molecules moves with the ion. In other words, the ion and its water sheath are a single kinetic entity. Thus, the picture (Fig. 3.8, region A) is of ions enveloped by a solvent sheath of oriented immobilized water molecules.

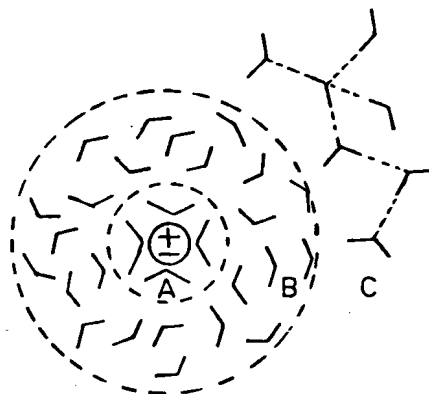


Fig.3.8- A simple model for the hydration of an ion. A, region of immobilization of water molecules. B, region of structure-breaking. C, structurally normal water.

At a distance sufficiently away from the ion, the influence of positive ion is negligible, because the ionic fields becomes attenuated virtually to zero and the normal structure of water remains undisturbed (region C). In the region between the solvent sheath and the bulk water (i.e. region B), the orientating influences of the ion and the water network operate; the former tries to align the water dipoles parallel to the spherically symmetrical ionic field, and the water network tries to restore the water in this region to its normal tetrahedral

arrangement. Caught between the two types of influences, the intermediate water adopts a compromise structure that is neither completely oriented nor disoriented. The compromising water molecules are not close enough to the ion to become oriented perfectly around it, nor are they sufficiently far away from the ion to be part of the structure of bulk water; hence depending on their distances from the ion, they orient out of the water network to varying degrees. In this intermediate region, the water structure is said to be partly broken down and the region is known as structure-breaking region.

3.3.5.3A Structure-breaking and structure-forming ions

Relatively small ions and multivalent ions such as Li^+ , Ca^{2+} and Al^{3+} increase the viscosity of water and thus are said to have a net structure-making effect. Their high electric fields not only polarise, immobilise and electrostrict the nearest neighbour water molecules but they induce additional order beyond the first water layer. The activation energy for the exchange of nearest neighbour water molecules about such ions is positive i.e. the primary hydration water is less mobile than the bulk water. On the other hand, large monovalent ions generally have a net structure-breaking effect. Because of the ion-dipole repulsion between the solvation shell molecules, the relatively weak electrostatic field about such

ions can cause polarization, immobilization and electrostriction of water molecules only in the first layer. Beyond this layer a strong structure-breaking effect persists. Thus, ions such as K^+ , Cl^- and I^- actually increase the fluidity of water.

By considering the Frank and Wen model of water near an ion, and the structure-breaking and structure-forming properties of the ions, Hertz *et al.*⁶⁶ proposed a model for explaining the diffusion coefficient-concentration curve, specially at higher concentrations. The brief outline of the model is described below.

3.3.5.4A The model of Hertz et al.

The essence of this model is the assumption that water-ion aggregates exist whose sizes and therefore diffusion velocities depend on the structure-breaking and structure-forming capacities of the different ions.

As we can see from the Fig. 3.9, the central ion, which is diffusing, is surrounded by two hydration spheres containing each four water molecules. If it is assumed that all these particles have correlated instantaneous velocities, they form an aggregate and the central reference ion is the part of this aggregate. The velocity of this central ion is denoted

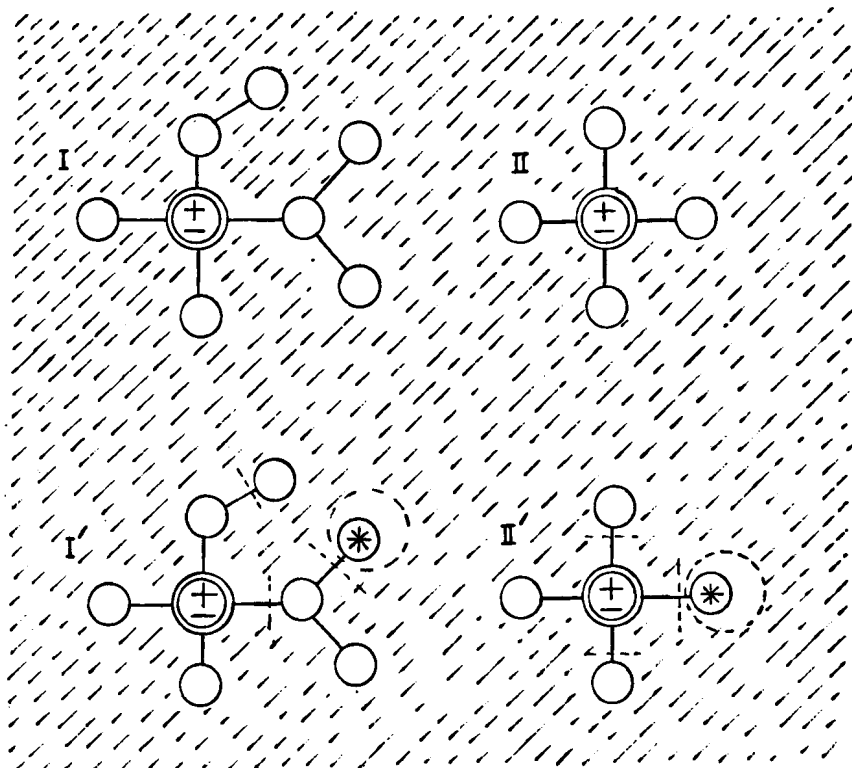


Fig.3.9-Schematic representation of the Hertz et al. model for self-diffusion of an ion.

as V and the water molecules which envelop the central ion also have essentially the same velocity as the central ion, so that

$$\vec{v}_1(1) \simeq \vec{v}_1(2) \simeq \dots \simeq \vec{v}_2(5) \simeq \dots \simeq \vec{v}_2(8) \simeq \vec{v}$$

All these water molecules have the correct relative orientations and distances such that they form a hydrogen bonded network. The superscript and subscript represent the numbering of the water molecule and hydration sphere respectively. The hatched area in the Fig. 3.9 is filled with water molecules which are not properly oriented so as to form hydrogen bonds with the water molecules in the first and the second hydration spheres. In the hatched area, the molecular velocities are uncorrelated with respect to the reference water.

Now, as depicted in Fig. 3.9, the central reference ion is part of the aggregate and hence its diffusion coefficient will be equal to that of the aggregate. As the aggregate size is large, the diffusion coefficient of the ion will be small, denoted by D_I . This would be the only diffusion coefficient of this ion, if the aggregate had an infinite life-time, but this is not so. According to Frank and Wen¹²², this aggregate size surrounding the ion fluctuates due to kinetic and potential energy fluctuations e.g. the original aggregate I may have lost all the members in the second hydration sphere resulting into aggregate II with diffusion coefficient D_{II} and as the aggregate II is smaller in size $D_{II} > D_I$.

Further, as shown in Fig. 3.9, the aggregate I' is same as aggregate I, but the couplings in the neighbourhood of the water molecule indicated by a star are modified. One possibility is that the bonds are decoupled indicated by the dashed lines. Now we have aggregates which are truncated compared to the original one. Let their diffusion coefficients be D_I° , D_I^{\prime} , $D_I^{\prime\prime}$ where the number of primes denotes the number of decoupled H-bonds, therefore we have,

$$D_I < D_I^{\circ} < D_I^{\prime} < D_I^{\prime\prime}$$

Similarly the truncated first sphere configuration for aggregate II, as sketched in Fig. 3.9 II' have the order :

$$D_{II} < D_{II}^{\circ} < D_{II}^{\prime} < D_{II}^{\prime\prime}$$

The dashed circle in aggregate I and II shows that the water molecule with a star is expanded so as to be a larger particle, with coupling to its neighbour unaltered and having the diffusion coefficients

$$D_I^*, (D_I^* < D_I) \quad \text{and} \quad D_{II}^*, (D_{II}^* < D_{II})$$

for the aggregate I and II respectively.

As a consequence of the fluctuating aggregate size,

the mean diffusion coefficient of an ion which is experimentally observed is given by the following expression :

$$D_{ion} = P_0 D_0^+ + \dots + P_I D_I + \dots \\ + P_I^I D_I^I + P_I^{II} D_I^{II} + \dots \\ + P_{II} D_{II} + \dots \\ + P_{II}^I D_{II}^I + P_{II}^{II} D_{II}^{II} + \dots$$

where D_0 is the diffusion coefficient of an ion in a configuration with all neighbours unbound to the central ion, P is the probability of occurrence of the particular aggregate and dots have the meaning of all other aggregates.

The structure-breaking or structure-forming ions cause the change in the aggregate size around the central ion. In the case of structure-breaking ions, the aggregate sizes are reduced due to the truncation of hydrogen bonds while the structure-forming ions increase the total aggregate size.

3.4A Interpretation of the Results

The deviations observed between the theoretical and experimental values of diffusion coefficients in all the systems studied can be explained only qualitatively in the light of various types of interactions discussed above.

To interpret the results of ion-diffusivity in gel medium, one has to take into consideration the role of gel molecules in determining the experimental values of diffusion coefficients. As described in the previous section, the obstruction and adsorption effects reduce the diffusion rate while water-gel interaction enhances the diffusion rate in gel medium in comparison with the value expected in pure aqueous medium. It is noticed from the Figs. 3.1-3.7 that the observed tracer-diffusion coefficient values of various ions studied are lower than the theoretical ones in the lower concentration range. This observation is attributed to the dominance of the obstruction and adsorption effects over the gel-water interactions. However, at higher concentrations, adsorption effect as discussed in Section 3.3.2A decreases, at the same time obstruction effect is also known to decrease with increasing concentration¹¹³. Thus, the contribution of these retarding effects is reduced and therefore the water-gel interaction becomes more prominent.

In addition to this, the ion-water and ion-ion interactions which enhance the diffusion rate play an important role at these concentrations. The overall result of all these effects lead to higher D^* values than that predicted by the theory. Further, as can be seen from the Tables 3.2 - 3.10,

the deviations from the theoretical values vary with concentration for a particular system and also vary from system to system indicating that the degree of interaction of these effects varies with the nature of the electrolyte as well as its concentration.

Further, it is also evidenced from the Figs. 3.1-3.7 that at higher concentrations, the experimental values are not only higher than theoretical one, but they also change the trend in the D_{expt}^* versus \sqrt{C} plot i.e. instead of a decrease in D_{expt}^* with increasing concentration, we observe an increasing trend in diffusion coefficient with concentration of the electrolyte. This reversal of trend in diffusion coefficient-concentration curve gives rise to a minimum. The occurrence of such a minimum in the D_{expt}^* versus \sqrt{C} plot has been reported by several workers both in aqueous^{31,114} and in gel^{106,108,124} medium. However, the position of the minimum varies from system to system, e.g. it occurs at 10^{-4} M for tracer-diffusion of Mn^{2+} in MgCl_2 system while in case of tracer-diffusion of Zn^{2+} in SrCl_2 system it is observed at 5×10^{-2} M.

The presence of such a minimum in the D_{expt}^* versus \sqrt{C} curve can be satisfactorily explained qualitatively on the basis of the model of Hertz et al.⁶⁶ (see 3.3.5.4A) and also

the
with/aid of Wang's³¹ model which takes into consideration the changes in the physical properties such as dielectric constant at microscopic level in the solution with increasing electrolyte concentration. Let us discuss the trend in diffusion-coefficient observed over the entire range of concentration studied in a particular system. Fig. 3.1 (Table 3.2) reveals that the rate of diffusion of Mn^{2+} in $MnCl_2$ decreases with concentration upto 5×10^{-4} M and then rises giving rise to a minimum in the $D_{Mn^{2+}}^*$ versus \sqrt{C} curve. The initial decrease in diffusion coefficient with concentration is in qualitative agreement with the Onsager's theory. In the lower concentration range, the ions are fully hydrated and as the average distance between the ions is very large, hydration and ion-solvent interactions remain the same and ion-ion interactions are also negligible at lower concentrations. Hence, the only effect of increasing salt concentration in this range is to increase the long-range ionic attraction (i.e. the relaxation effect) which gives decreasing trend in D_{expt}^* with concentration.

However, when the concentration of the ion increases beyond 5×10^{-4} M in $MnCl_2$ system, the average distance between ions goes on decreasing and so also the number of water molecules between them. According to Wang, as the distance

between two ions is reduced, it becomes difficult for the water molecules to orient themselves for maintaining the stable semicrystalline structure of water which exists at infinite dilution. Hence, the semi-crystalline structure of water gets distorted giving a decrease in the local dielectric constant of the solvent water. This decrease in dielectric constant increases the self-energy of the ions in the normal state while the energy of the activated state remains unaffected. Thus the total energy barrier for diffusion of ions is reduced and hence the rate of diffusion increases with concentration. The increase in the D_{Mn}^{*2+} with concentration of $MnCl_2$ beyond the minimum indicates that the effect of increase of self-energy dominates over the relaxation effect. A similar treatment can also be applied to other systems in order to account for the observed minimum in the D_{expt}^{*} versus \sqrt{C} plot.

The observed trend in D_{expt}^{*} beyond the minimum in various systems can also be explained alternatively by considering the model of Hertz et al.⁶⁶ which assumes the formation of water-ion aggregates whose sizes and therefore diffusion velocities depend on the structure-breaking and structure-forming properties of the different ions. The ion-water aggregates are formed in the solution of the electrolyte and the diffusing ion at the centre of aggregate is enveloped

by the first and the second hydration spheres of water molecules. The size of these aggregates gets affected by the structure-breaking or structure-forming properties of the approaching ion. The fluctuating aggregate sizes as mentioned earlier, then determine the magnitude of diffusion coefficient. In the present systems studied, it is well established that the chloride^{122,125} and sulphate¹²⁶ ions are structure-breaking in nature. Hence, the approach of such ions towards the central reference ion gives rise to decoupling of the hydrogen bonds. As the hydrogen bonds get decoupled, the aggregate size becomes small and as the concentration of the electrolyte increases, more and more hydrogen bonds get decoupled giving a larger proportion of smaller aggregate sizes which results in an increase of the diffusion coefficient with concentration of the electrolyte as observed in all the systems studied.

Though we can justify the presence of minimum in the D_{expt}^* versus \sqrt{C} curve, with the help of the model of Wang³¹ and of Hertz et al.⁶⁶, it is difficult to account for its occurrence at different concentrations in various systems. However, it appears to be the resultant of various types of interactions taking place in a given system controlling the overall diffusion process.

Section B : Variation of Electrolyte-Diffusion Coefficient with Concentration of the Electrolyte

This section covers the results obtained in the study of electrolyte-diffusion of MnCl_2 and MnSO_4 labelled with ^{54}Mn , and CuSO_4 labelled with ^{64}Cu . The concentration range chosen for these studies was 10^{-5} to 0.1 M and diffusion coefficients were measured in 1% agar gel at 25°C . These diffusion coefficients are compared with that expected from the Onsager-Fuoss theory for electrolyte-diffusion.

3.1B Theoretical Value of D'

As mentioned earlier, the diffusion coefficient of an electrolyte is definitely get influenced by the concentration dependent electrophoretic effect and the activity coefficient of it. Taking into consideration these two factors, Onsager and Fuoss arrived at the following expression :

$$D' = 1000 RT (\nu_1 + \nu_2) \left(\frac{\bar{M}}{C} \right) \left(1 + C \cdot \frac{\partial \ln \gamma_{\pm}}{\partial C} \right) \quad \dots (1.17)$$

where the electrophoretic term $\left(\frac{\bar{M}}{C} \right)$ and the thermodynamic term $\left(1 + C \cdot \frac{\partial \ln \gamma_{\pm}}{\partial C} \right)$ are explained by equations 1.14 to 1.16 and 1.13 respectively in Chapter 1. On the other hand, the limiting value of D' at infinite dilution, where $\left(1 + C \cdot \frac{\partial \ln \gamma_{\pm}}{\partial C} \right) \rightarrow 0$, is given by the Nernst expression:

$$D_0 = \frac{RT}{F^2} \cdot \frac{\nu_1 + \nu_2}{\nu_1 |Z_1|} \cdot \frac{\lambda_1^\circ \cdot \lambda_2^\circ}{\lambda_1^\circ + \lambda_2^\circ} \quad \dots (3.21)$$

The equivalent conductances for different ions required in theoretical calculation of D' were taken from the literature¹²⁷ and the values of ϕ , $A' \sqrt{C}$ and S_f are taken from The Physical Chemistry of Electrolytic Solutions by Harned and Owen¹²³, while the constants A' and B required in equation (1.17) are computed from the values of activity coefficients of the electrolytes at two different concentrations, using the relation

$$\log f_{\pm} = \frac{-S_f \sqrt{C}}{1 + A' \sqrt{C}} + B C \quad \dots (3.22)$$

The numerator of the first term of equation (3.22) on the right hand side gives the effect of the Coulomb forces between the ions considered as point charges, while the denominator represents the effect of the restriction on Coulomb forces imposed by the finite sizes of the ions. The term $B C$ in equation (3.22) describes the effect of change of dielectric constant with electrolyte concentration. When the term $B C$ is positive for an electrolyte, a lowering of dielectric constant is produced by the addition of ions and ions are 'salted out'

causing an increase in the activity coefficient. This increase in activity coefficient with concentration is responsible for the increase in thermodynamic factor which in turn increases the diffusion coefficient of an electrolyte and a minimum in D' versus \sqrt{C} plot occurs. On the other hand, when the term $B C$ is negative, the dielectric constant is increased by the addition of the electrolyte, the ions are 'salted in' and the activity coefficient is decreased showing an absence of minimum in D' versus \sqrt{C} curve.

The values of different parameters required in the calculation of theoretical diffusion coefficient of various electrolytes are presented in Table 3.11.

Table 3.11 : The values of various parameters required in the calculation of theoretical diffusion coefficient at 25°C for different electrolytes

Parameter	Electrolyte	MnCl ₂	MnSO ₄	CuSO ₄
γ_1		1	1	1
γ_2		2	1	1
$ Z_1 $		2	2	2
$ Z_2 $		1	2	2
λ_1°		53.5	53.5	53.6
λ_2°		76.35	80.0	80.0
S_f		1.7635	4.0727	4.0727
A_f		2.7016	1.3557	1.4071
B		0.1745	0.7910	0.6910

Substituting all these values into equation (1.13), we get expressions of D'_{theo} for different electrolytes at 25°C as follows :

$$D'_{\text{MnCl}_2} = 7.4327 \times 10^{13} \left[16.892 - \frac{5.4136\sqrt{C}}{1+2.7016\sqrt{C}} + 143.2 C \phi A' \sqrt{C} \right] \times 10^{-20}$$

$$\times \left[1 - \frac{2.0304\sqrt{C}}{(1+2.7016\sqrt{C})^2} + 0.8037 C \right] \quad \dots (3.23)$$

$$D'_{\text{MnSO}_4} = 4.9551 \times 10^{13} \left[17.216 - \frac{1.2661\sqrt{C}}{1+1.3557\sqrt{C}} + 299.92 C \phi A' \sqrt{C} \right] \times 10^{-20}$$

$$\times \left[1 - \frac{4.6893\sqrt{C}}{(1+1.3557\sqrt{C})^2} + 3.6433 C \right] \quad \dots (3.24)$$

$$D'_{\text{CuSO}_4} = 4.9551 \times 10^{13} \left[17.235 - \frac{1.2546\sqrt{C}}{1+1.4071\sqrt{C}} + 299.92 C \phi A' \sqrt{C} \right] \times 10^{-20}$$

$$\times \left[1 - \frac{4.6893\sqrt{C}}{(1+1.4071\sqrt{C})^2} + 3.1832 C \right] \quad \dots (3.25)$$

The values of D'_{theo} calculated using equations (3.23-3.25) and the different functions incorporated in it are presented in Tables 3.12-3.14 along with the D'_{expt} values obtained in the various systems studied. The results are also shown graphically in Figs. 3.10-3.12 as a function of square root of concentration of the electrolyte.

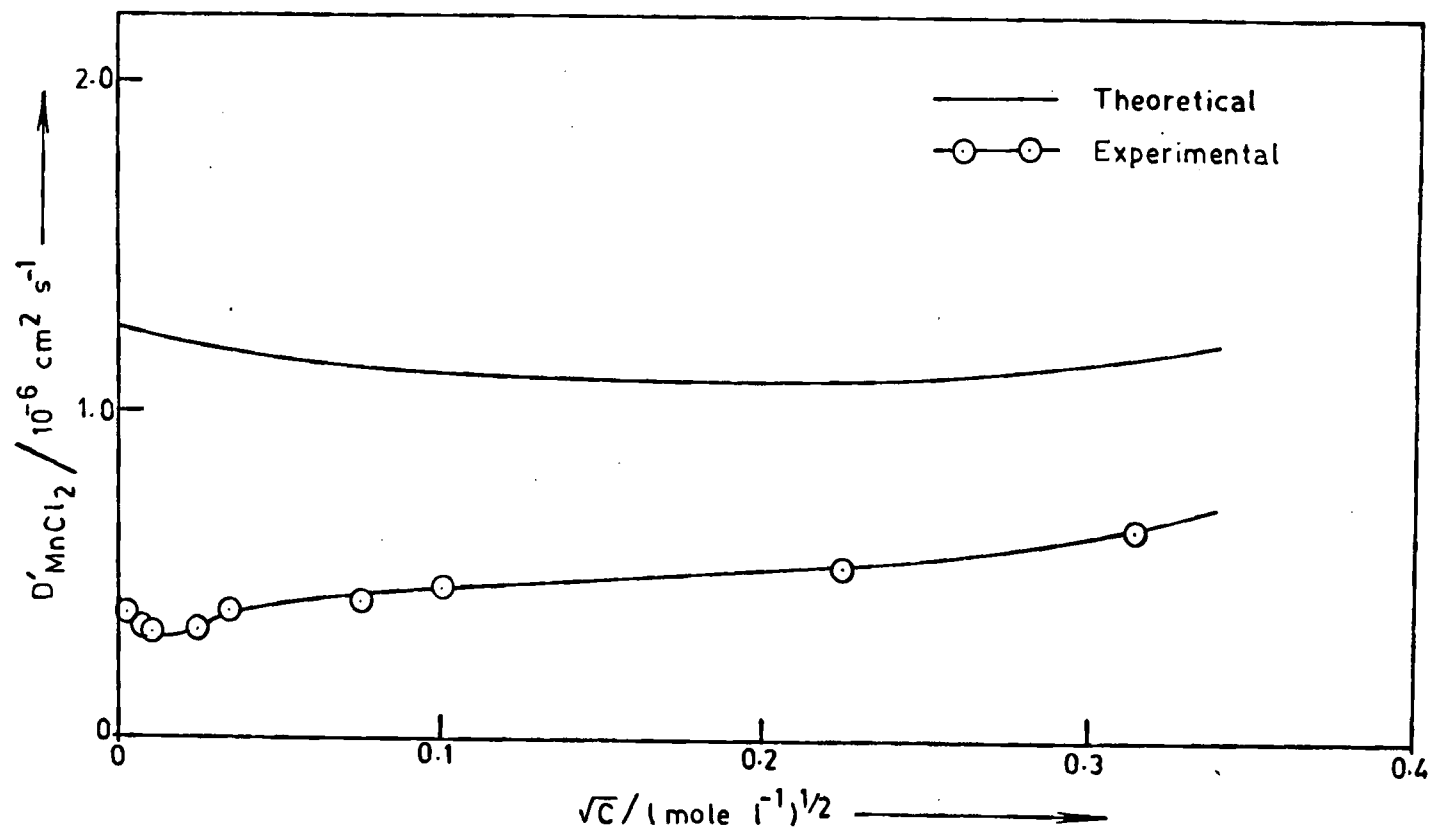


Fig. 3.10-Variation of D'_{MnCl_2} with the square root of concentration of manganese chloride in 1% agar gel at 25°C .

Table 3.12 : Variation of D'_{MnCl_2} with concentration of MnCl_2 in 1% agar gel at 25°C

Con/M	$\phi A'\sqrt{C}$	$\frac{\bar{M}}{C} \times 10^{-20}$	1+c. $\frac{\partial \ln \eta}{\partial C}$	$D'_{\text{MnCl}_2} / 10^{-6} \text{ cm}^2 \text{ s}^{-1}$	
				Theore- tical	Experi- mental
0	-	-	-	1.257	-
1×10^{-5}	3.3550	16.8798	0.9936	1.247	0.361
5×10^{-5}	2.8178	16.8746	0.9862	1.237	0.330
1×10^{-4}	2.4178	16.8739	0.9808	1.230	0.320
5×10^{-4}	1.7040	16.8998	0.9600	1.206	0.344
1×10^{-3}	1.4071	16.9357	0.9463	1.191	0.393
5×10^{-3}	0.7632	17.1170	0.9028	1.149	0.411
1×10^{-2}	0.5469	17.2489	0.8821	1.131	0.439
5×10^{-2}	0.2037	17.5978	0.8637	1.130	0.510
0.1	0.1191	17.6763	0.8936	1.174	0.634

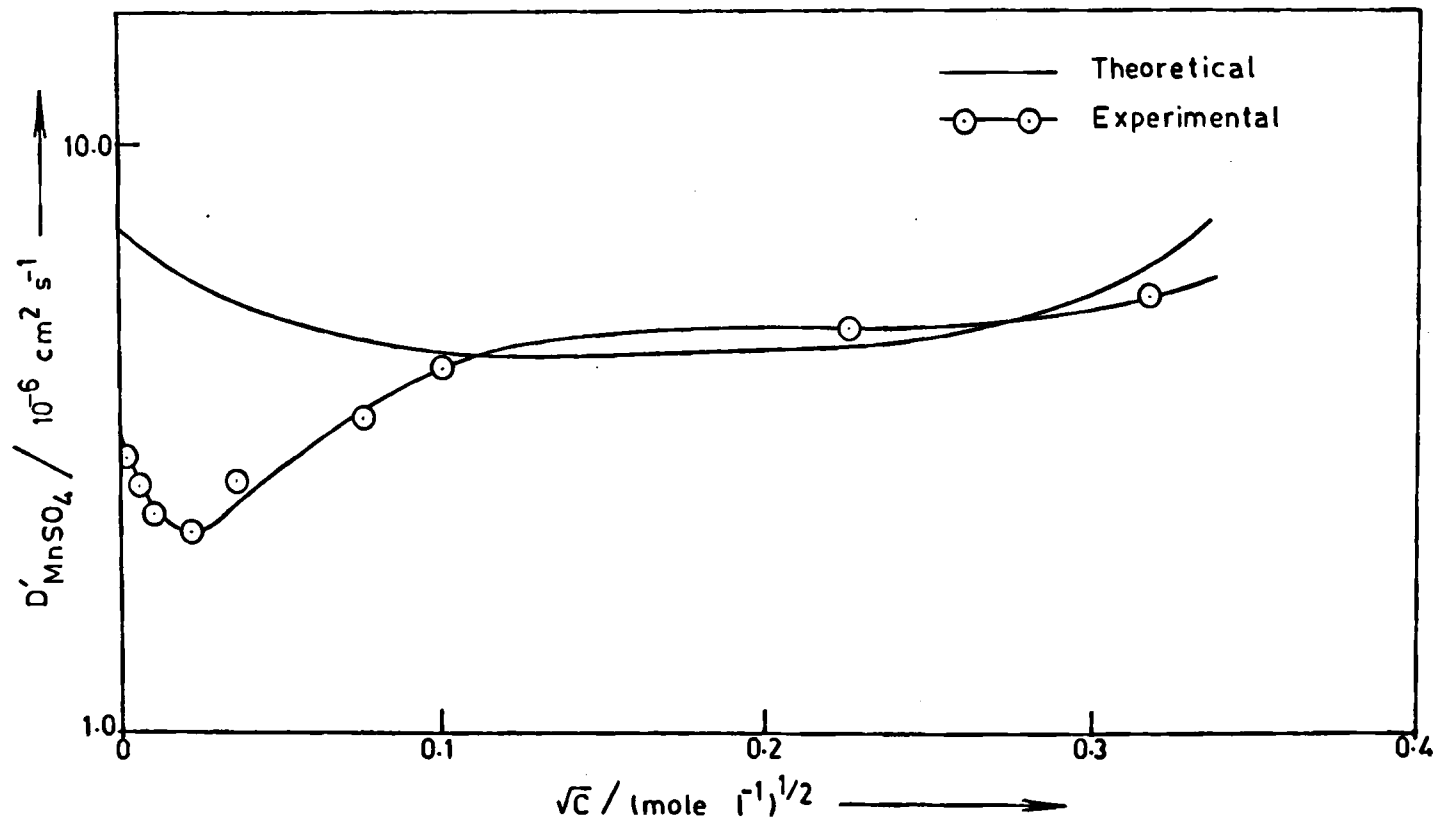


Fig.3.11-Variation of D'_{MnSO_4} with the square root of concentration of manganese sulphate in 1% agar gel at 25°C.

Table 3.13 : Variation of D'_{MnSO_4} with concentration of MnSO_4 in 1% agar gel at 25°C

Con/M	$\phi A'\sqrt{C}$	$\frac{\bar{M}}{C} \times 10^{-20}$	$1+C \cdot \frac{\partial \ln \gamma_{\pm}}{\partial C}$	$D'_{\text{MnSO}_4} / 10^{-6} \text{ cm}^2 \text{ s}^{-1}$	
				Theoretical	Experimental
0	-	-	-	8.537	-
1×10^{-5}	3.3550	17.2220	0.9853	8.408	4.241
5×10^{-5}	3.3550	17.2574	0.9676	8.274	3.875
1×10^{-4}	3.1455	17.2978	0.9547	8.183	3.496
5×10^{-4}	2.3331	17.5383	0.9030	7.847	3.236
1×10^{-3}	2.0105	17.7805	0.8672	7.640	3.913
5×10^{-3}	1.2334	19.0533	0.7421	7.008	4.962
1×10^{-2}	1.0133	20.1453	0.6727	6.715	5.575
5×10^{-2}	0.4351	24.2739	0.5647	6.792	6.061
0.1	0.3249	26.6825	0.6393	8.433	6.647

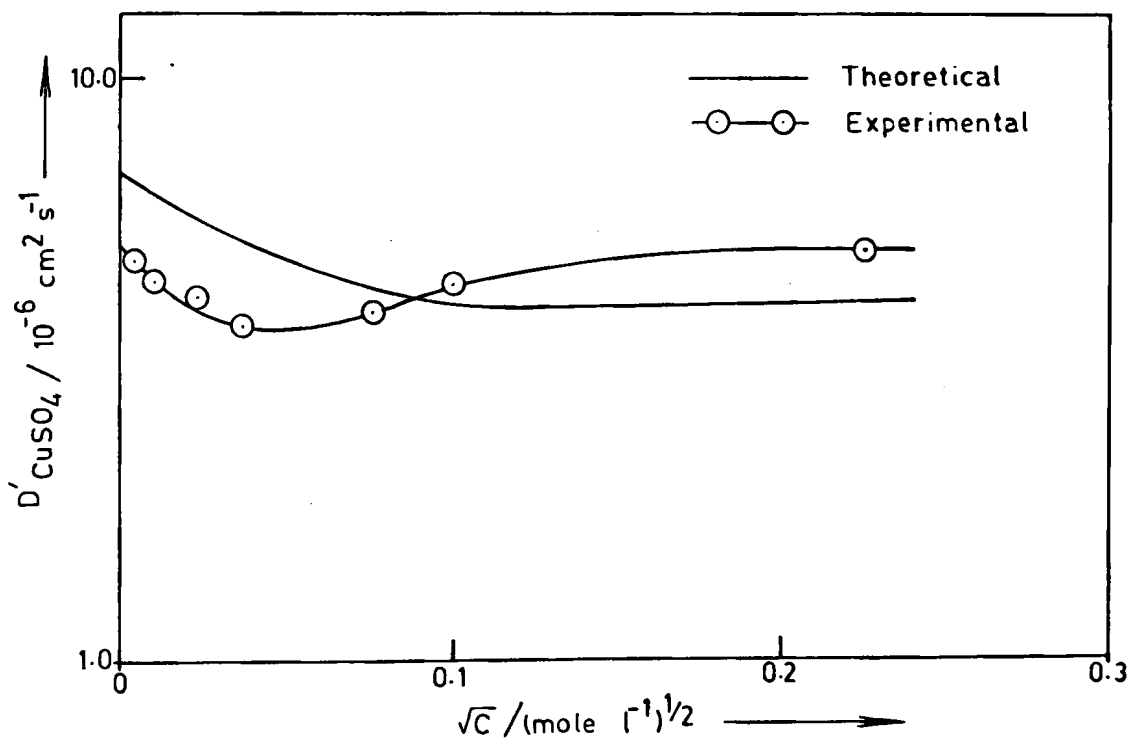


Fig.3.12 - Variation of D'_{CuSO_4} with the square root of concentration of copper sulphate in 1% agar gel at 25°C .

Table 3.14 : Variation of D'_{CuSO_4} with concentration of CuSO_4 in 1% agar gel at 25°C

Con/M	$\phi A' \sqrt{C}$	$\frac{\bar{M}}{C} \times 10^{-20}$	$1+C \cdot \frac{\partial \ln \gamma_{\pm}}{\partial C}$	$D'_{\text{CuSO}_4} / 10^{-6} \text{ cm}^2 \text{ s}^{-1}$	
				Theoretical	Experimental
0	-	-	-	8.547	-
5×10^{-5}	3.3550	17.2765	0.9676	8.233	7.182
1×10^{-4}	3.1189	17.3161	0.9540	8.136	6.980
5×10^{-4}	2.3051	17.5534	0.9030	7.854	6.726
1×10^{-3}	1.9689	17.7375	0.8612	7.590	6.126
5×10^{-3}	1.2403	19.0142	0.7416	6.983	6.300
1×10^{-2}	0.9821	20.0705	0.6714	6.677	6.875
5×10^{-2}	0.4675	24.0322	0.5529	6.573	7.345

3.2B Description of the Results

A glance at Figs. 3.10-3.12 and Tables 3.12-3.14 indicates that the experimental value of diffusion coefficient is always less than the theoretical one in MnCl_2 and MnSO_4 systems, while this is true in CuSO_4 system only upto 10^{-3} M concentration. Though the reverse trend (i.e. $D'_{\text{expt}} > D'_{\text{theo}}$) is observed in the latter system beyond 10^{-3} M concentration, the experimental values of diffusion coefficient are still less than the Nernst limiting value. Further, as can be seen from the Figs. 3.10-3.12 that a minimum is present in both theoretical and experimental diffusion curves; it occurs at 5×10^{-2} M in MnCl_2 and CuSO_4 system and at 10^{-2} M in MnSO_4 system in the former case and at 1×10^{-4} M (MnCl_2), 5×10^{-4} M (MnSO_4) and 1×10^{-3} M (CuSO_4) in the latter case. Thus, the minimum in the experimental curve occurs at the concentration which is very much lower than that predicted by the theory in all the systems studied.

3.3B Interpretation of the Results

Survey of the literature shows that the diffusion of number of alkali^{63,129-131}, alkaline earth^{70,73,62} and transition^{132,133} metal salts has been studied by several workers, both in pure aqueous solutions and in agar gel medium.

In most of the cases, the measured diffusion coefficient deviates from the theory, particularly for unsymmetrical and higher valence type electrolytes. For example, in the diffusion of CaCl_2 ⁷⁰, $\text{K}_4[\text{Fe}(\text{CN})_6]$ ¹²⁹ and Na_2SO_4 ¹³⁰ in the aqueous solution, a large divergence between theoretical and experimental diffusion coefficient was observed. This is mainly because of the difficulties involved in extending the theoretical equation to higher concentrations. As mentioned earlier, the Onsager-Fuoss¹² theory is based on the Debye-Huckel¹³ theory of electrolytes and because of the extremely complicated nature of the problem, the development of the latter theory is still awaited. Hence, the deviations observed in the present studies cannot be accounted for quantitatively. Further, the presence of gel in the diffusion medium should be duly considered in explaining the observed results.

The different interactions which influence the rate of diffusion of an electrolyte in gel medium are : (1) adsorption, (2) obstruction, and (3) electrophoretic effect and (4) ion-ion interactions at higher concentrations. Among the various factors that govern the overall experimental diffusion coefficient, contribution of electrophoretic effect to the observed diffusion coefficient can only be quantitatively determined while that of others is qualitative in nature.

As discussed in Section A, the obstruction and adsorption effects lower the value of diffusion coefficient in gel medium while gel-water interaction increase it. The results presented in Tables 3.12 and 3.13 reveal that the obstruction effect together with the adsorption effect dominates over the water-gel interaction at all the concentrations in MnCl_2 and MnSO_4 systems. In CuSO_4 system (Table 3.14), however, these effects dominate only upto 10^{-3} M concentration and higher experimental values observed beyond this concentration indicate the dominance of water-gel interaction over the other two interactions.

The shift in the experimental minimum towards the lower concentration side in relation to the theoretical minimum in the present work is similar to that observed by Patil and Adhyapak⁹⁷ in the diffusion of ZnCl_2 . This was accounted for by considering increasing ion-ion interactions and change in hydration of the ions with concentration of the electrolyte; which were not considered by Onsager and Fuoss in their theoretical treatment. The present results obtained in different systems are explained in the light of above concept.

When the concentration of the electrolyte increases, the self-energy of the central ion also increases¹³⁴. This is

to be expected, since at higher concentrations, the electric field near the central ion gets reduced by the opposing field of the ionic cloud and the central ion is desolvated effectively. This process is accompanied by an increase of lateral repulsions between the solvent dipoles of solvent molecules as these are forced against one another by interactions with nearby ions. The overall result is an increase in the activity coefficient of the electrolyte in real solution. Hence the thermodynamic term, which is a function of activity coefficient (equation 1.13), also increases giving a higher value of D'_{expt} than that predicted by the Onsager-Fuoss theory and we get an increase of D'_{expt} with concentration. It seems from Figs. 3.10-3.12 (Tables 3.12-3.14) that the effect of increase of activity coefficient starts operating at concentrations less than that predicted by the theory and hence the minimum in the D'_{expt} versus \sqrt{C} curve gets influenced and shifted to the lower concentration side.



— • CHAPTER 4 • —

• EFFECT OF GEL CONCENTRATION AND TEMPERATURE
ON THE DIFFUSION OF SOME LABELLED
IONS AND ELECTROLYTES •

CHAPTER 4

EFFECT OF GEL CONCENTRATION AND TEMPERATURE ON THE DIFFUSION OF SOME LABELLED IONS AND ELECTROLYTES

It has been shown by many workers^{116,135-137} that although agar gel provides a good stationary medium for the diffusion studies by reducing the errors due to thermal convection and mechanical disturbances to a minimum, the diffusion in agar gel undoubtedly gets influenced by its macromolecular structure. As mentioned in the previous chapter, the magnitude of the diffusion coefficient gets altered in gel medium as compared to its theoretically predicted value in pure aqueous solution.

The effect of gel macromolecules on diffusion is studied elaborately in this chapter by varying the gel concentration as well as temperature of the system. The study covers two aspects, dealt in separate sections. Section A of this chapter deals with the study of the obstruction effect in various systems under different conditions of temperature and concentration of the electrolyte while Section B deals with the determination of the activation energy for the process of diffusion for different ions and electrolytes at different gel

concentrations.

Section A : Obstruction effect

Stiles and Adair⁴⁷ were the first to study the diffusion in gels. Salvinien¹³⁸ employed cylindrical diffusion method to measure the diffusion coefficient of the electrolyte. The diffusion coefficient thus determined was found to depend on the concentration of the gel medium used. Bechhold and Ziegler⁴⁶ in their studies on diffusion of the juice of red beet found a decrease in diffusion rate by about 15% when the concentration of agar was varied from 1 to 4%. Friedman¹³⁶ in his studies on the diffusion of non-electrolytes also observed a linear dependence of the diffusion coefficients on agar gel concentration and the diffusion coefficient of urea was found to decrease by 36% when the gel percentage was varied from 0.8 to 5.15%. Further, from these studies, he determined the pore-size of the 2% agar gel which was found to be 0.29 nm.

The decrease in diffusion coefficient with increasing gel concentration observed by many workers is thought to be due to the operation of the following factors :

- (1) A reduction of diffusion space by the volume of the gel structure.
- (2) An increased resistance to motion due to the proximity of the cell wall.

- (3) An increased viscosity of the free liquid due to the presence of dissolved substances.

Survey of the literature shows that though a decrease in diffusivity rates of electrolytes^{46,106,116,135,139,140} and nonelectrolytes^{118,136,141} in the agar gel medium is observed, no systematic work as regards the obstruction effect and its dependence on various parameters has been reported, apart from the work of Thomas and coworkers^{116,135} and Patil and Adhyapak^{106,140}. Hence, it was thought of interest to study this effect by varying the different parameters of the system.

4.1A Present Work

The present work deals with the studies of effect of temperature and concentration of the electrolyte on the obstruction effect in various systems. In addition to this, the influence of different electrolytes on tracer-diffusion of Zn^{2+} and Cu^{2+} ions is also examined.

In order to study the above parameters, diffusion rates were measured in a medium of varying gel percentage in the range of 1-2.5%. The different systems chosen for these studies are :

Self-diffusion of (1) Mn^{2+} ions in MnCl_2 ,
(2) Mn^{2+} ions in MnSO_4 and
(3) Cu^{2+} ions in CuSO_4 .

Electrolyte-diffusion of (1) MnCl_2 ,
(2) MnSO_4 and
(3) CuSO_4 .

Tracer-diffusion of (1) Zn^{2+} in different chlorides and
(2) Cu^{2+} in different sulphates.

4.2A Results and Discussion

The variation of diffusion coefficient with the weight fraction of gel for self- and electrolyte-diffusion in MnCl_2 and MnSO_4 systems at 10^{-3} M concentration and in CuSO_4 system at 5×10^{-3} M concentration is shown in Tables 4.1-4.3. These results are also shown graphically in Figs. 4.1-4.3. In order to study the effect of concentration on the obstruction effect, we have chosen the MnSO_4 system in which self-diffusion of Mn^{2+} ions is carried out for three different concentrations at 30°C . These results are presented in Fig. 4.4. Further, Figs. 4.5 and 4.6 show the effect of different electrolytes on the tracer-diffusion of Zn^{2+} and Cu^{2+} ions respectively.

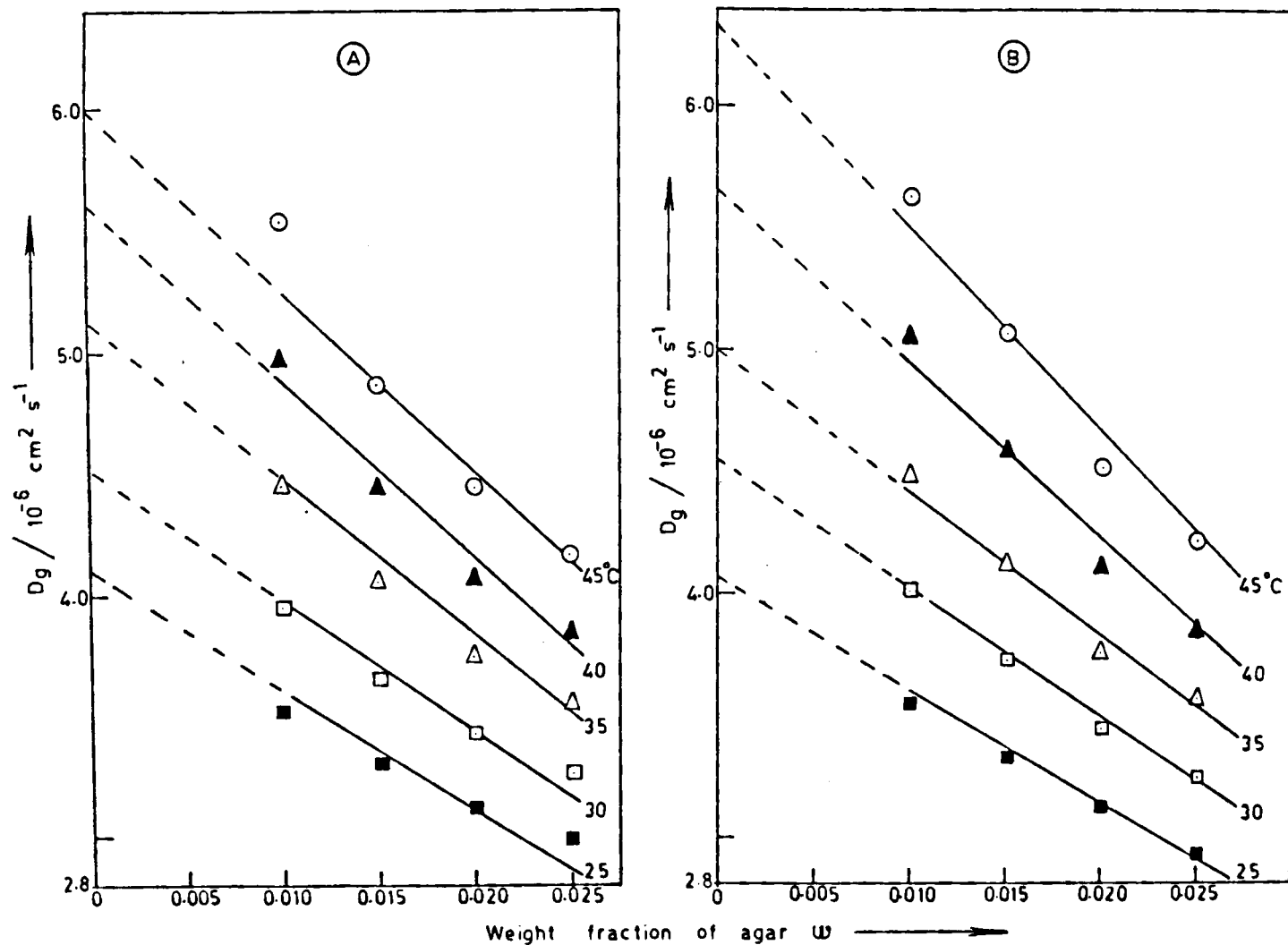


Fig.4.1-Obstruction effect in the (A) electrolyte-diffusion of $MnCl_2$ and (B) self-diffusion of Mn^{2+} in $MnCl_2$ at 10^{-3} M concentration.

Table 4.1 : Variation of diffusion coefficient with weight fraction of gel at different temperatures for (A) electrolyte-diffusion of MnCl_2 and (B) self-diffusion of Mn^{2+} in MnCl_2 at 10^{-3} M concentration

(A) Electrolyte-diffusion of MnCl_2

Temp/°C \ w	$D_g/10^{-6} \text{ cm}^2 \text{ s}^{-1}$				α value
	0.01	0.015	0.020	0.025	
25	3.521	3.316	3.145	3.027	12.19
30	3.968	3.664	3.440	3.294	12.43
35	4.461	4.043	3.757	3.530	12.69
40	4.993	4.443	4.088	3.879	12.98
45	5.567	4.866	4.435	4.189	12.50

(B) Self-diffusion of Mn^{2+} in MnCl_2

25	3.561	3.336	3.122	2.944	11.33
30	4.008	3.720	3.435	3.234	11.60
35	4.500	4.141	3.772	3.544	11.42
40	5.030	4.591	4.123	3.872	11.43
45	5.600	5.070	4.502	4.216	11.90

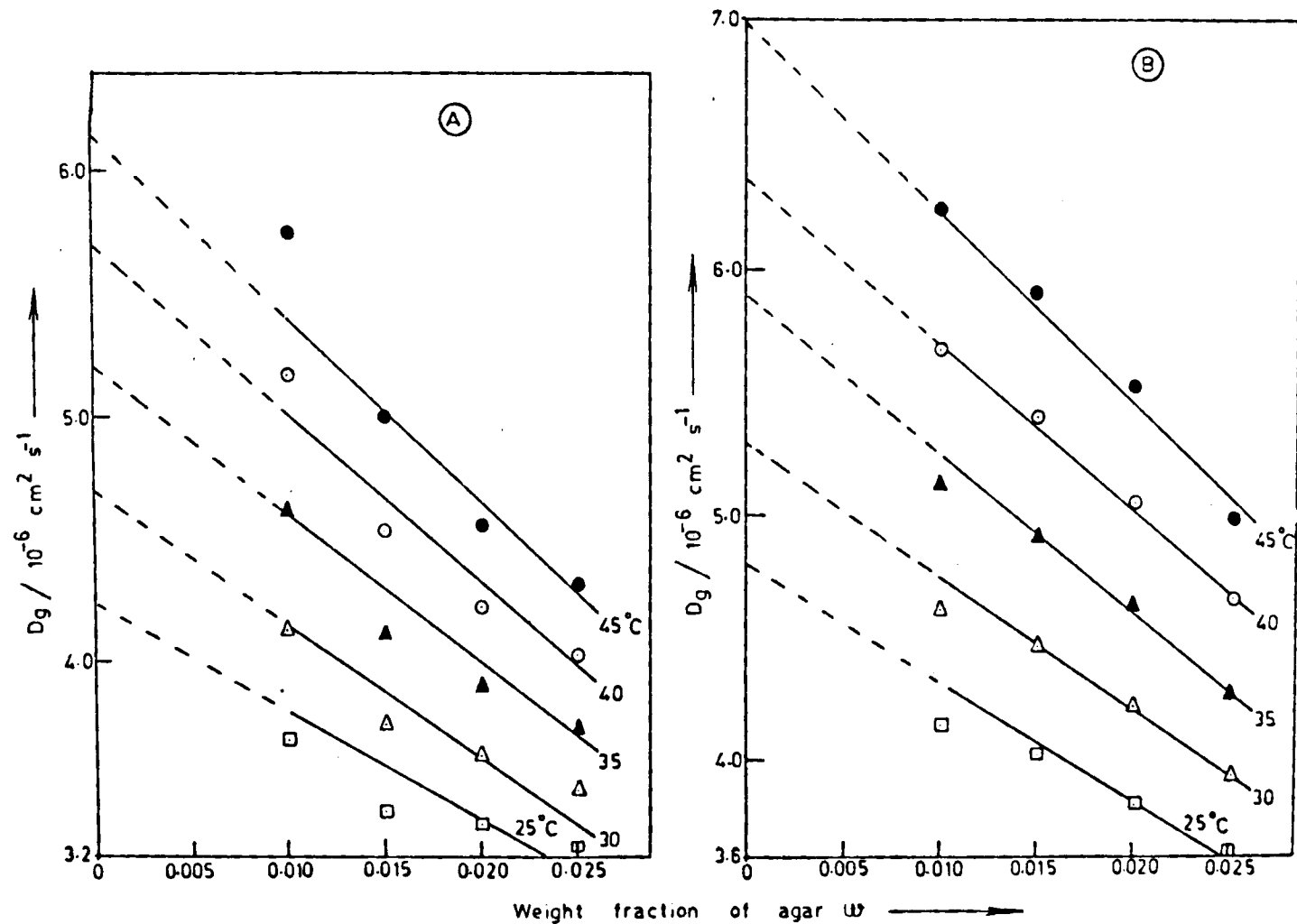


Fig. 4.2-Obstruction effect in the (A) electrolyte-diffusion of MnSO_4 and (B) self-diffusion of Mn^{2+} in MnSO_4 at 10^{-3} M concentration.

Table 4.2 : Variation of diffusion coefficient with weight fraction of gel at different temperatures for (A) electrolyte-diffusion of MnSO_4 and (B) self-diffusion of Mn^{2+} in MnSO_4 at 10^{-3} M concentration.

(A) Electrolyte-diffusion of MnSO_4

Temp/°C	w	$D_g/10^{-6} \text{ cm}^2 \text{ s}^{-1}$				α value
		0.01	0.015	0.020	0.025	
25		3.685	3.395	3.311	3.249	11.32
30		4.142	3.756	3.601	3.497	11.82
35		4.647	4.148	3.911	3.763	11.53
40		5.192	4.564	4.234	4.034	11.69
45		5.774	5.001	4.571	4.316	11.94

(B) Self-diffusion of Mn^{2+} in MnSO_4

25	4.128	4.038	3.818	3.616	10.41
30	4.600	4.461	4.205	3.934	10.37
35	5.118	4.918	4.623	4.274	10.59
40	5.670	5.402	5.065	4.629	10.18
45	6.259	5.914	5.530	4.999	10.71

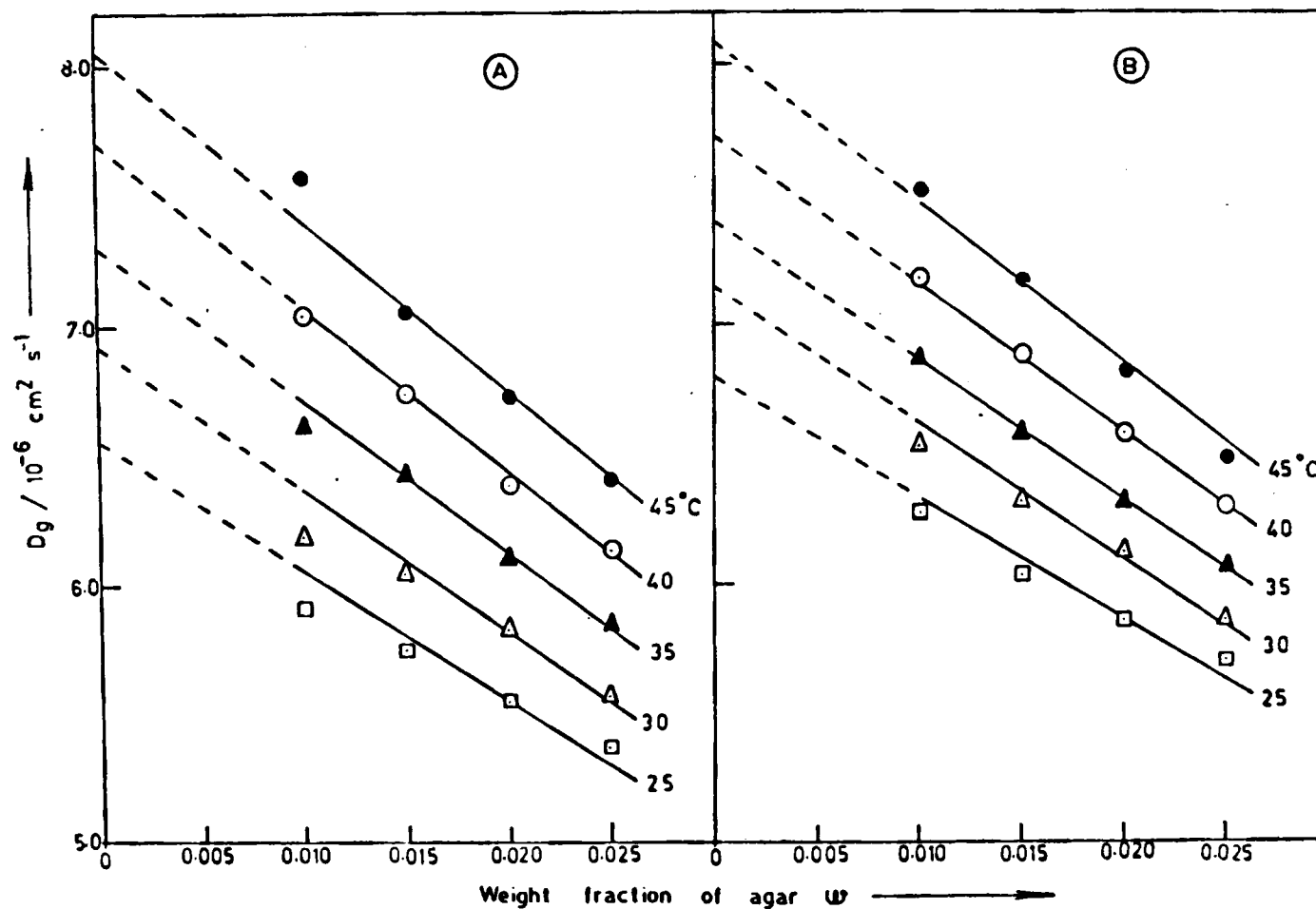


Fig.4.3-Obstruction effect in the (A) electrolyte-diffusion of CuSO_4 and (B) Self-diffusion of Cu^{2+} in CuSO_4 at $5 \times 10^{-3} \text{ M}$ concentration.

Table 4.3 : Variation of diffusion coefficient with weight fraction of gel at different temperatures for (A) electrolyte-diffusion of CuSO_4 and (B) self-diffusion of Cu^{2+} in CuSO_4 at 5×10^{-3} M concentration

(A) Electrolyte-diffusion of CuSO_4

Temp/°C	w	$D \times 10^{-6} \text{ cm}^2 \text{ s}^{-1}$				α value
		0.01	0.015	0.020	0.025	
25		6.021	5.792	5.561	5.262	7.31
30		6.342	6.082	5.801	5.510	7.94
35		6.701	6.412	6.121	5.810	8.21
40		7.062	6.722	6.401	6.101	7.30
45		7.400	7.082	6.722	6.414	8.03

(B) Self-diffusion of Cu^{2+} in CuSO_4

25	6.021	5.792	5.561	5.262	6.91
30	6.342	6.082	5.801	5.510	7.16
35	6.701	6.412	6.121	5.810	7.25
40	7.062	6.722	6.401	6.101	7.12
45	7.400	7.082	6.722	6.414	7.42

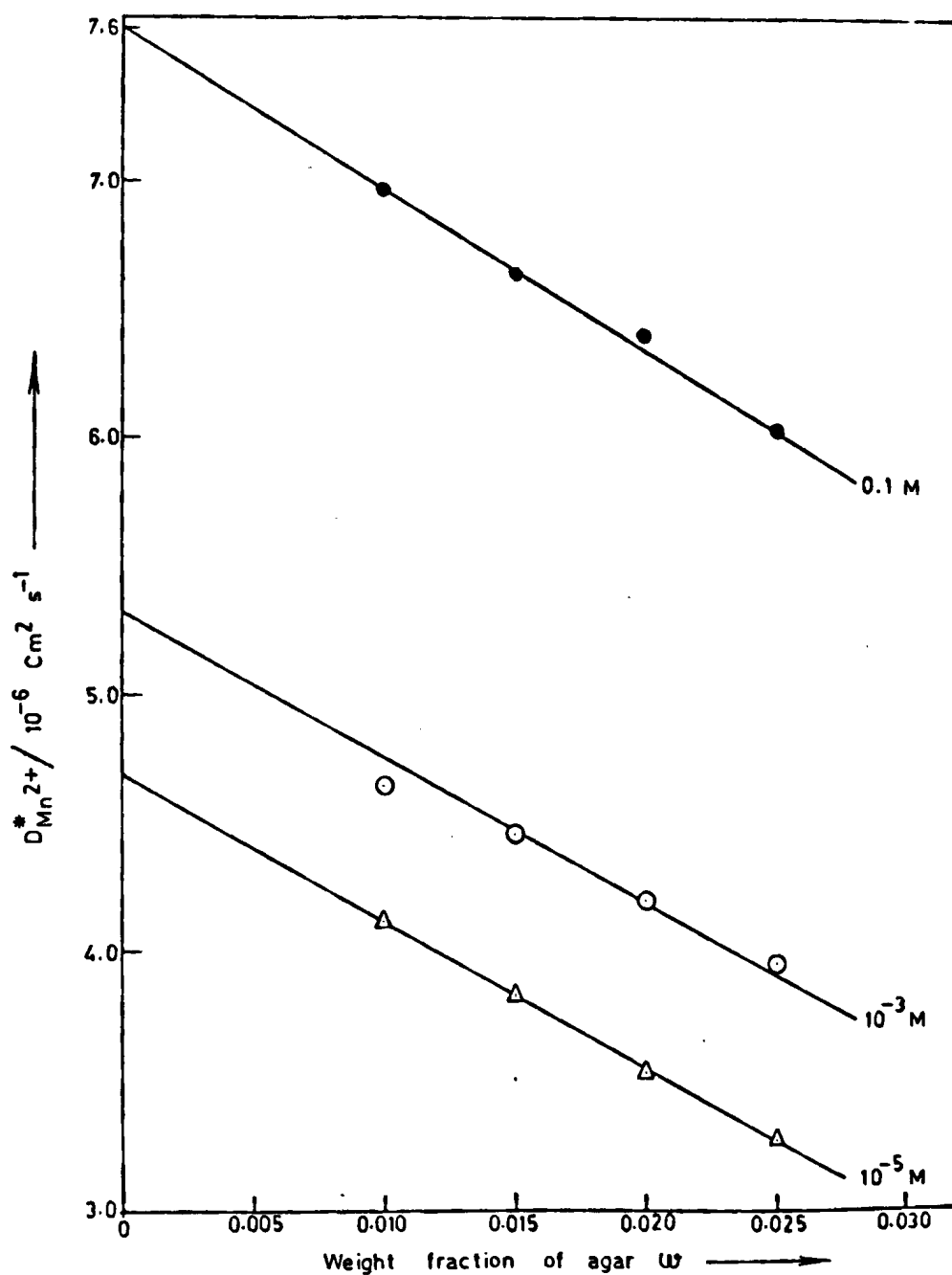


Fig 4.4-Obstruction effect in the self-diffusion of Mn^{2+} ions at different concentrations of $MnSO_4$ at 30°C

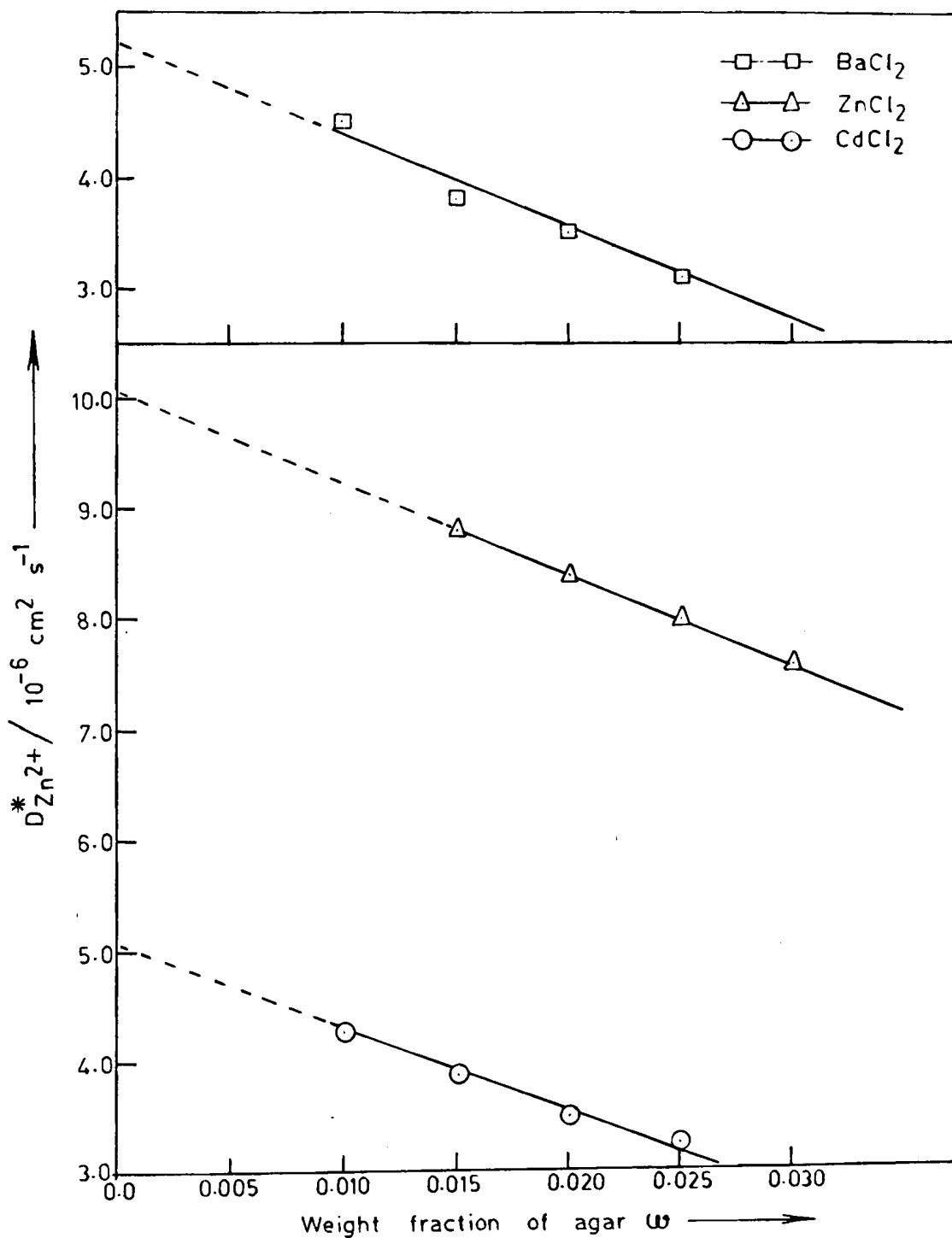


Fig.4.5-Obstruction effect in the tracer-diffusion of Zn^{2+} ions at 30°C in presence of different electrolytes.

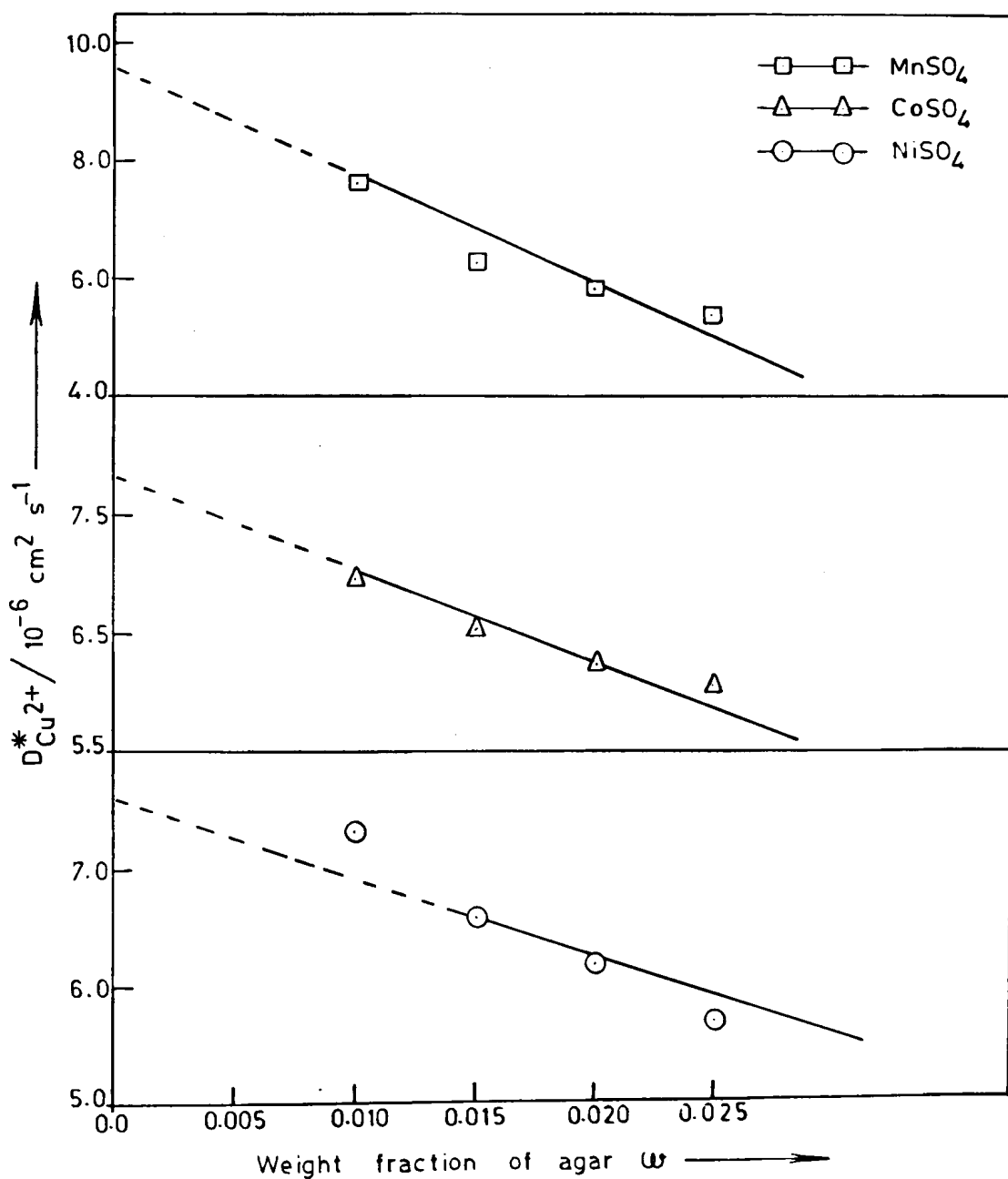


Fig.4.6-Obstruction effect in the tracer-diffusion of Cu^{2+} ions at 30°C in presence of different electrolytes.

The common feature to be noted from Figs. 4.1-4.6 is that the diffusion coefficient decreases linearly with increasing gel concentration in all the systems studied in agreement with the previous reports^{116,135,137,140}. This decrease is expected from the obstruction theory of Slade et al.¹³⁵ obeying a relation of the type

$$D_g = D_s - aW \quad \dots (4.1)$$

where D_g is the diffusion coefficient in gel medium, D_s is the extrapolated value of D_g to zero agar content for the given concentration of the electrolyte and a is the slope of the plot of D_g versus W . The decrease in diffusion coefficient with increasing gel concentration is attributed to the three-dimensional irregular network of agar macromolecules which have a much smaller diffusion coefficient due to high molecular weight than the diffusing ions. These large and almost stationary agar macromolecules obstruct the movement of ions. The ion near an agar molecule has to diffuse along longer path in order to get to the other side of the agar molecule. This lengthening of the diffusion path increases with increasing gel concentration and therefore one expects a lowering of diffusion coefficient with increasing gel concentration as observed.

Slade et al.¹³⁵ and Langdon and Thomas¹¹⁶ described

this obstruction in the diffusion path in terms of formation factor F , which is defined as the ratio of diffusion coefficient in aqueous solution to that in the gel medium. Thus,

$$F = \frac{D_s}{D_g} \quad \dots (4.2)$$

Substitution of the value of D_g from equation (4.1) gives

$$F = \frac{1}{1 - \frac{a}{D_g} \cdot \omega} = \frac{1}{1 - \alpha \omega} \simeq 1 + \alpha \omega \quad \dots (4.3)$$

where $\alpha = a/D_g$. \dots (4.4)

The obstruction effect in terms of α defined by equation (4.4) is calculated from the D_g ~~versus~~ ω plots. The values of α obtained in various systems under different experimental conditions are recorded in Tables 4.1-4.6.

Table 4.4 : Mean α -values for different systems

System	Mean α -value
<u>Self-diffusion</u>	
Mn^{2+} in MnCl_2	11.54
Mn^{2+} in MnSO_4	10.45
Cu^{2+} in CuSO_4	7.17
<u>Electrolyte-diffusion</u>	
MnCl_2	12.56
MnSO_4	11.66
CuSO_4	7.97

Table 4.5 : Effect of concentration on the α -value
for the self-diffusion of Mn^{2+} ions in
 MnSO_4

Concentration/mol l^{-1}	α -value
10^{-5}	13.02
10^{-3}	10.45
0.1	8.37

Table 4.6 : Effect of electrolyte on the α -value
for tracer-diffusion of Zn^{2+} and Cu^{2+}
ions

System	α -value
<u>Tracer-diffusion of Zn^{2+} ions</u>	
in ZnCl_2	8.54
in CaCl_2	14.90
in BaCl_2	16.03
<u>Tracer-diffusion of Cu^{2+} ions</u>	
in NiSO_4	8.83
in CoSO_4	10.12
in MnSO_4	18.04

A careful examination of the Tables 4.1-4.6 leads to the following important observations.

- (1) For a particular concentration of the electrolyte, α -value is independent of temperature (Tables 4.1-4.3).
- (2) For a particular system, α -value is higher for electrolyte-diffusion as compared to its value for the self-diffusion (Table 4.4).
- (3) At a given temperature, α -value decreases with increasing concentration of the electrolyte (Table 4.5).
- (4) In tracer-diffusion, α -value decreases with increasing charge density of cation of the electrolyte (Table 4.6).

Constant value of α for different temperatures for a given system indicates that no significant change in the geometry of macromolecules obstructing the path of diffusion occurs over the temperature range studied. On the other hand, the different experimental α -values observed for various systems studied are attributed to different degrees of interactions occurring between ions and gel molecules at different concentrations depending on the nature of the ions involved.

4.2.1A Theoretical value of α

Before discussing the results observed in the different systems, it is worthwhile to compare the experimental value of

α with that predicted by the theory. Theoretical value of α can be computed from a knowledge of the gel structure and transport properties of the heterogeneous media. If the gel is assumed to be a collection of randomly oriented three-dimensional network of needles, expression of formation factor F in terms of different parameters is given by^{116,142}

$$F = 1 + \varphi (\beta - 1) \quad \dots (4.5)$$

where φ is the effective volume fraction of gel molecules and β is the shape factor ($= 5/3$ for needles). As we have used the weight fraction instead of volume fraction in calculating the experimental value of α , equation (4.5) becomes

$$F = 1 + \frac{1}{\alpha_0} (\beta - 1) W \quad \dots (4.6)$$

Substituting the values of different parameters in equation (4.6), we get

$$F = 1 + 0.42 W \quad \dots (4.7)$$

and comparison of equations (4.3) and (4.7) leads to

$$\alpha_{\text{theo}} = 0.42$$

As can be seen from Tables 4.4 to 4.6 that the experimental value of α is very much greater than the theoretical value in each system suggesting that the gel structure is far more effective in obstructing the motion of the ions than

predicted by the theory. In fact, there is ample evidence in the literature^{116,135-137,140,141} to show that there is always a great disparity between the observed and theoretical α values. Further, even though different expressions are used for describing the obstruction effect by various workers^{116,135,143}, the agreement between the theory and experiment is always poor. The major cause for this large deviation is thought to be due to the extensive hydration of agar macromolecules which was not taken into account in deriving the expression for the obstruction effect. This extensive hydration increases the effective size of agar molecules leading to a larger obstruction to the diffusing ions than that anticipated by considering its size merely on the basis of the molecular weight of the unhydrated form of agar.

4.2.2A Estimation of hydration of agar

An estimate of the hydration of agar can be made using the treatment given by Kang¹⁴⁴.

Let C_a be the concentration of anhydrous agar (g/cm^3 of solution), C_w be the total concentration of water and W be the weight fraction of anhydrous agar in solution, then we have

$$\frac{C_a}{C_w} = \frac{W}{1-W} \quad \dots (4.8)$$

and

$$C_a \bar{V}_a + C_w/d_w = 1 \quad \dots (4.9)$$

where \bar{V}_a is the apparent specific volume of anhydrous agar with the density d_a in its aqueous solution and d_w is the density of pure water.

The hydration of agar in terms of grams of bound water per gram of anhydrous agar (H) is related to the volume fraction of agar (φ) by the relation

$$\varphi = C_a (\bar{V}_a + \frac{H}{d_w}) \quad \dots (4.10)$$

Substitution of the value of C_a from equations (4.8) and (4.9) and expressing \bar{V}_a in terms of density of agar, equation (4.10) takes the following form

$$\varphi = \frac{\frac{1}{d_a} + \frac{H}{d_w}}{\frac{1}{d_a} + \frac{1}{d_w} \left(\frac{1-w}{w} \right)} \quad \dots (4.11)$$

In the present case, the maximum concentration of agar used for the study of diffusion is 2.5%. Hence the weight fraction of agar is 0.025 which is far less than 1. Under this condition equation (4.11) reduces to

$$\varphi = \left(\frac{1}{d_a} + \frac{H}{d_w} \right) \cdot d_w \cdot w \quad \dots (4.12)$$

Substituting the value of β in equation (4.5) and comparing it with equation (4.3) one arrives at the following expression :

$$\alpha = \left(\frac{1}{d_a} + \frac{H}{d_v} \right) \cdot d_v \cdot (\beta - 1) \quad \dots (4.13)$$

Using equation (4.13) and experimental value of α , the mass of bound water per gram of anhydrous agar (H) is calculated. The values of H for different systems are recorded in Table 4.7.

Table 4.7 : Hydration value of agar in terms of grams of bound water per gram of anhydrous agar in different systems studied.

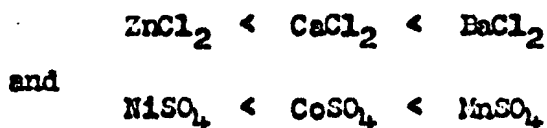
System	Hydration value
<u>Self-diffusion</u>	
Mn ²⁺ in MnCl ₂	16.69
Mn ²⁺ in MnSO ₄	
at 10 ⁻⁵ M	13.91
at 10 ⁻³ M	15.05
at 0.1 M	11.93
Cu ²⁺ in CuSO ₄	10.13
<u>Tracer-diffusion of Zn²⁺ ion</u>	
in ZnCl ₂	12.19
in CaCl ₂	21.73
in BaCl ₂	23.42
<u>Tracer-diffusion of Cu²⁺ ion</u>	
in NiSO ₄	12.70
in CoSO ₄	14.56
in MnSO ₄	26.44
<u>Electrolyte-diffusion</u>	
MnCl ₂	18.21
MnSO ₄	16.87
CuSO ₄	11.33

Higher values of Π presented in Table 4.7 for all the systems studied imply that obstruction to diffusion is caused not so much by the agar macromolecules themselves as by immobilized sheath of bound water molecules.

Examination of the Table 4.4 reveals that the experimental α -value is higher for electrolyte-diffusion than that for self-diffusion process for a given concentration of the electrolyte. Further, study of effect of concentration of electrolyte on the α -value shows that it decreases with increasing concentration of the electrolyte (Table 4.5). These observations are in agreement with that observed by Patil and Adhyapak¹¹³ in their diffusion studies in cadmium acetate system and are explained by considering the competitive hydration between ions and agar molecules. In the case of self-diffusion, the electrolyte concentration is constant throughout the gel column while in the case of electrolyte-diffusion, only the central zone contains the electrolyte and pure gel columns on either sides of it. Thus, in self-diffusion, number of ions which compete with agar macromolecules for water are more as compared to that in electrolyte-diffusion. Therefore, hydration of agar will be less in self-diffusion than that in electrolyte-diffusion which reflects in the value of obstruction effect observed in both the systems and we get lower value of α in

self-diffusion studies than in electrolyte-diffusion studies in each system. The decreased value of α with increasing concentration of the electrolyte is also in agreement with this concept. As the concentration of electrolyte increases, the number of ions competing for hydration also increases which cause a lowering in hydration of agar molecules and therefore giving less obstruction in the diffusion.

Further, an examination of Table 4.6 reveals that the observed trend in α for the tracer-diffusion of Zn^{2+} and Cu^{2+} ions in different supporting electrolytes is in the order



respectively.

The observed trend is again in agreement with the above concept of the competition between ions and agar molecules for hydration.

Consider, for example, the tracer-diffusion of zinc ions in different electrolytes. Among the three systems studied, zinc ion has a higher charge density as compared to calcium and barium ions. Hence it will attract more water molecules towards it as compared to the other two ions. Thus in ZnCl_2 system,

comparatively fewer water molecules are available for hydration of agar than are available in the CaCl_2 and BaCl_2 systems. This results in a lower obstruction value for the diffusion of Zn^{2+} ions in ZnCl_2 system than in the CaCl_2 and BaCl_2 systems. Thus, the observed trend in α is consistent with the trend in charge density of the ions. Similar argument can be applied for explaining the observed trend in α values for tracer-diffusion of Cu^{2+} ions in different transition metal sulphates.

Section B : Temperature dependence of diffusion coefficient

In this section, the effect of gel concentration on the activation energy required for diffusion in the different systems at a specified concentration of the diffusing species is investigated over the temperature range of 25-45°C. It also includes the study of tracer-diffusion of Mn^{2+} and Zn^{2+} ions in 1% agar gel in the presence of different supporting electrolytes over the same temperature range as mentioned above. The results obtained in different systems along with possible explanation are discussed in the following sections.

4.1B Effect of Gel Concentration on the Activation Energy for the Process of Self- and Electrolyte-Diffusion

Effect of gel concentration on the energy of activation required for the self- and electrolyte-diffusion processes in $MnCl_2$ and $MnSO_4$ systems at 10^{-3} M and in $CuSO_4$ system at 5×10^{-3} M is studied by varying the gel concentration between 1-2.5%. These results are presented in Figs. 4.7-4.9. It is to be noted that the values for diffusion coefficients plotted in Figs. 4.7-4.9 are taken from the Tables 4.1-4.3 from the Section A of this chapter.

It can be seen from Figs. 4.7-4.9 that the diffusion

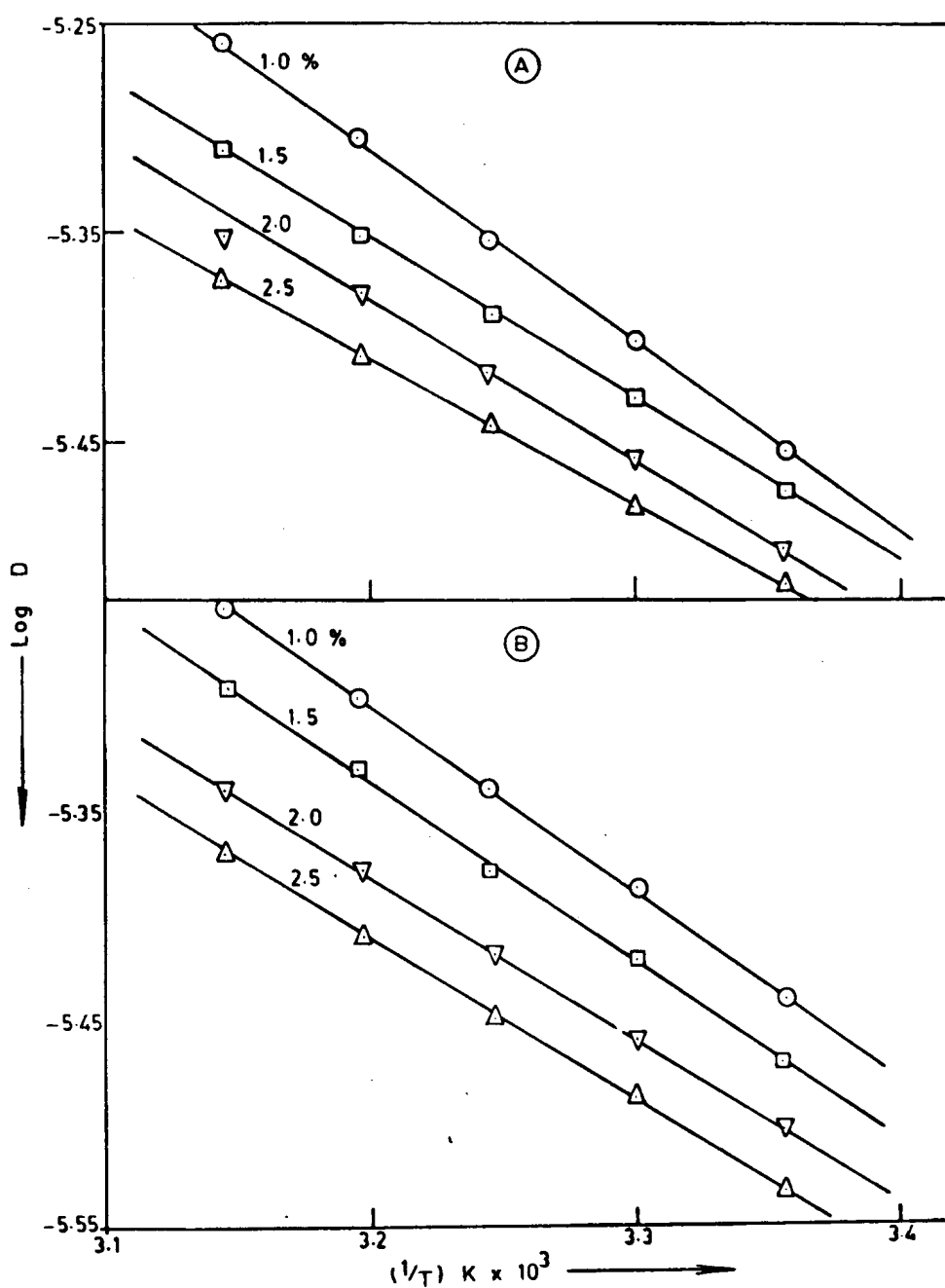


Fig.4.7- Activation energy for (A) electrolyte-diffusion of MnCl_2 and (B) self-diffusion of Mn^{2+} ions in MnCl_2 at 10^{-3} M concentration in different gel concentrations.

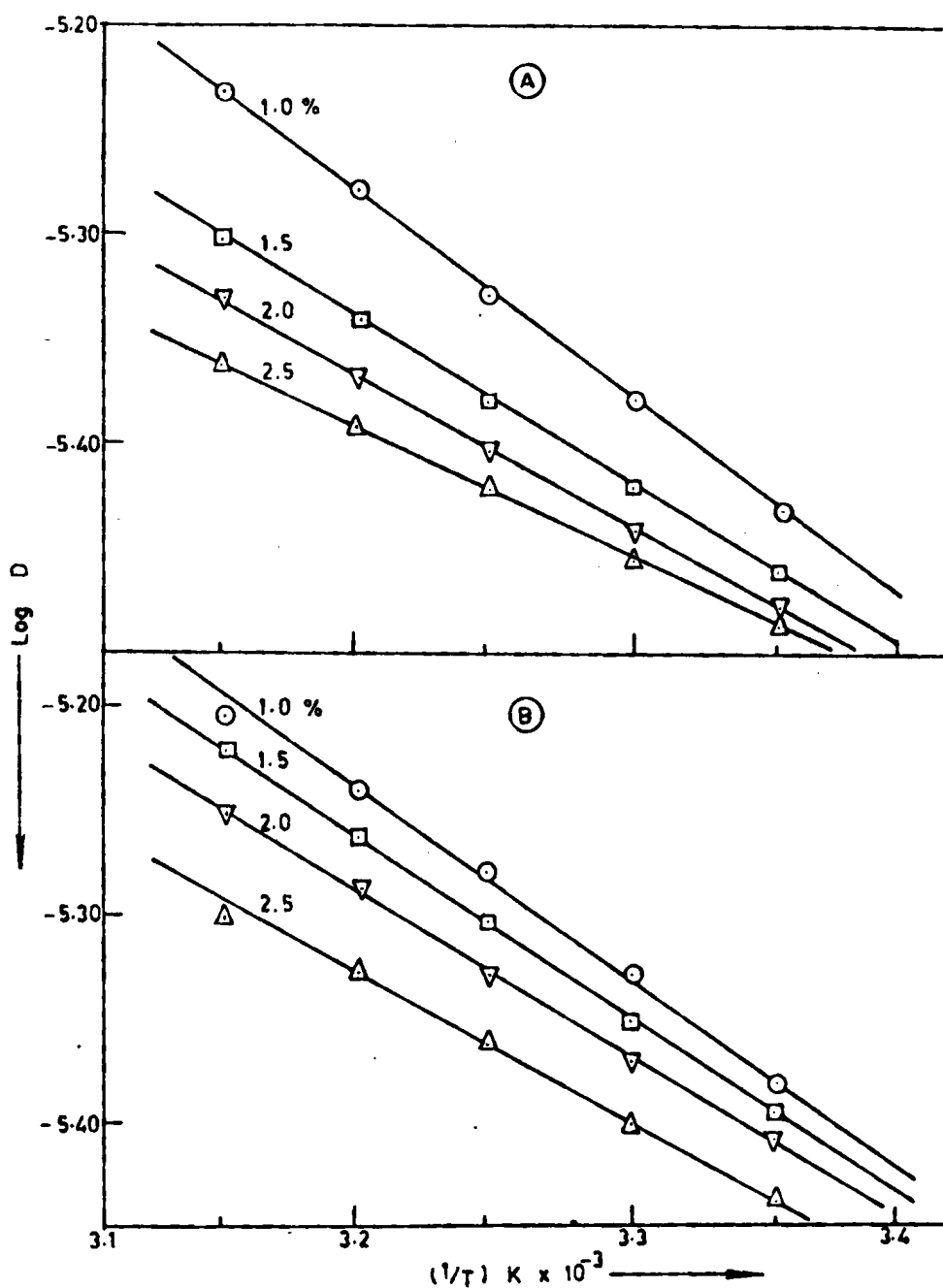


Fig.4.8- Activation energy for (A) electrolyte-diffusion of MnSO_4 and (B) self-diffusion of Mn^{2+} ions in MnSO_4 at 10^{-3} M concentration in different gel concentrations.

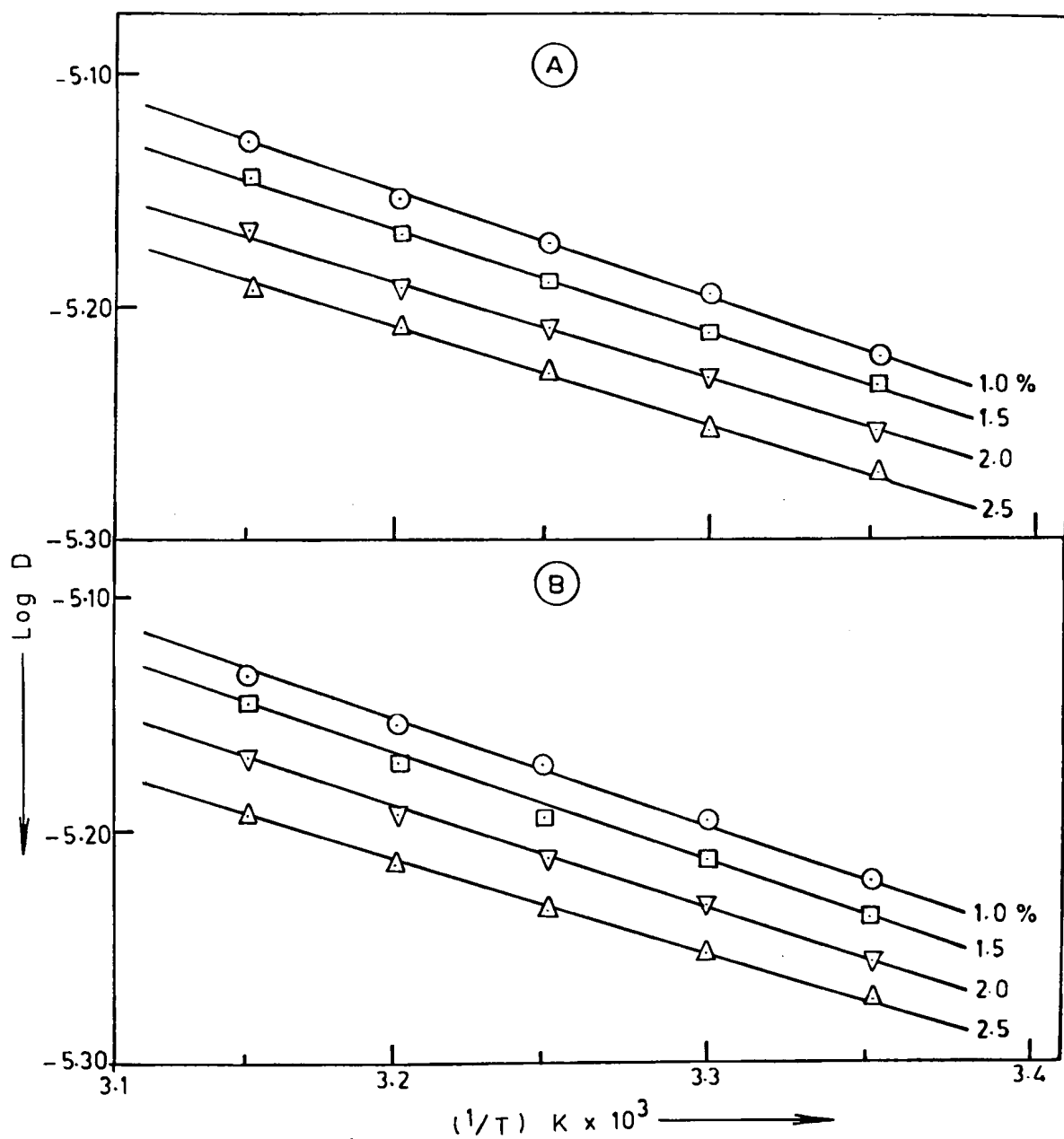


Fig. 4.9-Activation energy for (A) electrolyte-diffusion of CuSO_4 and (B) self-diffusion of Cu^{2+} ions in CuSO_4 at $5 \times 10^{-3} \text{ M}$ concentration in different gel concentrations.

coefficient increases with temperature in agreement with the transition state theory. With the increase of temperature, a larger fraction of diffusing species acquires the requisite amount of energy in order to cross the potential energy barrier required for the process of diffusion and hence diffusion coefficient increases with increasing temperature as observed.

The values of energy of activation E and D_0 for all the systems are calculated by the least square fitting of the data plotted in Figs. 4.7-4.9 and using the classical Arrhenius equation

$$D = D_0 e^{-E/RT} \quad \dots (4.14)$$

and are presented in Table 4.8 along with the standard deviations.

Table 4.8 : Variation of E and D_0 with gel concentration in different systems.

System	Gel percentage	$E/\text{kJ mol}^{-1}$	$D_0/10^{-3} \text{ cm}^2 \text{ s}^{-1}$
<u>Self-diffusion</u>			
Mn^{2+} in MnCl_2	1.0	17.9 ± 0.2	4.7 ± 0.4
	1.5	16.6 ± 0.1	2.6 ± 0.1
	2.0	14.5 ± 0.1	1.0 ± 0.03
	2.5	14.2 ± 0.3	0.9 ± 0.1
Mn^{2+} in MnSO_4	1.0	16.5 ± 0.6	3.1 ± 0.8
	1.5	15.1 ± 0.3	1.7 ± 0.2
	2.0	14.7 ± 0.3	1.4 ± 0.2
	2.5	12.9 ± 0.4	0.6 ± 0.09
Cu^{2+} in CuSO_4	1.0	7.7 ± 0.1	0.134 ± 0.005
	1.5	6.8 ± 0.1	0.093 ± 0.002
	2.0	6.0 ± 0.1	0.064 ± 0.002
	2.5	5.1 ± 0.1	0.044 ± 0.002
<u>Electrolyte-diffusion</u>			
MnCl_2	1.0	18.1 ± 0.3	5.1 ± 0.7
	1.5	15.2 ± 0.5	1.5 ± 0.3
	2.0	13.0 ± 0.2	0.7 ± 0.06
	2.5	12.9 ± 0.1	0.5 ± 0.03

Table 4.8 (contd.)

System	Gel percentage	$E/\text{kJ mol}^{-1}$	$D_0/10^{-3} \text{ cm}^2 \text{ s}^{-1}$
MnSO_4	1.0	17.8 ± 0.2	4.6 ± 0.4
	1.5	15.3 ± 0.2	1.6 ± 0.1
	2.0	12.7 ± 0.4	0.5 ± 0.1
	2.5	11.2 ± 0.2	0.3 ± 0.02
CuSO_4	1.0	10.5 ± 0.3	0.38 ± 0.05
	1.5	8.2 ± 0.2	0.152 ± 0.003
	2.0	7.8 ± 0.1	0.126 ± 0.004
	2.5	6.7 ± 0.1	0.078 ± 0.02

Examination of Table 4.8 reveals that both E and D_0 values decrease with increasing gel concentration in all the systems studied. For example, E and D_0 values for electrolyte-diffusion of $MnCl_2$ at 10^{-3} M concentration decrease from 13.1 to 12.9 kJ mol $^{-1}$ and 5.1 to 0.5×10^{-3} cm 2 s $^{-1}$ respectively as the gel concentration increases from 1 to 2.5%. This observation is in agreement with the expectation from earlier studies on other systems^{104,106,107,140,145} and is satisfactorily explained in terms of the transition state theory of diffusion as first postulated by Fujii and Thomas¹³⁹ in 1958 and then confirmed in a series of systems in our laboratory^{104,106,107,140,145}.

4.1.1B Application of transition state theory of diffusion in gel medium

According to Eyring and coworkers¹⁵⁻¹⁷, the diffusion process can be treated by means of the theory of absolute reaction rate. They assumed that the liquid is made up of holes which move about in matter and through these holes, diffusion of the different species occurs.

When an ion diffuses through the medium it jumps from one position to another and this jump distance, i.e. the component in the direction of diffusion of the average

elementary displacement required to produce an exchange of two ions, is denoted by λ . As discussed in Chapter 1, this jump distance is related to the diffusion coefficient by the following relation

$$D = \lambda^2 K' \quad \dots (1.25)$$

where K' is the specific reaction rate for diffusion given by the expression

$$K' = \frac{kT}{h} \cdot \frac{F^\ddagger}{F} \cdot e^{-\epsilon_0/kT} \quad \dots (4.15)$$

Substitution of value of K' in equation (1.25) leads to

$$D = \lambda^2 \frac{kT}{h} \cdot \frac{F^\ddagger}{F} \cdot e^{-\epsilon_0/kT} \quad \dots (4.16)$$

where F^\ddagger and F are partition functions of the system in the activated and normal states respectively and ϵ_0 is the activation energy per molecule at absolute zero. Since $\left(\frac{F^\ddagger}{F}\right) \cdot e^{-\epsilon_0/kT}$ is equal to K^\ddagger , the equation (4.16) becomes

$$D = \lambda^2 \frac{kT}{h} \cdot K^\ddagger \quad \dots (4.17)$$

and the thermodynamic relation for K^\ddagger in this equation is given by

$$K^\ddagger = e^{-\Delta F^\ddagger/RT}$$

where

$$\Delta F^\ddagger = \Delta H^\ddagger - T \Delta S^\ddagger$$

Hence equation (4.17) can be written as

$$D = \lambda^2 \frac{kT}{h} \cdot e^{\Delta S^\ddagger/R} \cdot e^{-\Delta H^\ddagger/RT} \quad \dots (4.18)$$

The ΔH^\ddagger in the above equation is related to the energy of activation by the following relation

$$\Delta H^\ddagger = E - RT + P \Delta V^\ddagger$$

As the diffusion is accompanied by a negligible volume change, equation (4.18) becomes

$$\begin{aligned} D &= \lambda^2 \frac{kT}{h} (e^{-E/RT+1}) \cdot e^{\Delta S^\ddagger/R} \\ &= e \lambda^2 \frac{kT}{h} \cdot e^{-E/RT} \cdot e^{\Delta S^\ddagger/R} \quad \dots (4.19) \end{aligned}$$

where E is the experimental activation energy for diffusion, ΔS^\ddagger is the entropy of activation which is defined as the change in entropy in the formation of the ion-pair of activated complex and the other symbols have their usual meaning. A comparison of the equations (4.14) and (4.19) gives the value of D_0 as

$$D_0 = e \lambda^2 \frac{kT}{h} \cdot e^{\Delta S^\ddagger/R} \quad \dots (4.20)$$

Thus, in terms of transition state theory of diffusion, D_0 measures the contribution to the diffusion coefficient of $\lambda^2 (kT/h) \cdot \exp(\Delta S^\ddagger/R)$.

As there is a relatively small rearrangement of the energy between various degrees of freedom in the formation of the activated state, ΔS^\ddagger may be expected to be small and hence it is reasonable to assume the entropy of activation to be independent of gel percentage. Under these circumstances, lowering in D_0 value implies that λ value also decreases with increasing gel percentage. Further, if we consider cubical packing in the liquid, then it can be visualized that one molecule oscillates about the origin and the six nearest neighbours are fixed in their mean positions along the three axes. This type of geometry predicts each molecule to be at a distance $V^{1/3}$ from the origin, when V is the volume. Then, if we consider the diffusion in one direction only, the λ value is to vary with $V^{1/3}$ and hence with $W^{-1/3}$ where W is the weight percentage of agar. Therefore, one expects D_0 to vary with $W^{-2/3}$. This is confirmed by the linear relationship observed in the D_0 versus $W^{-2/3}$ plots (Fig. 4.10) in all the systems studied.

The decrease in D_0 with increasing gel concentration indicates that the presence of these obstructing macromolecules manifest by a decrease in the value of λ , the longer elementary jumps being blocked. Therefore, the activation energy becomes likewise smaller for the more concentrated gels.

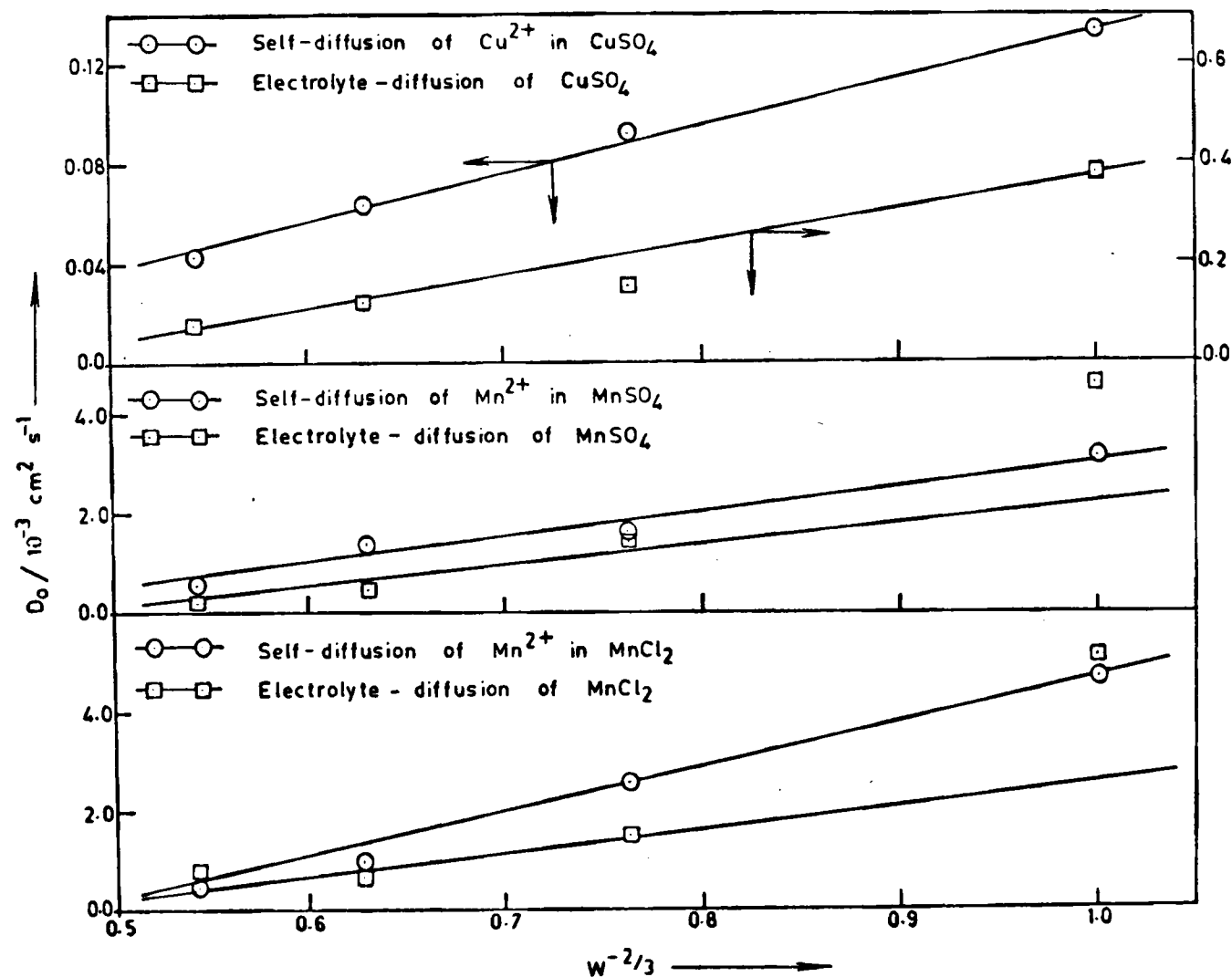


Fig. 4.10 - Variation of D_0 with $w^{-2/3}$ in different systems.

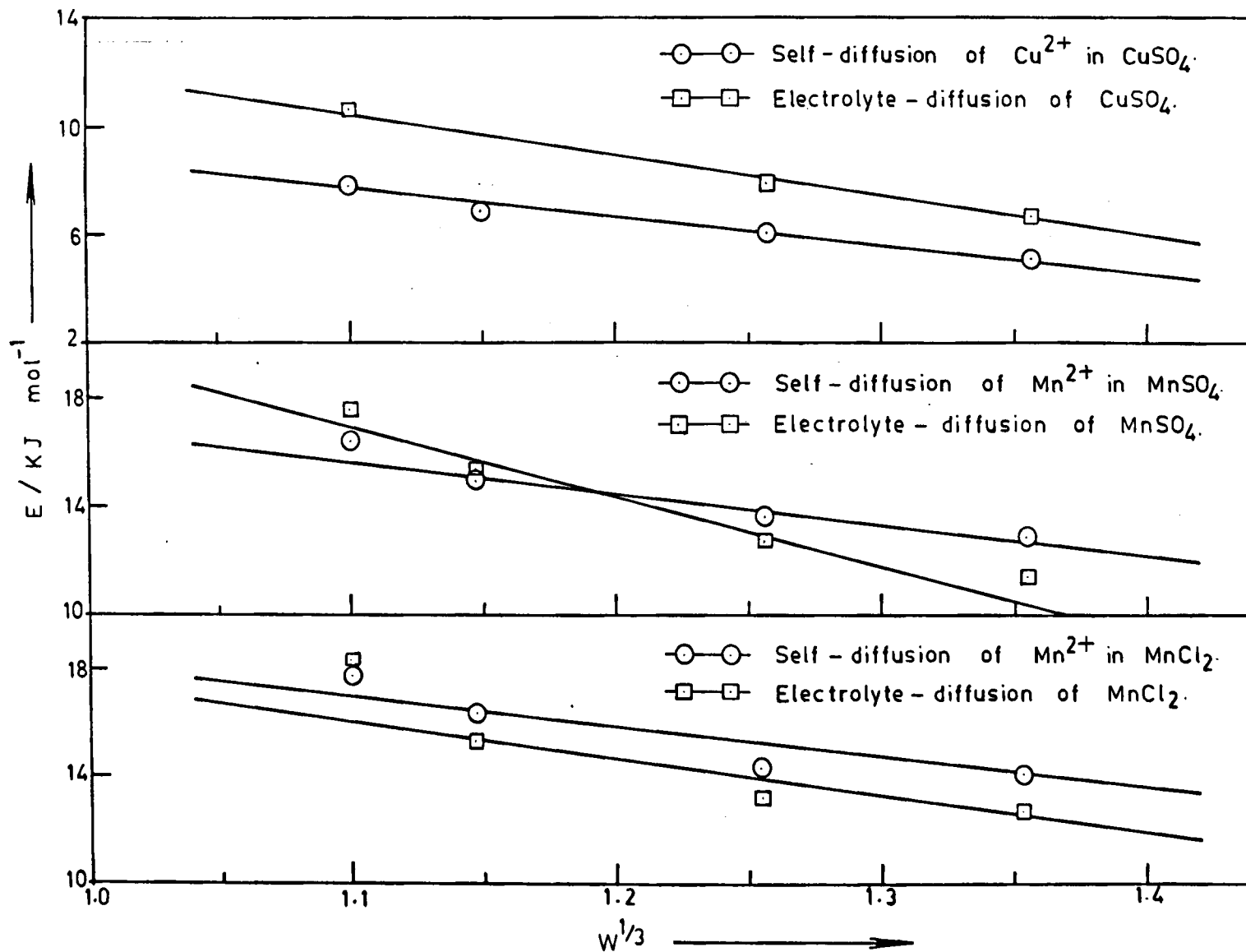


Fig. 4.11 - Variation of E with $W^{1/3}$ in different systems.

The decreasing trend in the energy of activation with increasing gel percentage (Table 4.8) is consistent with the above picture and it can be seen from Fig. 4.11 that the activation energy varies linearly with one-third power of gel percentage ($W^{1/3}$) for all the systems studied.

4.2B Effect of Supporting Electrolytes on the Activation Energy in Tracer-diffusion of Mn^{2+} and Zn^{2+} Ions

In order to study the effect of an electrolyte on the activation energy for the tracer-diffusion process, the tracer-diffusion coefficients of Mn^{2+} and Zn^{2+} ions were determined in different metal chlorides at various temperatures at 10^{-3} M concentration and the corresponding results are shown graphically in Figs. 4.12 and 4.13 respectively. The effect of transition metal sulphates on the activation energy for the tracer-diffusion of Mn^{2+} ions is also studied at 10^{-5} M concentration. The Arrhenius plots are shown in Fig. 4.14. The values of energy of activation calculated from the slopes of the Arrhenius plots along with the standard deviations for the process of tracer-diffusion in different systems are presented in Table 4.9.

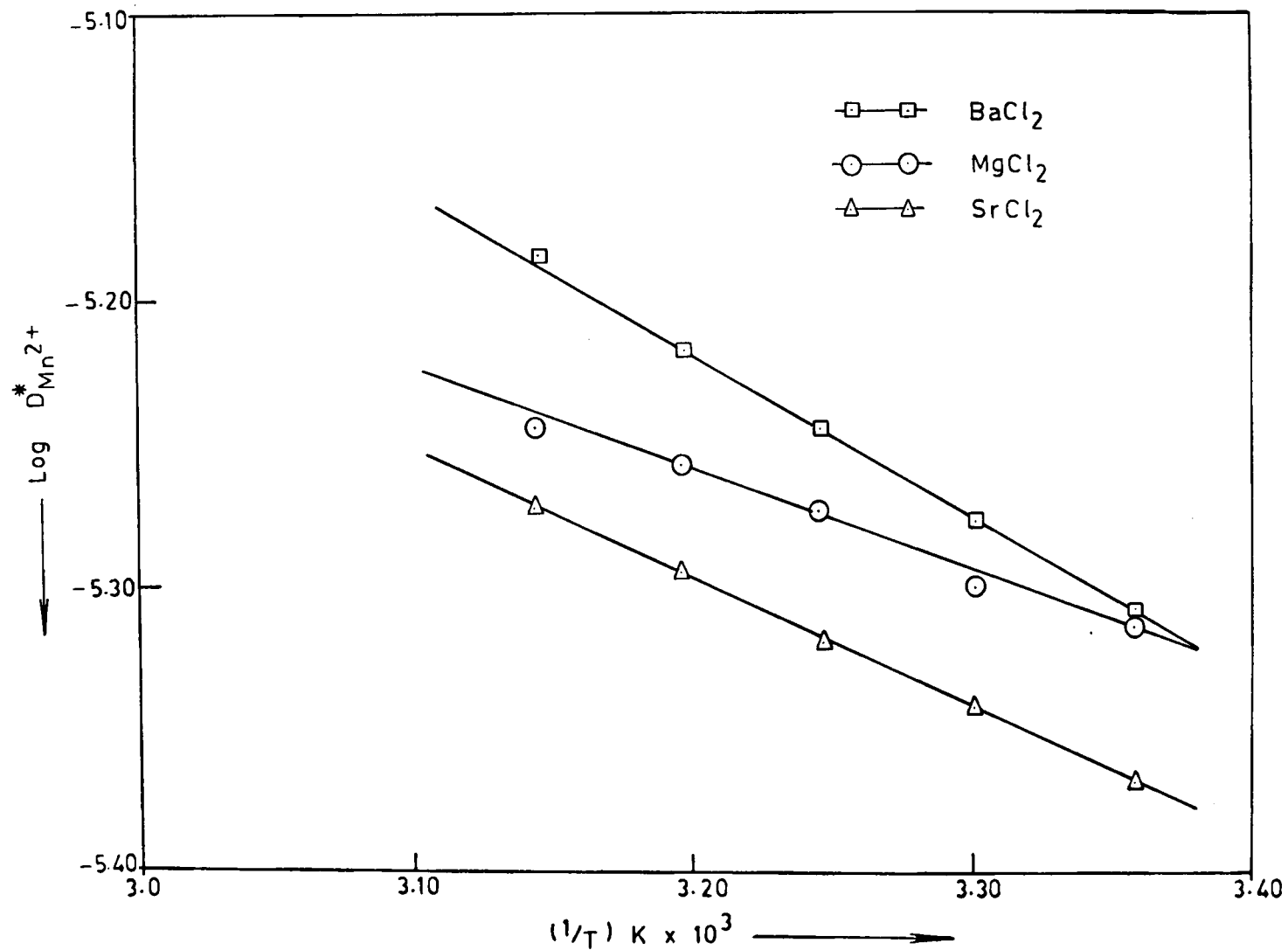


Fig. 4.12 - Activation energy for the tracer-diffusion of Mn^{2+} ions (10^{-3} M) in different electrolytes in 1% agar gel.

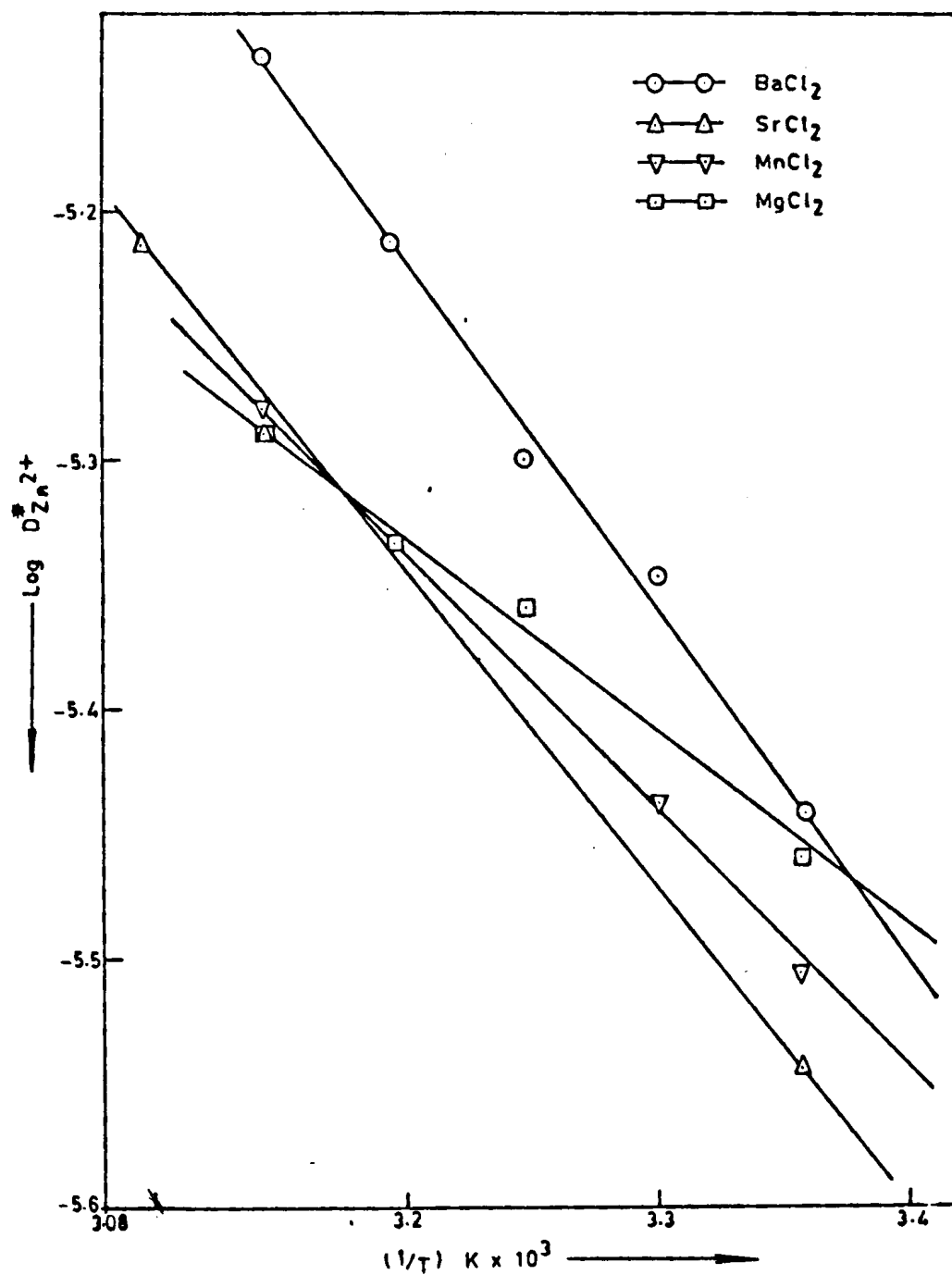


Fig.4.13- Activation energy for the tracer-diffusion of Zn²⁺ ions (10⁻³M) in different electrolytes in 1% agar gel.

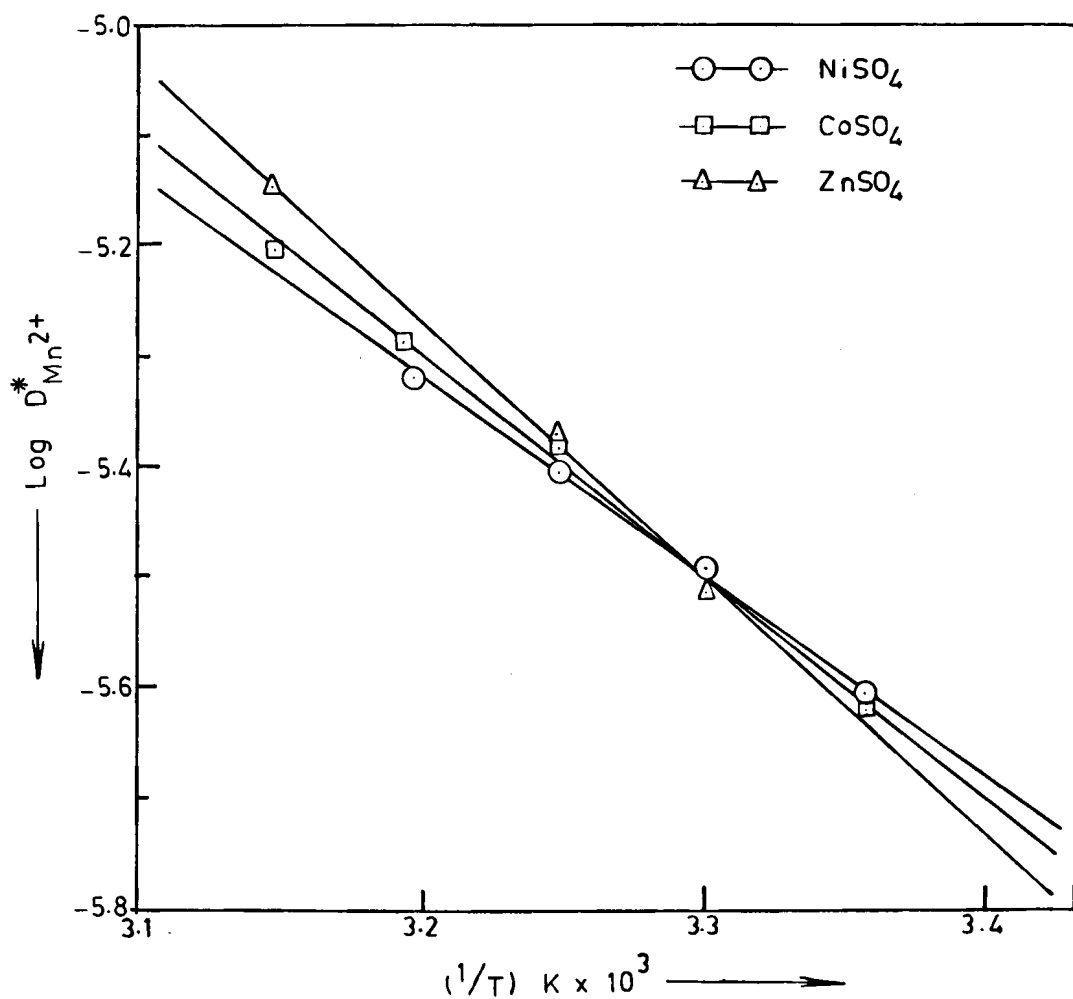


Fig.4.14 - Activation energy for the tracer-diffusion of Mn^{2+} ions (10^{-5}M) in different electrolytes in 1% agar gel.

Table 4.9 : Activation energy for tracer-diffusion of Zn^{2+}
and Mn^{2+} ions in different supporting electrolytes

System	$E/\text{kJ mol}^{-1}$
<u>Tracer-diffusion of Zn^{2+}</u>	
in MgCl_2	15.4 ± 1.1
in MnCl_2	20.4 ± 0.7
in SrCl_2	24.1 ± 0.9
in BaCl_2	27.0 ± 1.4
<u>Tracer-diffusion of Mn^{2+}</u>	
in MgCl_2	6.9 ± 0.7
in SrCl_2	8.8 ± 0.8
in BaCl_2	11.0 ± 0.8
<u>Tracer-diffusion of Mn^{2+}</u>	
in H_2SO_4	34.4 ± 1.7
in CoSO_4	38.0 ± 1.4
in ZnSO_4	44.3 ± 2.5

It is evident from Table 4.9 that the activation energy for the tracer-diffusion of Zn^{2+} and Mn^{2+} ions in different chlorides decreases in the following order :

(1) for the diffusion of Zn^{2+} ions



(ii) for the diffusion of Mn^{2+} ions



while the trend in the activation energy for the tracer-diffusion of Mn^{2+} ions in different transition metal sulphates shows the following order :



The observed trend in the activation energy in different systems can be explained qualitatively by considering the distortion in the water structure caused by ions and agar molecules.

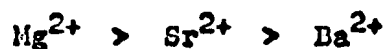
During the formation of a gel, water molecules are held up in the fibres of the agar gel network by hydrogen bonding¹¹⁷, adsorption¹¹⁸ and dipole-dipole interactions¹¹⁹ which develop a loose structure throughout the gel network due to tetrahedral coordination of water dipoles. However, this loose gel-water structure through which the diffusion occurs, melts in the presence of electrolytes due to the greater attractive forces

of ions which hold the water dipoles more firmly than the agar molecules. The extent of local melting of the gel-water structure is expected to depend on the charge and size of the ionic species. If the charges on the different ions are same, a smaller size of the ion indicates more charge density on the ion and hence it has greater attractive forces which in turn are responsible for more distortion in the gel-water structure. Let us consider as an example, the tracer-diffusion of Zn^{2+} ions in different supporting electrolytes. The charge densities of the bivalent ions of the different electrolytes in which the diffusion is studied have the following order :

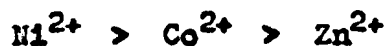


This order shows that magnesium ion attracts more water dipoles towards it, barium ions the least and the others lie inbetween, which means that magnesium ions melt the gel-water structure to a greater extent as compared to other three ions causing more distortion in the diffusion column. This distortion in the short range crystalline structure of water causes a decrease in the local dielectric constant of the medium, thereby increasing the self-energy of the ion in the normal state which in turn reduces the total energy barrier for diffusion. This picture indicates that the activation energy in the presence of these ions should be in the reverse order of their charge

density which is confirmed by the observed trend in the present studies. The trend observed in the activation energy for tracer-diffusion of Mn^{2+} ions in different metal chlorides and sulphates can also be explained on a similar argument, the order of charge density of bivalent cations in both the systems being



and



respectively. The corresponding activation energies are exactly in the reverse order in agreement with the above concept.



—● SUMMARY ●—

SUMMARY

The thesis presents the work done on tracer-diffusion of some labelled transition metal ions in different transition metal chlorides and sulphates as well as electrolyte-diffusion of manganese chloride, manganese sulphate and copper sulphate labelled with respective cations in agar gel medium. It consists of four chapters : The first chapter is an introductory one, the second chapter covers the experimental part and the third and fourth chapters deal with the discussion of the results obtained in the present studies.

The first chapter covers the introduction of the subject of diffusion and related theories. Onsager and Onsager-Fuoss theories of self- and electrolyte-diffusion respectively are discussed in detail from which the corresponding equations of diffusion coefficient are derived. It also includes a brief discussion of the transition state theory as applied to the phenomenon of diffusion. At the end of this chapter, the work done on self- and electrolyte-diffusion studies by earlier workers both in solution state and in gel medium is reviewed briefly.

The principle of zone-diffusion technique used for determining the diffusion coefficient is discussed in Chapter 2 along with the boundary conditions of the technique. A solution of the Fick's II law for the given boundary conditions is derived. The expression thus obtained was used for calculating the experimental diffusion coefficient.

The applicability of the Onsager and Onsager-Fuoss theory to the experimental data of tracer and electrolyte-diffusion coefficients respectively, obtained for various systems is examined in Chapter 3 and the corresponding results are discussed in two separate sections.

Section A deals with the studies on tracer-diffusion of Mn^{2+} , Cu^{2+} and Zn^{2+} ions in different supporting electrolytes while Section B presents the results of electrolyte-diffusion of MnCl_2 , MnSO_4 and CuSO_4 over a wide range of concentration of 25°C .

The more important observations related to the tracer-diffusion studies (Section A) are summarized below.

(1) A minimum in the experimental D^* versus \sqrt{C} curve at lower concentrations is a characteristic of all the systems studied against its absence in the theoretical curve.

(2) D_{expt}^* is found to be lower than the D_{theo}^* at lower concentrations while the reverse is observed at higher concentrations with the exception of the results obtained in tracer-diffusion of Cu^{2+} ions.

(3) Initially the diffusion coefficient decreases with concentration of the electrolyte in qualitative agreement with the theory but beyond a certain concentration it starts increasing.

These discrepancies in the observed results over the entire range of concentration are explained on the basis of gel-water, ion-water and ion-ion interactions as well as adsorption and obstruction effects due to the gel macromolecules. The increasing trend of diffusion coefficient after the minimum is accounted with the help of Wang's model which considers the changes in the physical properties occurring at the microscopic level at higher concentrations of the electrolyte due to ion-ion and ion-water interactions. These results are also interpreted in terms of structure-breaking properties of the ions affecting the sizes of ion-water aggregates by decoupling of the hydrogen bonds (Hertz et al. model).

In Section B of this chapter, the results on electrolyte-diffusion studies are discussed, the important observations being :

(1) The experimental value of diffusion-coefficient is always less than the theoretical one in MnCl_2 and MnSO_4 systems and upto 10^{-3} M concentration in CuSO_4 system.

(2) The minimum in the experimental D' versus \sqrt{C} curve occurs at concentration which is very much lower than that predicted by the theory in all the systems studied.

The observed results are explained in terms of different types of interactions occurring in gel-water-electrolyte system. The shift in the experimental minimum towards the lower concentration side in relation to the theoretical minimum is attributed to desolvation of the ions with increasing concentration of the electrolyte.

The effect of gel macromolecules on diffusion is studied elaborately in Chapter 4 by varying the gel concentration as well as temperature of the system. Section A of this chapter deals with the study of obstruction effect in different systems while Section B consists of determination of activation energy for the process of diffusion for different ions and electrolytes.

The study of obstruction effect under different conditions of temperature and concentration of the electrolyte leads to the following observations :

- (1) For a particular concentration of the electrolyte, obstruction effect calculated in terms of α is independent of temperature.
- (2) At a given temperature, α -value decreases with increasing concentration of the electrolyte,
- (3) For a particular system, the α -value is higher for electrolyte-diffusion as compared to that for self-diffusion.
- (4) In tracer-diffusion, the α -value decreases with increasing charge density of cation of the electrolyte.
- (5) In all the systems, experimental value of α is found to be very much greater than that predicted by the theory.

Higher value of α compared to the theoretical one is attributed to the extensive hydration of agar macromolecules. Further, the higher value of α observed for electrolyte-diffusion than that for self-diffusion process, for a given concentration of the electrolyte and decreasing trend in it with concentration of the electrolyte, are explained by considering the competitive hydration between ions and agar macromolecules. The effect of different cations on the α -value for tracer-diffusion is also explained using the same concept.

In Section B of this chapter, a study of the effect of gel concentration on the activation energy for

the diffusion process in different systems shows that (1) the activation energy decreases with increasing gel percentage (w) and it varies linearly with $w^{1/3}$, (2) the D_0 value also decreases with increasing gel percentage and shows a linear relationship with $w^{-2/3}$. These observations are explained on the basis of the transition state theory of diffusion.

The study of effect of the supporting electrolyte on the activation energy for the tracer-diffusion process shows that the activation energy for tracer-diffusion of Zn^{2+} and Mn^{2+} ions in different chlorides decreases in the following order :

(1) for tracer-diffusion of Zn^{2+} ions



(2) for tracer-diffusion of Mn^{2+} ions



while the trend in activation energy for the tracer-diffusion of Mn^{2+} ions in different transition metal sulphates shows the following order :



The observed trend in the activation energy in different systems is explained qualitatively in terms of charge density of the ions and the distortion caused by them in the gel-water structure.



REFERENCES

1. Graham, T., Phil.Trans., 142, 1, 305 (1850);
141, 483 (1861); 144, 177 (1854); 151, 183 (1861).
2. Fick, A., Pogg. Ann., 94, 59 (1855).
3. Berthollet, C.L., 'Essai de Statique Chimique'
Paris, 1803.
4. Fourier, J.B., J.Theorie Analytique de la Chaleur,
Paris, 1822.
5. Onsager, L., Ann.N.Y.Acad.Sci., 46, 241 (1945).
6. Long, H., Ann.Physik., 9, 613 (1830).
7. Nernst, W., Z.Phys.Chem., 2, 613 (1833).
8. Schreiner, E., Tidskr.Kem.O.Bergvaeson, 2, 151 (1922).
9. Gibbs, J.W., Collected Works, Longmans, Green,
New York, Vol. 1, p. 429 (1928).
10. Guggenheim, E.A., J.Phys.Chem., 33, 842 (1929).
11. Hartley, G.S., Phil.Mag., 12, 473 (1931).
12. Onsager, L. and Fuoss, R.M., J.Phys.Chem.,
36, 2689 (1932).
13. Debye, P. and Huckel, E., Physik.Z., 24, 185, 305 (1923).
14. Gosting, L.J. and Harned, H.S., J.Am.Chem.Soc.,
23, 159 (1951).
15. Kincaid, J.F., Eyring, H. and Stearn, A.E.,
Chem.Rev., 23, 301 (1941).
16. Glasstone, S., Laidler, K. and Eyring, H., 'The Theory
of Rate Processes, McGraw-Hill, New York (1941).

17. Hirschfelder, J.O., Stevenson, D. and Eyring, H., J.Chem.Phys., 5, 896 (1937).
18. Clack, B.W., Proc.Phys.Soc.London, 36, 313 (1924).
19. Northrop, J.H. and Anson, M.L., J.Gen.Physiol., 12, 543 (1929).
20. Hartley, G.S. and Rummides, D.F., Proc.Roy.Soc., 168A, 401 (1933).
21. McBain, J.W. and Liu, T.H., J.Am.Chem.Soc., 53, 59 (1931).
22. McBain, J.W. and Dawson, C.R., Proc.Roy.Soc., 148A, 32 (1935).
23. Mouquin, H. and Cathcart, W.H., J.Am.Chem.Soc., 52, 1791 (1935).
24. Valko-E, Trans.Faraday Soc., 31, 230 (1935).
25. Gordon, A.R., Ann.N.Y.Acad.Sci., 46, 232 (1945).
26. Stokes, R.H., J.Am.Chem.Soc., 72, 763 (1950); 73, 3527 (1951).
27. Harned, H.S. and French, D.M., Ann.N.Y.Acad.Sci., 46, 267 (1945).
28. Arnikar, H.J. and Malshe, A.G., Proc. of Indian Science Congress (1967).
29. Anderson, J.S. and Saddington, K., J.Chem.Soc., S331 (1949).
30. Carslaw, H.S. and Jaeger, J., 'The Conduction of Heat in Solids', Oxford, Clarendon Press, 1st ed., 1947; 2nd ed., 1959.
31. Wang, J.H., J.Am.Chem.Soc., 74, 1182 (1952).
32. Mills, R. and Godbole, E.W., Aust.J.Chem., 11, 1 (1958).

33. Mills, R. and Kennedy, J.W., J.Am.Chem.Soc., 75, 5696 (1953).
34. Krauss, C.J. and Spinks, J.W.T., Canad.J.Chem., 32, 71 (1954).
35. Burkell, J.E. and Spinks, J.W.T., Canad.J.Chem., 30, 311 (1952).
36. Haycock, E.W., Alder, B.J. and Hilderbrand, J.H., J.Chem.Phys., 21, 1601 (1953).
37. Johenson, P.A. and Babb, A.L., J.Phys.Chem., 60, 14 (1956).
38. Wang, J.H. and Miller, Sara, J.Am.Chem.Soc., 74, 1611 (1952).
39. Wang, J.H., J.Am.Chem.Soc., 73, 510, 4181 (1951).
40. Wang, J.H., J.Am.Chem.Soc., 74, 1612 (1952).
41. Mills, R. and Godbole, E.W., Aust.J.Chem., 12, 102 (1959).
42. Mills, R. and Adamson, A.W., J.Am.Chem.Soc., 77, 3454 (1955).
43. Paulson, S. and Snelman, O., Biochim.Biophys.Acta, 6, 48 (1950).
44. Hirai, N., Bull.Inst.Chem.Res., Kyoto Univ., 33, 21 (1955).
45. Graham, T., Ann., 121, 1 (1862).
46. Bechhold and Ziegler, Ann.Physik., 20, 4, 900 (1906).
47. Stiles and Adair, Biochem.J., 5, 631 (1921).
48. Herzog and Polotsky, Z.Physik.Chem., 87, 449 (1914).
49. Fricke, Z.Electrochem., 31, 430 (1925).
50. Ricketts, V.L. and Culberston, J.L., J.Am.Chem.Soc., 53, 4002 (1931).

51. Araki, C.H., Bull.Chem.Soc.Japan, 29, 543 (1956).
52. Markova, V.G., Goncharov, U.V., Yashkichev, V.I., Zh.Fiz.Khim., 49, 2133 (1974).
53. Harned, H.S. and Blake, C.H., J.Am.Chem.Soc., 72, 2265 (1950).
54. Stokes, R.H., J.Am.Chem.Soc., 72, 2243 (1950).
55. Wang, J.H. and Kennedy, J.W., J.Am.Chem.Soc., 72, 2080 (1950).
56. Harned, H.S. and Elander, M., J.Am.Chem.Soc., 75, 2853 (1953).
57. Kelemen, F., Bota, F. and Neda, A., Acad.Rep.Populare Romaine Studii Cercetari Fiz., 14, 583 (1963).
58. Turq, P., Lantelme, F. and Chemla, M., Electrochim.Acta, 14, 1031 (1969).
59. Popova, L.V., Izv.Vyssh.Ucheb.Zaved.Khim.Khim.Tekhnol., 12, 269 (1969).
60. Shukla, B.M., Singh, V.N., Proc.Chem.Symp. 2nd, 2, 317 (1970).
61. Fell, Christopher, J.E. and Hatchison, H.P., J.Chem.Eng.Data, 16, 427 (1971).
62. Gupta, R.P., Z.Phys.Chem.(Neue Folge), 81, 236 (1972).
63. Thomas, H.C., Ku James, C.J.Phys.Chem., 77, 2233 (1973).
64. Mills, R. and Godbole, E.W., J.Am.Chem.Soc., 82, 2395 (1960).
65. Ravdel, A.A., Porai-Koshits, A.B., Sazohov, A.M. and Shmuilovich, G.A., Zh.Fiz.Khim., 49, 1319 (1974).
66. Hertz, H.G., Holz, M. and Mills, R., J.Chim.Phys. Physiochim.Biol., 71, 1355 (1974).
67. Agar, J.N. and Lobov, H.M., J.Chem.Soc.Faraday Trans.I, 71, 1659 (1975).

63. Sood, M.L. and Kaur, G., Z.Phys.Chem.(Leipzig), 259, 535 (1973).
69. Sood, M.L. and Kaur, G., Acta Cienc Indica, 2, 341 (1976).
70. Robinson, R.A. and Chia, C.L., J.Am.Chem.Soc., 74, 2776 (1952).
71. Harned, H.S. and Polestra, F.M., J.Am.Chem.Soc., 75, 4168 (1952).
72. Hall, J.R., Wishaw, B.F. and Stokes, R.H., J.Am.Chem.Soc., 75, 1556 (1953).
73. Harned, H.S. and Polestra, F.M., J.Am.Chem.Soc., 76, 2064 (1954).
74. Yamaoto, J., Tottori Daigaku Kogakulou Kenkyu Hokoku, 3, 53 (1973).
75. Fortes, J.M., Mercier, M. and Molenat, J., J.Chim.Phys.Physicochim.Biol., 71, 164 (1974).
76. Brown, D.A., Soil Sci.Soc.Am.Proc., 38, 533 (1974).
77. Petschel, M. and Richter, D., Isotopenpraxis, 10, 265 (1974).
78. Saxena, S.K., Boersma, L., Lindstrom, F.J. and Young, J.L., Soil Sci., 112, 14 (1974).
79. Harned, H.S., Parker, H.W. and Elander, M., J.Am.Chem.Soc., 77, 2071 (1955).
80. Sakuma, T., Hoshino, S. and Fujii, Y., J.Phys.Soc. Japan, 46, 617 (1979).
81. Harned, H.S. and Hildreth, C.L. Jr., J.Am.Chem.Soc., 73, 3292 (1951).
82. Sancho, J., Juan, B., Vidal-Abarca, Anales Real Soc. Espan.Fis.Quim.(Madrid), Ser.B, 58, 733 (1962).
83. Dombialska, A. and Chyzewski, A., Nukleonika, 12, 411 (1965).

84. Shukla, B.M. and Singh, V.N., Proc.Nucl.Radiat. Chem.Symp.3rd, 533 (1967).
85. Ermolaev, M.I. and Levchenko, G.V., Tr.Voronezh.Tekhnol.Inst., 12, 70 (1968).
86. Gupta, R.P. and Prasad, G., Z.Phys.Chem., (Frankfurt Ammain), 72, 255 (1970).
87. Woolf, L.A. and Hoveling, A.W., J.Phys.Chem., 74, 2406 (1970).
88. Olsztayn, M., Turq, P. and Chemla, M., J.Chim.Phys.Physicochim.Eiol., 62, 217 (1970).
89. Gupta, R.P., Z.Phys.Chem. (Frankfurt Ammain), 91, 277 (1974).
90. Reiners, G., Lorenz, W.J. and Hertz, H.G., Ber.Bunsengers Phys.Chem., 82, 733 (1978).
91. Paterson, R. and Lutfullah, J.Chem.Soc. Faraday Trans.I, 74, 93 (1978).
92. Stokes, R.H., J.Am.Chem.Soc., 75, 4563 (1953).
93. Sood, M.L., Acta Cienc.Indica, 2, 110 (1976).
94. Wishaw, B.F. and Stokes, R.H., J.Am.Chem.Soc., 76, 2065 (1954).
95. Harned, H.S. and Hudson, R.M., J.Am.Chem.Soc., 73, 3781 (1951).
96. Tanaka, K., Hashitani, J. and Tanamushi, R., Rikagaku Kenkyusho Hokoku, 51, 153 (1975).
97. Patil, S.F. and Adhyapak, N.G., Int.J.Appl.Radiat. and Iso., 33, 105 (1982).
98. Stokes, R.H., Woolf, L.A. and Mills, R., J.Phys.Chem., 61, 1634 (1957).
99. Stokes, R.H. and Woolf, L.A., J.Chim.Phys., 54, 906 (1957).

100. Mills, R., J. Am. Chem. Soc., 77, 6116 (1955).
101. Nielsen, J.M., Adamson, R. and Cobble, J.W., J. Am. Chem. Soc., 74, 446 (1952).
102. Vitagliano, V. and Lyons, P.A., J. Am. Chem. Soc., 78, 1549 (1956).
103. Friedman, A.M. and Kennedy, J.W., J. Am. Chem. Soc., 77, 4499 (1955).
104. Patil, S.F. and Adhyapak, N.G., Ind. J. Chem., 21A, 803 (1982).
105. Patil, S.F. and Adhyapak, N.G. and Ujlambkar, S.K., Radiochem. Radioanal. Lett., 49, 119 (1981).
106. Patil, S.F. and Adhyapak, N.G., Int. J. Appl. Radiat. Isot., 32, 631 (1981).
107. Patil, S.F. and Adhyapak, N.G., Proc. Nucl. Radiat. Symp., p. 233 (1980).
108. Patil, S.F. and Adhyapak, N.G., Int. J. Appl. Radiat. Isot., 32, 837 (1981).
109. Mills, R., March, M.H., Giaquinta, P.V., Farinello, M. and Tosi, M.P., Chem. Phys., 26, 237 (1977).
110. Yagodarov, V.P. and Khranov, A.S., Zh. Fiz. Khim., 50, 2997 (1976).
111. Arnikar, H.J., J. Inorg. Nucl. Chem., 11, 249 (1959).
112. Tripathi, R., Proc. Chem. Symp., p. 150 (1969).
113. Patil, S.F. and Adhyapak, N.G., Radiochem. Radioanal. Lett., 52, 177 (1982).
114. Mills, R., Rev. Pure Appl. Chem., 11, 78 (1961).
115. Singh, V.N., Tiwari, R.K., Fathak, B.K. and Singh, P.C., Ind. J. Technol., 12, 234 (1979).
116. Langdon, A.G. and Thomas, H.C., J. Phys. Chem., 75, 1821 (1971).

117. Jirgensons, B. and Straumanis, M.B., 'A Short Textbook of Colloid Chemistry', Pergamon Press Ltd., London (1945).
118. Felicetta, V.N., Markham, A.E., Peniston, Q.Q. and McCarthy, J.L., J. Am. Chem. Soc., 71, 2379 (1949).
119. Gilkman, S.A. and Shuhtsova, J.G., Colloid, J., 21, 25 (1953).
120. Bockris, J. O'M., 'Physical Chemistry Series 2, Vol. 6, Electrochemistry, Butterworths and Co., Publication (1976).
121. Bockris, J.O'M and Reddy, A.K.N., 'Modern Electrochemistry', Vol. 1, A Plenum/Rosetta Edition, New York (1977).
122. Frank, H.S. and Wen, Wen-Yang, Discuss-Faraday Soc., 24, 133 (1957).
123. Frank, H.S., Proc. Roy. Soc., A247, 431 (1958).
124. Arnikar, H.J. and Kalkar, C.D., J. Univ. Poona, Sci. Technol., 50, 45 (1977).
125. Samoilov, O.Ya, Discuss-Faraday Soc., 24, 141 (1957).
126. Kavanau, J.L., 'Water and Solute-Water Interactions', Holden-Day, Inc., San Francisco, London, Amsterdam (1964).
127. Larson, S.R., 'Handbook of Electrochemical Constants', Butterworths, London (1959).
128. Harned, H.S. and Owen, B.B., 'The Physical Chemistry of Electrolytic Solutions', 2nd edition, Reinhold Publ. Comp., New York, N.Y. (1950).
129. Harned, H.S. and Hudson, R.N., J. Am. Chem. Soc., 73, 5033 (1951).
130. Janz, G.J., Oliver, B.G., Lakshminarayanan, G.R. and Mayer, G.E., J. Phys. Chem., 74, 1235 (1970).
131. Sood, M.L., Kaur, G. and Choppra, S.L., Indian J. Chem., 18A, 131 (1979).

132. Reilly, P.J. and Stokes, R.H., Aust.J.Chem., 24, 1361 (1971).
133. Luk, Y., Nanis, L. and Litt, M., Ind.Eng.Chem. Fundam., 14, 92 (1975).
134. Bennetto, H.P. and Spitzer, J.J., J.C.S. Faraday Trans.I, 74, 2335 (1978).
135. Slade, A.L., Cremers, A.E. and Thomas, H.C., J.Phys.Chem., 70, 2840 (1966).
136. Friedman, L., J.Am.Chem.Soc., 52, 1311 (1930).
137. Arnkar, H.J., Patil, S.F., Adhyapak, N.G. and Potdar, J.K., Z.Phys.Chem.(Neue Folge), 51, 120 (1930).
138. Salvinien, J., J.Chim.Phys., 43, 465 (1951).
139. Fujii, T. and Thomas, H.C., J.Phys.Chem., 62, 1566 (1958).
140. Patil, S.F. and Adhyapak, N.G., Indian J.Chem., 20A, 1039 (1981).
141. Nakayama, F.S. and Jackson, R.D., J.Phys.Chem., 67, 932 (1963).
142. Schantz, E. and Lauffer, H.A., Biochemistry, 1, 653 (1962).
143. Brown, W., Kloow, G., Chitumbo, K., Amu, T., J.C.S. Faraday Trans.I, 72, 495 (1976).
144. Wang, J.H., J.Am.Chem.Soc., 76, 4755 (1954).
145. Patil, S.F. and Adhyapak, N.G., Radiochimica Acta, 30, 239 (1982).

List of Publications

1. Trace-ion diffusion of Mn^{2+} in 2-1 electrolytes,
S.F. Patil, N.G. Adhyapak and S.K. Ujlambkar,
Radiochem.Radical.Lett., 49, 119 (1981).
2. Diffusion studies of manganese sulphate and manganese
chloride in agar gel medium,
S.F. Patil, N.G. Adhyapak and S.K. Ujlambkar,
Int.J.Appl.Radiat.Isot., 33, 1433 (1982).
3. Effect of supporting electrolytes on the diffusion
of Zn^{2+} ions in agar gel medium,
S.F. Patil, N.G. Adhyapak, S.K. Ujlambkar and Kavaljit Kaur,
Int.J.Appl.Radiat.Isot., 34, 701 (1983).
4. Applicability of the transition state theory to diffusion
of manganese and copper ions and their salts in gel medium,
S.F. Patil, N.G. Adhyapak and S.K. Ujlambkar,
Int.J.Appl.Radiat.Isot. (in press).
5. Obstruction effect in the diffusion of cadmium acetate
and manganese chloride by agar gel,
S.F. Patil, N.G. Adhyapak and S.K. Ujlambkar,
presented at D.A.E. Symposium held at Banaras, 1981.
6. Effect of supporting electrolytes on the diffusion of
 Mn^{2+} ions in agar gel medium,
S.F. Patil, N.G. Adhyapak and S.K. Ujlambkar,
Radio and Radiat. Chem. Symp. AR 21 (1982).
7. Adsorption and Desorption of Ce^{+} Monolayer ; Copper-Aqueous
Electrolyte Solution Systems ,
F.A.Daniels , M.Y.Pandit .and S.K.Ujlambkar ,
Journal of the University of Poona , Science and Technology
Section , No. 54 ; pp. 45 to 50, 1981